

**UNIVERSITY OF SOUTHAMPTON**

**FACULTY OF MEDICINE, HEALTH AND LIFE SCIENCES**

**School of Medicine**

**Investigation of Potential Pro-Apoptotic and Differentiating  
Therapeutic Modalities in Breast Cancer Cells**

**by**

**Simon John Crabb**

**Thesis for the degree of Doctor of Philosophy**

**June 2006**

**UNIVERSITY OF SOUTHAMPTON**

**ABSTRACT**

**FACULTY OF MEDICINE, HEALTH AND LIFE SCIENCES**

**SCHOOL OF MEDICINE**

**Doctor of Philosophy**

**INVESTIGATION OF POTENTIAL PRO-APOPTOTIC AND  
DIFFERENTIATING THERAPEUTIC MODALITIES IN BREAST CANCER  
CELLS**

**by Simon John Crabb**

Improvements to breast cancer therapy will require better understanding of mechanisms to target cell cycle progression, apoptosis and differentiation. This thesis addresses two such examples using in-vitro models of these processes in breast cancer cells.

Firstly investigation addressed the ability of the anti-apoptotic protein BAG-1, which potentiates the oestrogen receptor in breast cancer, to also modulate PPAR $\gamma$  (peroxisome proliferator activated receptor  $\gamma$ ), a nuclear hormone receptor important for lipid and glucose homeostasis. PPAR $\gamma$  agonists represent a potential therapeutic approach for breast cancer, inducing cell cycle arrest, apoptosis and differentiation. Prostaglandin J2 (PGJ2) stimulated PPAR $\gamma$  mediated expression of HSP70, a BAG-1 binding partner, but not BAG-1 isoform expression. BAG-1 over expression did not alter PGJ2 dependent transcription, or interfere with PGJ2-induced cell cycle arrest or differentiation. However, BAG-1 did interfere with induction of cell death by PGJ2. Thus, BAG-1 is unlikely to directly modulate PPAR $\gamma$ , but its known over expression in some breast cancers might limit potential clinical efficacy of PPAR $\gamma$  agonists, by suppression of PPAR $\gamma$ -induced cell death pathways.

Secondly, a depsipeptide natural compound, Spiruchostatin A, was characterised with respect to its histone deacetylase (HDAC) activity and ability to induce cell cycle arrest, differentiation and cell death in breast cancer cells. Differences in potency, cell cycle arrest characteristics and induction of cell death were detected for Spiruchostatin A in breast cancer versus normal cells. Comparative investigation of the depsipeptide HDAC inhibitors Spiruchostatin A and FK-228 demonstrated class I HDAC selectivity in distinction to hydroxamate pan HDAC class I and II inhibitors. Class I HDAC selectivity allowed for the retention of anti breast cancer cell effects. However depsipeptide inhibitors displayed delayed but prolonged histone acetylation pharmacodynamics with implications for in-vivo surrogate markers of downstream biological effects of these compounds.

These findings have potential relevance for the utilisation of PPAR $\gamma$  agonists and HDAC inhibitors in breast cancer therapeutic development.

# List of Contents

<b>1</b>	<b>Introduction.....</b>	<b>14</b>
1.1	Overview.....	14
1.2	BAG-1 Structure, Expression, Interactions and Function .....	18
1.2.1	BAG-1 Exists As Multiple Isoforms With Differing Translational Processes .....	18
1.2.2	BAG-1 Isoforms Have Common C-Terminal Domains But Variable Amino-Terminals.....	23
1.2.3	BAG-1 Is An Anti-Apoptotic Protein .....	26
1.2.4	BAG-1 Has A Range Of Interaction Partners .....	27
1.2.5	BAG-1 Interaction With HSP Chaperones Is Central To Its Cellular Roles .....	27
1.2.6	BAG-1 Isoforms Have Variable Cellular Localisation Characteristics.....	30
1.2.7	The Role of BAG-1 in Breast Cancer and Other Malignancies.....	31
1.3	Nuclear Hormone Receptors and Their Interactions With BAG-1 .....	36
1.3.1	Mechanisms of Nuclear Hormone Receptor Function.....	36
1.3.2	Specific Examples of BAG-1 NHR Interaction and Relevance to Malignancy .....	42
1.3.3	Peroxisome Proliferator Activated Receptor $\gamma$ (PPAR $\gamma$ ) .....	45
1.3.4	In-Vitro and Animal Data To Support The Role Of PPAR $\gamma$ In Cancer .....	48
1.3.5	Human and Clinical Data Regarding PPAR $\gamma$ and Cancer .....	49
1.3.6	Evidence Regarding Interaction Of BAG-1 With PPAR $\gamma$ .....	50
1.4	Histone Deacetylase Inhibitors .....	52
1.4.1	Acetylation Is An Epigenetic Control Mechanism Of Gene Expression.....	52
1.4.2	HDAC And HAT Activity Are Aberrant In Malignancy .....	58
1.4.3	HDACs And HATs Also Target Non-Histone Proteins .....	58
1.4.4	HDACs Can Be Inhibited By Compounds Targeted To Their Active Sites.....	61
1.4.5	Biological Effects Of HDAC inhibitors.....	67
1.4.6	Differences Between HDAC Inhibitor Effects In Normal Versus Malignant Cells .....	69
1.4.7	Clinical Trials Involving HDAC Inhibitors .....	70
1.4.8	Spiruchostatin A Is A Homologue Of FK228 Amenable For Chemical Synthesis .....	74
<b>2</b>	<b>Project Aims and Outline of Investigation.....</b>	<b>78</b>
2.1	Interaction Between BAG-1 and PPAR $\gamma$ .....	78

2.2	Characterisation of the Novel HDAC Inhibitor Spiruchostatin A .....	79
2.3	Comparisons Between Cyclic Tetrapeptide and Hydroxamate HDAC Inhibitors .....	79
<b>3</b>	<b>Materials and Methods .....</b>	<b>81</b>
3.1	Reagents .....	81
3.1.1	General Buffers and Solutions .....	81
3.1.2	Protein Manipulation Solutions And Buffers .....	82
3.1.3	DNA Electrophoresis Reagents .....	83
3.1.4	Bacterial manipulation reagents.....	83
3.1.5	Mammalian Cell Culture.....	84
3.2	In-vitro Cell Culture Techniques .....	85
3.2.1	Cell Lines .....	85
3.2.2	Cell Culture and Cryopreservation Techniques .....	85
3.3	Protein Manipulation Techniques .....	88
3.3.1	Protein Quantification .....	88
3.3.2	Sodium Dodecyl Sulphate Polyacrylamide Gel Electrophoresis (SDS-PAGE).....	88
3.3.3	SDS-PAGE Sample Preparation For Histone Acetylation Experiments .....	89
3.3.4	Western Blot Analysis .....	89
3.4	DNA Manipulation Techniques .....	92
3.4.1	Bacterial Transformation .....	92
3.4.2	DNA Purification Methods .....	92
3.4.3	Restriction Endonuclease Digestion .....	93
3.4.4	Agarose Gel Electrophoresis.....	94
3.4.5	Summary of DNA Plasmid Constructs Used.....	94
3.5	Transcription Reporter Assays.....	96
3.5.1	tk.luc Control Reporter Construct For PPRE-tk-luc .....	96
3.5.2	Transcription Reporter Assays For PPAR $\gamma$ .....	96
3.5.3	Transcription Reporter Assays For VDR and VDR/PPAR $\gamma$ Comparisons .....	97
3.6	Cell Cycle and Cell Death Analysis by FACS.....	98
3.7	Nile Red Fluorescence Microscopy .....	99
3.8	Cell Proliferation Assays for HDAC Inhibitors.....	100
3.9	RNA Gene Expression Analysis .....	100
3.9.1	RNA Isolation and Purification.....	100

3.9.2	cDNA Production.....	101
3.9.3	RNA Expression Analysis .....	102
3.10	Statistical Analysis.....	102
<b>4</b>	<b>Interaction Between BAG-1 and PPAR<math>\gamma</math> .....</b>	<b>104</b>
4.1	Introduction.....	104
4.2	PPAR $\gamma$ Stimulation Increases HSP40 And HSP70 But Not BAG-1 Protein Expression.....	104
4.3	BAG-1 Does Not Modulate Downstream Transcriptional Effects Of PPAR $\gamma$ .....	107
4.4	The Influence of BAG-1 Isoforms on PPAR $\gamma$ Mediated Differentiation in Breast Cancer Cells.....	113
4.5	Effect of BAG-1 Isoforms on PGJ2 Induced Breast Cancer Cell Cycle Arrest and Cell Death.....	118
4.6	Discussion.....	123
<b>5</b>	<b>Characterisation of a Novel HDAC Inhibitor Spiruchostatin A.....</b>	<b>128</b>
5.1	Introduction.....	128
5.2	Spiruchostatin A Induces Histone Acetylation .....	128
5.3	Spiruchostatin A Induces Cell Cycle Arrest and Cell Death .....	132
5.4	Spiruchostatin A Induces Differentiation in Breast Cancer Cells .....	136
5.5	Spiruchostatin A Has Greater Potency In Malignant Compared To Normal Cells In-Vitro .....	138
5.6	Spiruchostatin A Exhibits Differences In Induction Of Cell Cycle Arrest And Cell Death Between Malignant And Normal Cells.....	140
5.7	Spiruchostatin A Causes Detachment of Adherent Cell Mono-Layers and Inhibits Differentiation Markers Prior To Inducing Cell Death .....	145
5.8	Discussion .....	149

<b>6</b>	<b>Comparison Between Bicyclic Tetrapeptide and Hydroxamate HDAC Inhibitors.....</b>	<b>154</b>
6.1	Introduction.....	154
6.2	Comparison Of The Effects Of Bicyclic Tetrapeptides And Hydroxamates On Cell Proliferation, Gene Expression And Cell Cycle Progression.....	157
6.3	Spiruchostatin A Exhibits Class I HDAC Selective Effects.....	166
6.4	Bicyclic and Hydroxamate HDAC Inhibitors Exhibit Differences In Histone Acetylation Pharmacodynamics .....	168
6.5	The Effect of Histone Acetylation Pharmacodynamics on Cell Cycle Progression.....	172
6.6	Investigation of Bicyclic Tetrapeptide Cellular Entry and Internal Reduction Mechanisms .....	176
6.7	Discussion .....	179
<b>7</b>	<b>Future Work.....</b>	<b>185</b>
	<b>References .....</b>	<b>189</b>

## List of Figures

Figure 1-1 Schematic representation of the CAP dependant ribosomal scanning mechanism for BAG-1L translation and IRES dependant translation for BAG-1S.....	21
Figure 1-2 Schematic diagram of the BAG1 isoform structures .....	25
Figure 1-3 The BAG-1–Hsc70 interaction.....	29
Figure 1-4 Generalised mechanism for chaperone function in NHR maturation, activation and downstream transcriptional modulation of target genes...40	
Figure 1-5 Structural organisation of the PPAR $\gamma$ receptor. ....	47
Figure 1-6 Schematic representation of histone acetylation as a model for transcriptional control by epigenetic mechanisms .....	56
Figure 1-7 Selected HDAC inhibitor structures.....	65
Figure 1-8 Schematic representation of TSA interaction with the HDAC active site .....	66
Figure 1-9 Activation of FK228 by reduction of the internal disulfide bond.....	76
Figure 1-10 Structures of FK228 and Spiruchostatin A and its inactive epimer .....	77
Figure 4-1 BAG-1 and HSP protein expression following PPAR $\gamma$ stimulation in MCF7 breast carcinoma cells.....	106
Figure 4-2 Analysis of PPAR $\gamma$ activity with PGJ2 stimulation with respect to dose, in MCF7 breast cancer cells.....	110
Figure 4-3 Effect of BAG-1L co-transfection on PPAR $\gamma$ stimulated downstream transcription in MCF7 breast cancer cells .....	111
Figure 4-4 Comparison of BAG-1L co-transfection in H376 cells on either VDR or PPAR $\gamma$ downstream transcription .....	112

Figure 4-5 Effect of PPAR $\gamma$ stimulation on MDA-MB-231 breast cancer cell morphology .....	115
Figure 4-6 Effect of PPAR $\gamma$ stimulation on average cell lipid droplet count assessed by Nile Red staining in MCF7 cells.....	116
Figure 4-7 The effect of BAG-1 over expression on differentiation induced by PPAR $\gamma$ stimulation in MCF7 stably transfected clones .....	117
Figure 4-8 Cell cycle analysis of MCF7 cells by flow cytometry following PPAR $\gamma$ stimulation.....	120
Figure 4-9 Cell cycle analysis in BAG-1 over expressing MCF7 clones following PPAR $\gamma$ stimulation.....	122
Figure 5-1 Protein acetylation and expression with respect to Spiruchostatin A dose in MCF7 and BT474 breast cancer cells.....	131
Figure 5-2 Cell cycle effects of Spiruchostatin A relative to dose in MCF7 breast carcinoma cells.....	134
Figure 5-3 Induction of cell death by Spiruchostatin A with respect to dose in breast cancer cells.....	135
Figure 5-4 Spiruchostatin A induced differentiation in MCF7 breast carcinoma cells .....	137
Figure 5-5 Cell proliferation following Spiruchostatin A exposure for MCF7 versus normal human dermal fibroblasts .....	139
Figure 5-6 Comparison of histone acetylation status following Spiruchostatin A exposure in MCF7 breast carcinoma cells and normal human dermal fibroblasts.....	142
Figure 5-7 Cell cycle progression following Spiruchostatin A exposure in MCF7 breast carcinoma cells and normal human dermal fibroblasts .....	143
Figure 5-8 Induction of cell death following Spiruchostatin A exposure in MCF7 breast carcinoma cells and normal human dermal fibroblasts .....	144



Figure 5-9 Effects of Spiruchostatin A in floating and adherent cell fractions in MCF7 breast carcinoma cells.....	148
Figure 6-1 Cell proliferation curves for Spiruchostatin A, FK228, TSA and SAHA in MCF7 breast cancer cells.....	160
Figure 6-2 Cell proliferation following bicyclic tetrapeptide or hydroxamate HDAC inhibitor exposure, in MCF7 breast carcinoma cells versus normal human dermal fibroblasts.....	161
Figure 6-3 Mean IC <sub>50</sub> values for Spiruchostatin A, FK228, TSA and SAHA in MCF7 breast carcinoma cells and normal human dermal fibroblasts....	162
Figure 6-4 Gene expression analysis following exposure to Spiruchostatin A, its structural epimer or FK228, TSA or SAHA .....	164
Figure 6-5 Cell cycle progression and apoptosis in MCF7 breast carcinoma cells following HDAC inhibition with Spiruchostatin A, TSA or SAHA .....	165
Figure 6-6 Histone and tubulin acetylation and p21 <sup>(WAF1/Cip1)</sup> expression characteristics for bicyclic tetrapeptides compared to hydroxamates in MCF7 breast carcinoma cells.....	167
Figure 6-7 Histone acetylation with respect to time for Spiruchostatin A and TSA treatment in MCF7 breast cancer cells.....	170
Figure 6-8 Histone acetylation following exposure to, and washout of, Spiruchostatin A, FK228, TSA or SAHA in MCF7 breast cancer cells	171
Figure 6-9 Cell cycle progression in MCF7 breast carcinoma cells following pulsed exposure to Spiruchostatin A, FK228, TSA or SAHA .....	174
Figure 6-10 Histone acetylation in MCF7 breast carcinoma cells following pulsed exposure to bicyclic tetrapeptides or hydroxamates .....	175
Figure 6-11 Effects of internal reduction, the presence of serum proteins and co-treatment with an inactive epimer on Spiruchostatin A induced histone acetylation .....	178

## List of Tables

Table 1-1 Human BAG-1 family proteins .....	22
Table 1-2 The significance of BAG-1 in malignancies other than breast cancer .....	35
Table 1-3 The interaction of BAG-1 isoforms and mutants with NHRs based on reporter construct assays .....	41
Table 1-4 Characteristics and classification of the human HDAC enzymes <sup>10,110</sup> .....	57
Table 1-5 Non-histone proteins regulated by acetylation status <sup>10,11,122</sup> .....	60
Table 1-6 HDAC inhibitor classes, examples and clinical trial status .....	64
Table 1-7 Clinical trials using HDAC inhibitors .....	73
Table 3-1 Cell lines used for this work .....	87
Table 3-2 Antibodies used in this study .....	91
Table 3-3 DNA expression plasmids used in this work .....	95
Table 3-4 Gene expression assays used for real time PCR for results presented in this thesis .....	103
Table 6-1 Inhibition values of Spiruchostatin A and TSA against HDAC1 and HDAC6 .....	156

## **Acknowledgements**

I would like to acknowledge and thank Dr Graham Packham and Professor Peter Johnson who acted as supervisors for the project presented in this work.

From Dr Packham's laboratory, Dr Adam Sharp, Mr Mathew Brimmell, Dr Melanie Howell, Dr Becky Pickering and Miss Fay Habens each provided help and instruction in the various techniques used within this thesis. Dr Angela Hague (Bristol University) provided help and advice regarding the performance of the vitamin D receptor reporter assays. In addition, I thank all current and past members of Dr Packham's laboratory who have been of assistance throughout this work.

I am grateful to Cancer Research UK, who funded my position as a Clinical Research Fellow, and work within Dr Packham's laboratory, to allow me to undertake the project presented in this thesis.

Finally, thankyou to Jane for making the coffee.

## Abbreviations

AR	Androgen receptor
BAG-1	Bcl-2 associated athanogene-1
DTT	1,4-Dithiothreitol
EGFR	Epidermal growth factor receptor
ER	Oestrogen receptor
GR	Glucocorticoid receptor
HAT	Histone acetyl transferase
HDAC	Histone deacetylase
HER2	Human epidermal growth factor receptor 2
HSP	Heat shock protein
IC <sub>50</sub>	Concentration for 50% inhibition of cell proliferation
MR	Mineralocorticoid receptor
NHR	Nuclear hormone receptor
NLS	Nuclear localizing sequence
NHDF	Normal human dermal fibroblasts
PCNA	Proliferating cell nuclear antigen
PGJ <sub>2</sub>	15-deoxy- $\Delta^{12,14}$ -prostaglandin J <sub>2</sub>
PPAR	Peroxisome proliferator activated receptor
PR	Progesterone receptor
RAR	Retinoic acid receptor
SAHA	Suberoylanilide hydroxamic acid (Vorinostat)
SD	Standard deviation
SEM	Standard error of the mean
TSA	Trichostatin A
TZD	Thiazolidinedione
VDR	Vitamin D receptor

# 1 Introduction

## 1.1 Overview

Breast cancer remains a major source of morbidity and mortality in the UK, with an incidence of over 40000 annually, the highest for all cancers in women. With an annual mortality in excess of 12000 it represents the second most common female cancer death.<sup>1</sup> Therapeutic options for breast cancer remain inadequate therefore and new options for treatment are required, both for this and other malignancies. For breast cancer, it is likely that further advances in survival rates will arise through improvements in systemic therapies, rather than modifications to other therapeutic approaches such as surgery or radiotherapy. This basic premise recognises that the key to disease control and eradication lies in systemic control of disease, either following potentially curative resection or in the palliative setting. Breast cancer is a good example of a malignancy where systemic therapeutic intervention already combines conventional cytotoxic chemotherapeutics with more targeted approaches that include hormonal intervention and now targeted antibody therapy. There remains a need for development of agents aimed at specific mechanisms that underpin key biological processes for the malignant cell. Examples of such processes include apoptosis, cell cycle progression and differentiation.

Development of agents which target these processes is an expanding area with great interest at the level of basic, translational and early phase trial work. With regard to targeting the cell cycle, a number of agents have been assessed which appear to act predominantly by targeting control mechanisms for cell cycle progression. The cell cycle represents a succession of tightly regulated events via which cells proliferate by passing through the stages of division. This is regulated by critical cell cycle machinery comprising of the cyclin dependant kinases (CDK) which are regulated positively by cyclins and negatively by naturally occurring CDK inhibitors. Carcinogenesis is often in part a result of disruption to the activity of these

regulating compounds, either through over-expression of cyclins or under-expression of CDK inhibitors, leading to excessive unregulated cell cycle progression. An example of drug like inhibitors of cell cycle control, and perhaps the furthest developed, is flavopiridol. This agent has been shown to act predominantly through inhibition of cyclin dependant kinases leading to cell cycle arrest and subsequently apoptosis. Encouraging results have been seen in breast and other malignant cell lines with this and other compounds. The sequencing with conventional cytotoxics seems particularly important in determining efficacy of such agents.<sup>2</sup>

With regard to differentiation, again a number of potentially useful drug like compounds have been developed with potential to modify malignant cell progression by targeting this cellular process. This approach is based on the knowledge that many neoplastic cells exhibit aberrant patterns of differentiation and that treatment with an appropriate agent can result in tumour reprogramming, resulting in the induction of terminal differentiation, a loss of proliferative capacity and subsequently apoptosis. Probably the most well established example of this in clinical practice is of the use of all-trans retinoic acid (ATRA) in acute promyelocytic leukaemia where ATRA treatment exerts a differentiating effect through the characteristic retinoic acid receptor t(15;17) fusion protein.<sup>3</sup>

In the targeting both of cell cycle progression and differentiation as key processes underpinning carcinogenesis, it is hoped that toxicity may be comparatively spared compared to conventional systemic cytotoxic therapies. However agents that interfere with these fundamental cellular processes clearly have the potential to impact on normal cells also and so this presumption requires careful assessment. In addition many examples of drug development towards potentially more intelligent targeted interventions for specific malignant processes are likely to progress to assessment in combination with conventional cytotoxic agents. The use of ATRA in acute promyelocytic leukaemia is a prime example. In this situation responses to the differentiating agent alone tend to be seen in the majority of patients but are commonly

short lived requiring co-treatment with chemotherapeutics.<sup>3</sup> Thus co-administration of agents with complementary mechanisms of action should be investigated from the point of initial cell line work through to clinical application.

This thesis addresses the pre-clinical development of therapeutic modalities with potential in breast cancer, to exploit aberrant cell cycle and differentiation processes, leading to inhibition of proliferation and cell death via apoptosis. Two such examples are explored which are both promising potential approaches to allow more intelligent targeting of malignant cell pathology with the hope arising that this would lead to better therapeutic:toxicity profiles.

The first involves a key interaction between the anti-apoptotic protein BAG-1 and its ability to modify the function of nuclear hormone receptors (NHR) including the oestrogen receptor (ER). BAG-1 is known to be over-expressed in breast cancer and act as a prognostic indicator. Work in the author's laboratory has previously shown that BAG-1 potentiates the activity of the ER.<sup>4</sup> A further potential NHR target in breast cancer is PPAR $\gamma$ . This key regulator of lipid homeostasis is known to exhibit decreased expression in a proportion of breast cancers. PPAR $\gamma$  ligands, which induce apoptosis, cell cycle arrest and differentiation, have raised interest as a potential hormonal therapeutic option in breast and other cancers. Data are presented to determine the ability of BAG-1 to modify PPAR $\gamma$  activity using such ligands in breast cancer cells (Crabb S et al, manuscript in preparation). Understanding this potential interaction may be important in the development of these agents as modulators of cell cycle progression, differentiation and subsequently apoptosis in breast cancer.<sup>5-11</sup>

Secondly, results are presented that address the role of HDAC inhibitors to modify epigenetic control mechanisms which again represents a promising potential therapeutic approach to modify the cell cycle and differentiation pathways in breast cancer and other malignancies. Development of structural variants of HDAC inhibitors is desirable to allow better understanding of their mechanisms of action

and future drug development<sup>12-14</sup> This work has addressed the in-vitro characterisation of a novel bicyclic HDAC inhibitor, Spiruchostatin A, with respect to its activity in breast cancer cells, as well as comparison to other structural HDAC inhibitor classes. This serves as a means to better understand the way in which these compounds may be of use in breast cancer as well as well as providing insight into the potential to develop HDAC class specific inhibitors (Crabb S et al, manuscript submitted).



## **1.2 BAG-1 Structure, Expression, Interactions and Function**

### **1.2.1 BAG-1 Exists As Multiple Isoforms With Differing Translational Processes**

The anti-apoptotic protein BAG-1 was originally discovered in 1995 by two independent groups who identified a novel interaction partner for Bcl-2 and the glucocorticoid receptor.<sup>15,16</sup> It has subsequently been determined that three BAG-1 isoforms are produced from a single gene located on chromosome 9 band 12 in the human.<sup>17</sup> Distinct translational initiation sites within a single mRNA sequence are responsible for the different isoforms observed. In the human, the major isoforms produced are BAG-1L (50 kDa) initiated at an upstream CUG codon, BAG-1M (46 kDa, also called RAP46 or HAP46) initiated at the first in-frame AUG codon, and BAG-1S (36 kDa) initiated from the second in-frame AUG codon. In the mouse two isoforms are described, BAG-1L (50kDa) and BAG-1 (32kDa). The most abundant isoform is generally BAG-1S, followed by BAG-1L and then BAG-1M although these patterns may alter in states of cell stress or malignancy. A fourth human isoform of 29kDa in size has been detected, but expression is inconsistent and at low levels, and its functional significance remains unclear.<sup>11,17-20</sup>

The BAG-1 promoter has been cloned and contains a CCAAT box, GC rich boxes and Sp1 transcription factor binding sites as typical promoter elements (but lacking a TATA box). The presence of a CpG-rich island raises the possibility of methylation as a control mechanism for BAG-1 transcription. Raised BAG-1 mRNA expression by survival factors is seen but the role of promoter activation remains to be fully elucidated.<sup>9</sup>

The translational mechanisms that produce the different isoforms of BAG-1 occur by two different processes (figure 1-1). Firstly, a conventional cap-dependant mechanism exists whereby a ribosome complex 'scans' from a 5' cap structure until

the first translation initiation codon, in the context of a good Kozak consensus sequence. This mechanism accounts for the translation of BAG-1L, BAG-1M and to a degree BAG-1S, and explains in part the relative lack of abundance seen for BAG-1M. The second mechanism is by internal ribosome entry sequence (IRES) dependant translation. This process allows a ribosomal complex to enter within an mRNA coding sequence at an IRES independent of and distinct from the cap structure. IRES elements are thought to exist in about 3% of cellular mRNAs including BAG-1 where it allows for the translation of the BAG-1S isoform. BAG-1S has GC-rich areas upstream of its AUG start codon with the potential to form extensive secondary structure characteristic of this mechanism. Thus IRES dependent translation may explain the relative abundance of BAG-1S in cells, despite its start codon existing within the full BAG-1 coding sequence and downstream of eight CUG and two AUG codons, some of which are in good Kozak consensus, which would be highly unusual based only on the cap dependant scanning mechanism for translation initiation. It may also be relevant to BAG-1 function in that IRES dependant transcription of BAG-1S can be maintained following heat shock as this form of translation is found to be maintained for polypeptide production at times of cellular stress when cap dependant transcription is compromised.<sup>21-23</sup> Thus variable translational mechanisms provide another level of functional variability for BAG-1, in addition to that conferred by variability in isoform length.

BAG-1 degradation is not well understood although the proteins generally seem to be very stable. One study has suggested that injured neuronal cells are susceptible to degradation of BAG-1 following protein modification, possibly as a result of ubiquitylation and associated with apoptosis. This process may be mediated by the Siah protein family.<sup>24</sup>

BAG-1 is one of a family of six proteins in the human which are grouped together based on the presence of the C-terminal BAG domain. The key function of this domain seems to be the interaction with the heat shock protein (HSP) family of

molecules through the HSP amino-terminal ATPase domain. Thus this family are likely to each have roles linked to the targeting of molecular chaperones with differences between them determined by variability in their amino terminal structures. (Table 1-1) In addition to a BAG domain (four in the case of BAG-5), these proteins each contain variable additional functional domains relevant to cellular localisation and protein interactions. BAG-1 remains the most extensively studied of the BAG family and less is known about the cellular roles of the other members. Only four have been confirmed in-vivo and shown to interact with the HSP family.<sup>25</sup>

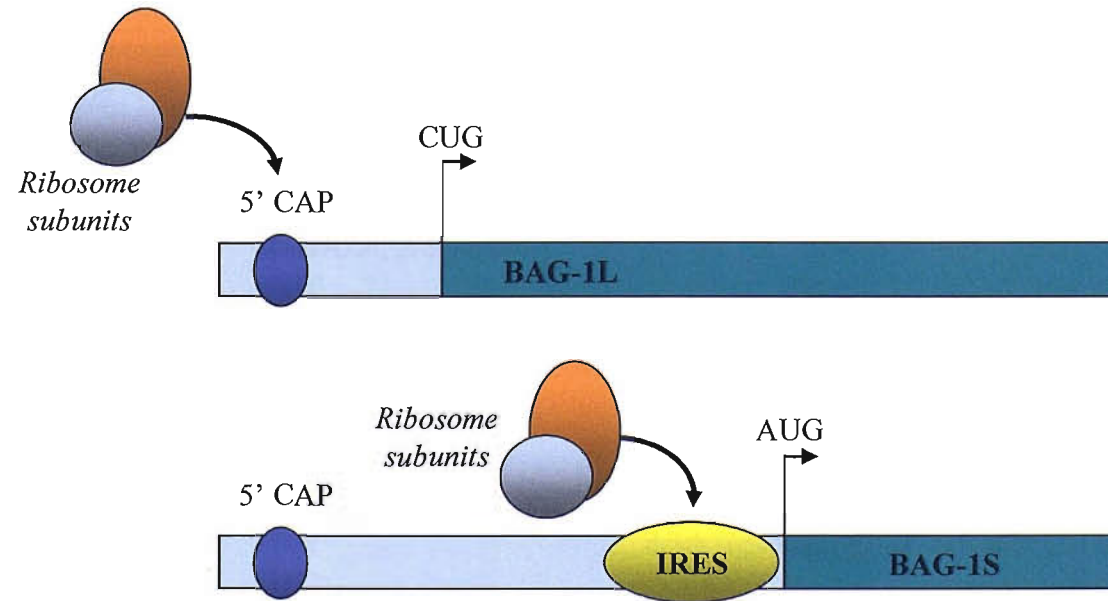


**Figure 1-1 Schematic representation of the CAP dependant ribosomal scanning mechanism for BAG-1L translation and IRES dependant translation for BAG-1S**

Member	Other Names	Chromosome	Known Interactions	Comments
BAG-1	RAP46, HAP46	9p22	Bcl-2, Raf-1, Siah1, HGFR, PDGFR, ER, AR, GR, RAR, TR, VDR, Rb, CHIP, GADD34, proteasome	
BAG-2		6p11.2-12.3		
BAG-3	CAIR-1, Bis	10q25.2-q26.2	PLC $\gamma$ , Bcl-2	Binds the SH3 domain of phospholipase C- $\gamma$ (PLC $\gamma$ ). Potential role in growth factor activation of calcium dependant signalling.
BAG-4	SODD	8p22	TNFR1, DR3	Binds TNF super family death domains. Prevents cell death signalling, NF- $\kappa$ B induction and caspase associated apoptosis.
BAG-5		14		
BAG-6	Scythe, BAT3	6p21.3	Reaper	Apoptosis regulating nuclear protein. Binds the pro- apoptotic Reaper and sequesters an unidentified apoptotic molecule blocking cytochrome c release.

**Table 1-1 Human BAG-1 family proteins**

### **1.2.2 BAG-1 Isoforms Have Common C-Terminal Domains But Variable Amino-Terminals**

BAG-1 isoforms share a common carboxy terminus sequence but exhibit different lengths at their amino termini. Thus the longer isoforms contain functional domains in the amino terminal (which are relevant for example to sub-cellular localisation) that are absent from the shorter forms (Figure 1-2). This explains differing localisation characteristics and may also be relevant in the differing functional activity patterns seen for the different isoforms.

Close to the carboxy terminal lies the BAG domain, spanning about 70 amino acids, which is common to all isoforms. It consists of two anti-parallel alpha-helices which are involved in the key interaction with HSPs, and a third helix which may maintain the structure of this region and mediate other protein interactions. BAG-1 may in part function as a bridging molecule by binding to the ATPase domain of HSPs via the BAG domain, facilitating recruitment to target molecules through further interactions mediated by variable amino terminal regions. Mutation of the BAG domain can block a range of BAG-1 functions suggesting the importance/requirement of HSP interaction for a number of its proposed roles.<sup>26-28</sup>

The BAG-1 carboxy-terminus is also able to interact with the serine/threonine kinase RAF1, which normally stimulates the MAP kinase cascade signalling pathway following RAS activation. BAG-1 interaction represents a mechanism for activation of this pathway independent of RAS and is an example of the ability of BAG-1 to modulate cell signalling paths relevant to cell proliferation. The interaction of RAF1 with BAG-1 is at a site which partially overlaps the BAG domain interaction site for HSP70. Thus BAG interaction with these two molecules appears to be competitive and dependant on the cellular state, with increased HSP70 production at times of cellular stress causing a rise in HSP70/BAG-1 complexes at the expense of RAF1/BAG-1 interaction. Thus has been proposed to represent a 'cellular switch' away from cellular RAF-1 mediated proliferation processes in a stressful

environment maybe to a less proliferative, quiescent state.<sup>25,29,30</sup> BAG-1 expression patterns are altered in human malignancy but the degree to which the interactions with HSPs and RAF1 might be deranged in the production of a malignant phenotype remains unknown.

All BAG-1 isoforms share a common ubiquitin like domain (ULD) and may play a role in the ubiquitin/proteasome system. Ubiquitin is a ~70 amino acid molecule that attaches to protein targets by a series of covalent recognition, activation and conjugation reactions. One of the major functions of ubiquitylation is to target proteins for ATP dependant degradation by the proteasome, which is the major non-lysosomal proteolytic mechanism for protein degradation. Thus, ubiquitylation is a mechanism for control of protein turnover. Like other ULD containing proteins, BAG-1 can be ubiquitylated. However rather than being subsequently degraded, it appears that it may facilitate interaction between the proteasome and chaperones such as HSPs.<sup>31,32</sup>

Further towards the amino terminal, BAG-1 isoforms contain variable numbers of an acidic amino acid rich repeat sequence conforming to a TR/QSEEX consensus sequence. Nine copies of these repeats are present in BAG-1L and BAG-1M but only three in BAG-1S. The exact function of this part of the molecule remains unclear, but it may be required for some BAG-1 functions, such as the interaction with the glucocorticoid receptor. It may also represent a domain that undergoes phosphorylation in-vivo but the functional significance of this is uncertain.<sup>9,33</sup>

Finally in the amino terminal of BAG-1L lies a nuclear localising sequence (NLS).

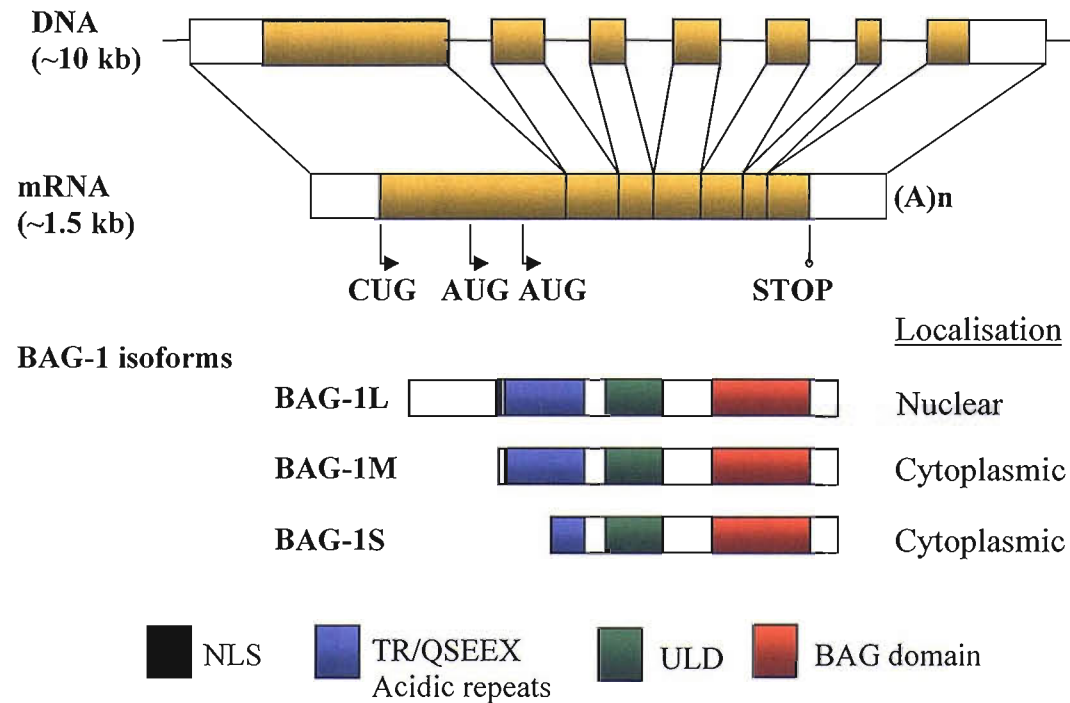


**Figure 1-2 Schematic diagram of the BAG1 isoform structures**

Human BAG-1 comprises seven exons and encompasses approximately 10kb resulting in an mRNA of approximately 1.5kb. Distinct translational CUG and AUG start sites exist for the three major BAG-1 isoforms within a common mRNA sequence. The domain structure of the three main isoforms is shown. Adapted from Townsend et al, with permission.<sup>9</sup> (ULD - ubiquitin like domain, NLS - nuclear localization sequence)



### 1.2.3 BAG-1 Is An Anti-Apoptotic Protein

BAG-1 suppresses apoptosis in a range of in-vitro settings. It has been shown to do so in response to a wide range of pro-apoptotic stimuli including Fas and TRAIL death receptor stimulation, serum and cytokine withdrawal, heat shock, hypoxia, dexamethasone, ATRA, radiation and cytotoxics such as etoposide and cisplatin.<sup>15,34-40</sup> Where studied, all three major isoforms seem to confer a pro-survival effect, however in many of the studies cited BAG-1S has been focussed on and detailed comparisons with BAG-1L and BAG-1M were not undertaken. There remain many gaps in our understanding of precisely which of the domain regions within the BAG-1 isoforms contribute to pro-survival functions but a C-terminal chaperone dependant mechanism has been shown to exist.<sup>9,38</sup>

The mechanism for BAG-1 functioning as an apoptotic molecule remains uncertain with clear evidence linking it to effector molecules not available. One possibility is via the Bcl-2 protein which was one of the first BAG-1 interaction partners discovered.<sup>15</sup> Bcl-2 is part of a family of structurally related proteins which act to suppress apoptosis or counter Bcl-2 action. It functions by localisation to the mitochondrial membrane and one of BAG-1s effects is prevention of release of pro-apoptotic, caspase activating factors such as cytochrome c from mitochondria. BAG-1 may in part act by modulating Bcl2 function therefore. BAG-1 interaction with Bcl-2 has been shown by a number of techniques but direct evidence of endogenous interaction and of Bcl-2 being an obligate mediator for the BAG-1 anti-apoptotic effect is lacking. An alternate mechanism might be the interaction of BAG-1 with RAF-1 or the heat shock family of molecular chaperones.

#### **1.2.4 BAG-1 Has A Range Of Interaction Partners**

BAG-1 has been found to interact with a range of partners in addition to RAF-1, Bcl-2 and HSPs as mentioned already. These include proteins important for cell survival such as Rb and p53.<sup>41,42</sup> Recently, BAG-1 has been found to interact with the cellular stress response protein GADD34 which mediates apoptosis, growth arrest and transcriptional and translational repression in response to a variety of stressful stimuli. This interaction appears to occur via the direct binding of BAG-1 and GADD34 in a complex together with variable other cofactors such as HSPs. BAG-1 was found to inhibit GADD34 bound PP1 phosphatase activity, cell growth suppression and generalised transcriptional suppression.<sup>43</sup>

Other BAG-1 interaction molecules include cell surface receptors (PDGFR, HGF), growth factors (heparin binding-epidermal growth factor-like growth factor), enzymes involved in ubiquitylation (Siah and CHIP) and DNA.<sup>31,37,38,44</sup>

#### **1.2.5 BAG-1 Interaction With HSP Chaperones Is Central To Its Cellular Roles**

The role of BAG-1 in many of its cellular functions is determined by its interactions with the 70kDa HSP molecular chaperones. There are four mammalian 70kDa HSPs of which HSC70, mHSP70 (mitochondrial) and BiP/GRP78 (endoplasmic reticulum) are constitutively expressed and HSP70 (nuclear) is inducible by cellular stress. They are key to the processes of folding of newly synthesised proteins, disassembly of oligomeric protein structures, facilitation of proteolytic degradation and control of activity of folded regulatory proteins such as transcription factors. Of the four, BAG-1 interacts with HSP70 and HSC70 and blocking these interactions can abrogate many of its functions. HSC70 is known to have an amino terminal ATPase domain, a central peptide binding domain and a C-terminal region able to

form a lid over the peptide binding pocket. Refolding of substrate proteins is dependant on ATP hydrolysis leading to an ADP bound state with closure of the peptide binding pocket and high affinity peptide binding compared to the ATP bound open state. Release of ADP and subsequent ATP binding allows release of the refolded substrate.

The carboxy terminal BAG domain of BAG-1 interacts with a 1:1 stoichiometry (figure 1-3), by binding the HSC70 ATPase domain using helices 2 and 3 of the BAG domain and stimulating ADP release. This interaction relies on key amino acid residues in these two helices which are conserved between species and which cause disruption to BAG-1 function if mutated.<sup>9,26,45</sup> This binding leaves the HSC70 peptide binding domain free for substrate interactions. Therefore BAG-1 may be able to interact with some targets as an indirect action via HSP binding. At least at the in-vitro level BAG-1 seems to be able to modify refolding of artificially denatured reporter proteins but discrepant results exist. For example Takayama et al<sup>46</sup> showed BAG-1S to inhibit refolding of heat denatured  $\beta$ -galactosidase and Zeiner et al<sup>47</sup> showed BAG-1M inhibited luciferase refolding. However Luders et al<sup>48</sup> have reported BAG-1M inhibition and BAG-1S stimulation of luciferase and  $\beta$ -galactosidase. Some of these differences may result from experimental differences but also may be explained by amino-terminal differences of the BAG-1 isoforms.<sup>9</sup>

Evidence for BAG-1 causing refolding in intact cells comes from studies by Nollen et al<sup>49,50</sup> who showed BAG-1 over expression to inhibit HSP70 mediated refolding of the heat sensitive reporter firefly luciferase following heat shock in a fibroblast cell line without alteration in HSP70 cellular localisation or levels. This effect was seen for BAG-1M and BAG-1S but not the nuclear BAG-1L (which may still have similar effects on refolding within the nucleus).

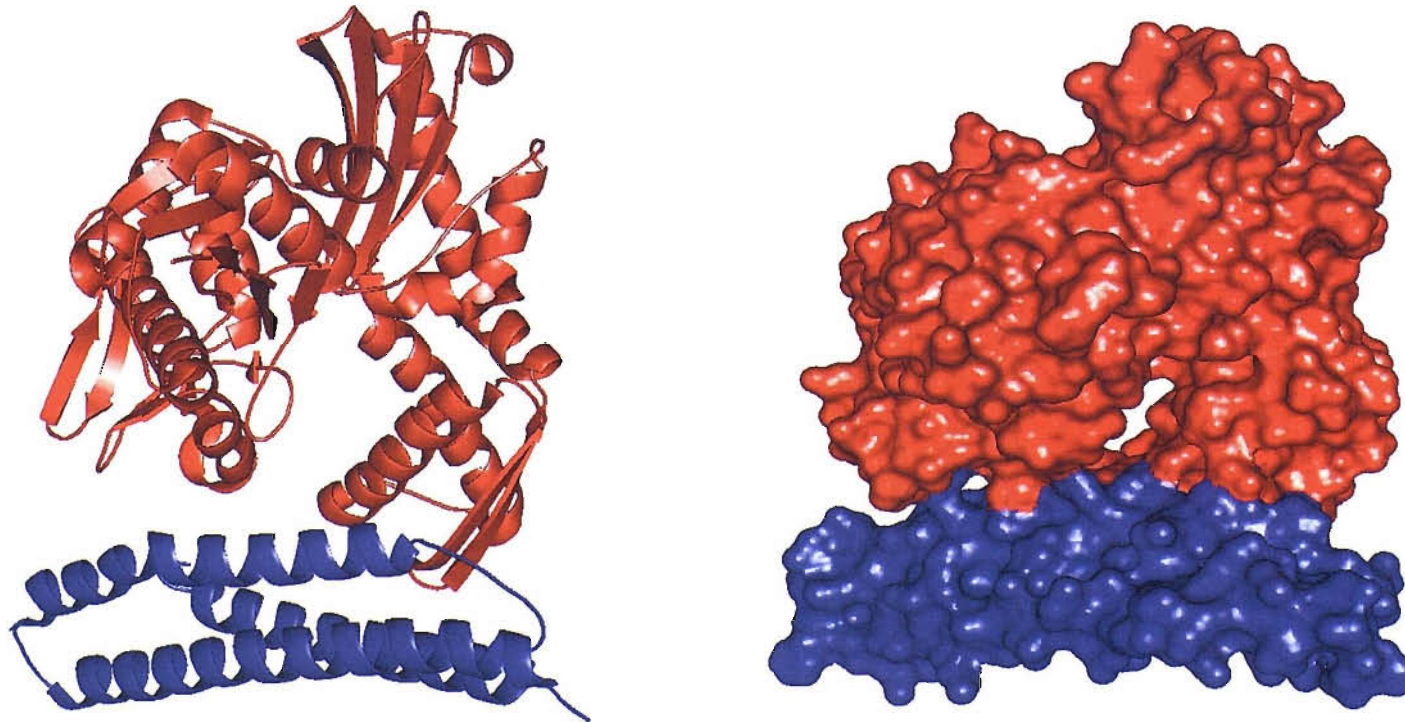


**Figure 1-3 The BAG-1–Hsc70 interaction**

The structure of the BAG-1 BAG domain (blue) bound to the ATPase domain of Hsc70 (red) is shown in ribbon and space-filling representations.<sup>26,27</sup> (Adapted from Sharp et al, 2004<sup>10</sup>)

### 1.2.6 BAG-1 Isoforms Have Variable Cellular Localisation Characteristics

Generally, BAG-1L is found to localise to the nucleus and BAG-1S to the cytoplasm, whilst BAG-1M is able to locate between the two depending on cellular state. However re-localisation between the nucleus and cytoplasm may occur following situations such as cellular stress or interaction with NHRs and may be deranged in malignancy. The variable localisation of BAG-1 isoforms is explained by the different amino terminal sequences of these proteins. BAG-1L contains a PRMKKKT nuclear localising sequence (NLS) within its unique amino terminal which is similar to the SV40 Tag NLS sequence (PKKKRKV).<sup>18-20,51</sup> Part of this sequence (the third to seventh amino acids) exists at the extreme end of the amino terminal of BAG-1M but its functional significance is unclear. Optimal localisation of BAG-1L seems also to require components in amino acids 1 to 50 found to the amino side of this NLS sequence, which if deleted leave a mutant protein with a 'more promiscuous' localisation pattern to both the nucleus and cytoplasm.<sup>52</sup>

In addition, a proposed bipartite NLS sequence (KKNSPQEEVELKCLKH), present in the common segment of all three isoforms, may have relevance in explaining the variability of localisation seen at differing times depending on cell state and provide a mechanism for BAG-1S and M to enter the nucleus.<sup>16</sup> Isoform specific effects, such as interaction with NHRs as described in section 3, may in part be explained by these localisation differences.

### 1.2.7 The Role of BAG-1 in Breast Cancer and Other Malignancies

The relevance of BAG-1 in carcinogenesis has been most extensively investigated in breast cancer. BAG-1 has been shown to be detectable in normal breast tissue specimens, breast carcinoma specimens and also breast cancer tumour cell lines. In both biopsy specimens and cell lines, the presence of BAG-1 staining and also its intensity has been found to be greater in ER $\alpha$  positive cells.<sup>51</sup> High levels of BAG-1 expression have also been seen in DCIS specimens which represent an early pre-invasive state with a risk of progression to overt malignancy. This suggests that changes in BAG-1 regulation might be important at an early stage in carcinogenesis and tumour development.<sup>51,53</sup>

In terms of data relating BAG-1 expression with clinical and pathological outcome variables in patient cohorts, five large immuno-histochemical studies comprising variable subject characteristics exist.<sup>4,53-56</sup> Inconsistencies between studies exist which may in part be explained by differences in clinical characteristics and treatment modalities employed for the patient cohorts studied, as well as variable methods used for immuno-histochemical analysis.<sup>7,57</sup> Cytoplasmic BAG-1 staining was increased consistently across these studies in two thirds or more of cases. Increased nuclear staining is less consistently seen with rates which range between 20 and 70%, with rates for both increased nuclear and cytoplasmic staining between 1 and 60%.

A strong correlation between lower tumour grade and increased nuclear BAG-1 expression was seen in three studies.<sup>4,55,56</sup> Cytoplasmic BAG-1 staining was found to correlate with ER status in pre but not post menopausal patients in a study of patients with early stage disease treated with a diverse set of modalities by Townsend et al<sup>56</sup>. Nuclear and cytoplasmic BAG-1 staining correlated both to ER $\alpha$  and progesterone receptor (PR) expression in a cohort of patients with early stage breast cancer who had all received adjuvant hormonal therapy.<sup>4</sup> Other clinico-

pathologic characteristics have correlated less clearly with BAG-1 staining patterns in these studies.

Three studies have shown BAG-1 staining to correlate with survival with important conflicting results. Tang et al<sup>55</sup> found BAG-1 to be significantly associated with shorter disease free and overall survival in multivariate analysis but not after univariate analysis in a cohort of patients with mixed pathological and clinical characteristics. However, Turner et al<sup>53</sup> found BAG-1 over-expression correlated with improved overall distant metastasis free survival (79 vs. 34% at 10 years) and overall survival (82 vs. 42% at 10 years) in a group of patients with early stage breast cancer treated with variable treatment modalities, which was maintained in multivariate analysis. Cytoplasmic (but not nuclear) BAG-1 over expression also correlated with improved survival. Improved overall and distant metastasis free survival for patients, who over-expressed BAG-1, was maintained in a subset that was axillary lymph node negative. This raises the question of whether BAG-1 staining could be useful to stratify low risk node negative early breast cancer patients. Clearly this would require confirmatory prospective data. More recently Cutress et al<sup>4</sup>, found that increased nuclear (but not cytoplasmic) BAG-1 status correlated with a significantly increased overall survival in univariate analysis (hazard ratio for death with positive nuclear BAG-1 staining 0.334). This study benefits from having assessed a more homogenous cohort of patients who all had early breast cancer treated with surgery followed by adjuvant hormonal therapy but not chemotherapy.

How can one explain the variations in results between these studies and why does an anti-apoptotic protein such as BAG-1 correlate with improved outcome in two of them? Firstly there are differences in critical patient cohort characteristics between these studies. Tang et al used a mixed group of patients with both early stage (i.e. potentially cured) and metastatic disease whereas the other two studies contained only early stage disease. It also used a different antibody (rabbit polyclonal versus mouse monoclonal) and BAG-1 staining scoring method (intensity versus H score).

The Turner study looked at patients with variable treatment with some patients receiving adjuvant chemotherapy and a low percentage of ER positive cases compared to a standard population. Cutress et al however, looked at patients who had all received adjuvant hormonal therapy but not chemotherapy. As such the prognosis of these three cohorts and their response to therapy would be expected to be quite different. Ultimately tightly controlled patient group characteristics, larger study design or prospective design are the way to improve on these problems in future investigation but this adds significantly to the difficulty of performing such studies.<sup>7</sup>

To explain the finding in two of these studies of an improved outcome to therapy in the face of BAG-1 over expression it has been suggested that as BAG-1 acts to enhance ER function then this may represent a mechanism for driving carcinogenesis in ER positive breast cancer which is well recognised as a good prognostic and predictive subtype. This raises the question of what role BAG-1 may have in ER negative disease where other factors are presumably required to result in the metastatic phenotype.

Separate from the issue of BAG-1 as a prognostic marker in breast cancer, is its potential as a predictive marker for determining therapeutic outcome. One study exists where investigators assessed retrospectively just under half of the biopsy specimens for a randomised phase III study looking at second line docetaxel versus methotrexate and 5FU in 283 patients with advanced breast cancer.<sup>54</sup> They were unable to determine a predictive relationship for any of the apoptosis regulators which they assessed, including BAG-1, and BAG-1 did not correlate with survival in this cohort. The study did not specify for sub-cellular localisation of BAG-1 staining and the patient cohort had relapsed disease compared to early stage breast cancer in some of the other studies mentioned above.

In a second pilot study 29 patients undergoing neoadjuvant doxorubicin containing chemotherapy for early breast cancer had pre and post treatment biopsy samples



taken. All pre-treatment tumour biopsies and 40-100% of neoplastic cells expressed BAG-1 in the cytoplasm and to a variable degree in the nucleus. No correlation between pre-chemotherapy expression of BAG-1 and subsequent pathological response to cytotoxic therapy was seen and paired pre- and post treatment specimens showed similar levels of BAG-1 expression when residual tumour could be assessed.<sup>58</sup> Thus based on this limited data there is no evidence for BAG-1 as a predictive marker at present but investigation in early stage patients with consistent cohort characteristics and suitable sample size would be of interest.

A number of other malignancies have been shown to have alterations in BAG-1 expression patterns and subsequent correlations with clinico-pathological outcome measures and are summarised in table 1-2. As with the data relating to breast cancer variable results are seen depending on the localisation of BAG-1 isoforms assessed, and again questions regarding sample size and the retrospective nature of much of the data may confound the results.

<b>Tumour type</b>	<b>Significance of BAG-1</b>	<b>References</b>
Oesophageal squamous cell carcinoma	Nuclear BAG-1 expression correlates with depth of tumour invasion and shorter overall survival	59
Colorectal carcinoma	Nuclear BAG-1 expression correlates with presence of distant metastases and decreased overall survival	60
Tongue squamous cell carcinoma	BAG-1 expression correlates with poorer disease specific survival	61
Non-small cell lung cancer	Overall and cytoplasmic BAG-1 expression correlates with improved overall survival	62
Chronic lymphocytic leukaemia	Increased BAG-1 expression correlated with failure to achieve complete response to chemotherapy	63
Laryngeal squamous cell carcinoma	Nuclear BAG-1 staining correlates with reduced failure free survival following radical radiotherapy	64
Malignant glioma	BAG-1 expression documented in glioma cell lines and biopsy samples	65
Cervical carcinoma	BAG-1 over expressed in human cervical cancer cell lines and tissue samples and conferred resistance to DNA damaging agents	39
Endometrial carcinoma	BAG-1 expression increased in high grade carcinoma compared to secretory epithelium	66
Oral squamous cell carcinoma	BAG-1 expression correlates with presence of nodal metastases and tumour grade	67,68

**Table 1-2 The significance of BAG-1 in malignancies other than breast cancer**

## **1.3 Nuclear Hormone Receptors and Their Interactions With BAG-1**

### **1.3.1 Mechanisms of Nuclear Hormone Receptor Function**

Nuclear hormone receptors (NHR) are key molecules in the control of a wide variety of patterns of transcriptional regulation. As such they help to control a diverse array of cellular processes, such as cell proliferation, motility, cell division, apoptosis, differentiation and morphogenesis. NHRs are also critical in the progression, at least initially, of certain malignancies of which breast and prostate cancers are prime examples. Modulation of their function is a mainstay of therapy in these diseases.<sup>5,69</sup>

All NHRs have a common structural pattern. A central DNA binding domain is critical in allowing binding to highly specific DNA response element sequences. In the C-terminal region lays a ligand binding domain to specific hormonal and non-hormonal compounds, which together with the interaction with specific response elements determines the specificity of downstream biological function. In addition receptors contain variable amino and carboxy domains as well as variable hinge region sequences between the DNA and ligand binding domains. The mechanism of action of NHRs follows a common pattern that is similar for most examples of these receptors. Firstly ligand binding leads either to homo or hetero dimerization. This is followed by binding to specific DNA response elements in promoter or enhancer regions, leading to subsequent modulation of expression of specific transcriptional targets. Some NHRs are also capable of response element binding and transcriptional modification in the absence of ligand binding (e.g. TR, VDR, RAR, and RXR).<sup>70,71</sup>

Nuclear receptor function is controlled through the interaction of co-activator and co-repressor molecules at two activation domains termed activation domain 1 in the amino terminal and activation domain 2 in the carboxy terminal ligand binding

domain. Examples of co-activator proteins include CBP/p300 (CREB binding protein), the p160 family such as steroid receptor co-activator-1 (SRC-1), transcriptional mediator/intermediary factor-2 (TIF-2) and pCIP (CBP/p300 co-integrator associated protein each of which exhibit histone acetyl-transferase (HAT) activity. A further group of co-activators including the thyroid receptor associated protein complex (TRAP) or vitamin D receptor interacting protein complex (DRIP) which enhance receptor activity by recruiting RNA polymerase II to enhance transactivation.<sup>5,71</sup>

Further complexity is added to this mechanism because NHR maturation and function is dependant on protein complex formations with chaperone molecules of which BAG-1 is an example. Interaction of co-chaperones is complex, often with formation of a chaperone:NHR complex that determines the way in which the NHR subsequently regulates downstream transcription. Initial interaction is often in the cytoplasm, however it has become clear that transport of the co-chaperone-receptor complex once formed, can under certain circumstances subsequently relocate to the nucleus, or it may be formed in the nucleus itself.<sup>5</sup>

A generalised scheme for the maturation, ligand binding and function of NHRs is shown in figure 1-4. Two points should be borne in mind when considering this model. Firstly much of the data leading to this schema was developed around the glucocorticoid receptor (GR) and PR with varying levels of information to indicate how far it can be extrapolated to other receptors. Secondly much of the data are derived from in-vitro reticulocyte lysate systems raising issues regarding the degree to which it reflects interactions within the cell. These issues are important in BAG-1 interactions particularly in terms of stoichiometry to HSPs and in terms of cellular compartment localisation. The first stage of the maturation process of the NHR involves complex formation at the hormone binding domain by the chaperones HSP70 and HSP40. This allows subsequent binding by an HSP90 dimer via its co-chaperone adaptor protein HSP70/HSP90 organising protein (HOP). As with many other chaperone processes, NHR-chaperone complex interactions are ATP

dependant processes. The next stage of receptor maturation involves binding of the HSP90 co-chaperones p23 and one of the immunophilins and the release of HOP, HSP40 and HSP70 resulting in a conformation in which the aporeceptor can be bound by ligand. This HSP90 bound state is thought to be required to allow stabilisation of the receptor conformation. Interruption of this complex, for example by HSP90 inhibition with geldanamycin leads to increased sensitivity to proteolytic degradation of the receptor. Ligand binding and release of p23, HSP90 and immunophilins results in an activated receptor with a stable more compact conformation that is capable of binding DNA. The ligand bound receptor complex enters the nucleus at this stage following rebinding by HSP70. When looking at glucocorticoid or progesterone receptor function in-vitro there are five obligate complex members in this pathway, namely HSP40, HSP70, HSP90, p23 and HOP. Further non-obligate partners in NHR functional chaperone complexes include HSP interacting protein (HIP), the immunophilins FKBP52 and FKBP51, cyclosporine-A-binding immunophilin cyclophilin 40 (Cyp40), protein phosphatase PP5 and BAG-1.<sup>72,73</sup>

BAG-1M and BAG-1L (but not BAG-1S) inhibit functional activity of the GR.<sup>33</sup> Data for BAG-1 interaction with the mechanism of GR processing by chaperones suggests multiple potential actions. Firstly Kanelakis et al showed in reticulocyte lysate systems that at low 'physiological' ratios to HSP70/HSC70 that BAG-1 induced HOP release from HSP90 but did not alter GR:HSP90 complex assembly. However at higher ratios approaching stoichiometry to HSP70/HSC70, inhibition of GR folding to a steroid binding form with reduced assembly of the GR:HSP70 complex was seen.<sup>74</sup> However two papers by Andrew Cato's group have shown by fluorescence microscopy that BAG-1 co-localises with the GR:HSP70 from the cytoplasm to the nucleus and inhibits GR DNA binding. The inhibition and transfer to the nucleus appears to require the carboxy terminal BAG domain important for HSP interaction but also an intact hinge region of the GR.<sup>33,75</sup> The multiple effects shown for BAG-1 in interaction with the GR and the lack of data regarding its

involvement with chaperone complex modulation of other NHRs hampers our understanding of the variation seen in BAG-1/NHR interaction for other receptors.

BAG-1 isoforms have been shown to interact with a range of NHRs (but not all) and thus modulate their functions, and specific examples are considered in the following section. However contradictions within the literature remain to be explained by a consistent and cohesive model for BAG-1/NHR interaction. For example BAG-1 will inhibit the glucocorticoid receptor but not the structurally similar mineralocorticoid receptor.<sup>33</sup> The oestrogen and androgen receptors are potentiated by BAG-1L but not M or S<sup>4,76</sup>, whereas retinoic acid receptors are inhibited by BAG-1S (L and M isoforms not known) but glucocorticoid receptors are inhibited by BAG-1L and M but not S.<sup>33</sup>

Table 1-3 summarises the data regarding the interaction of BAG-1 with nuclear hormone receptors based on reporter construct assays using response elements to the respective NHRs. The following section deals with some specific examples.

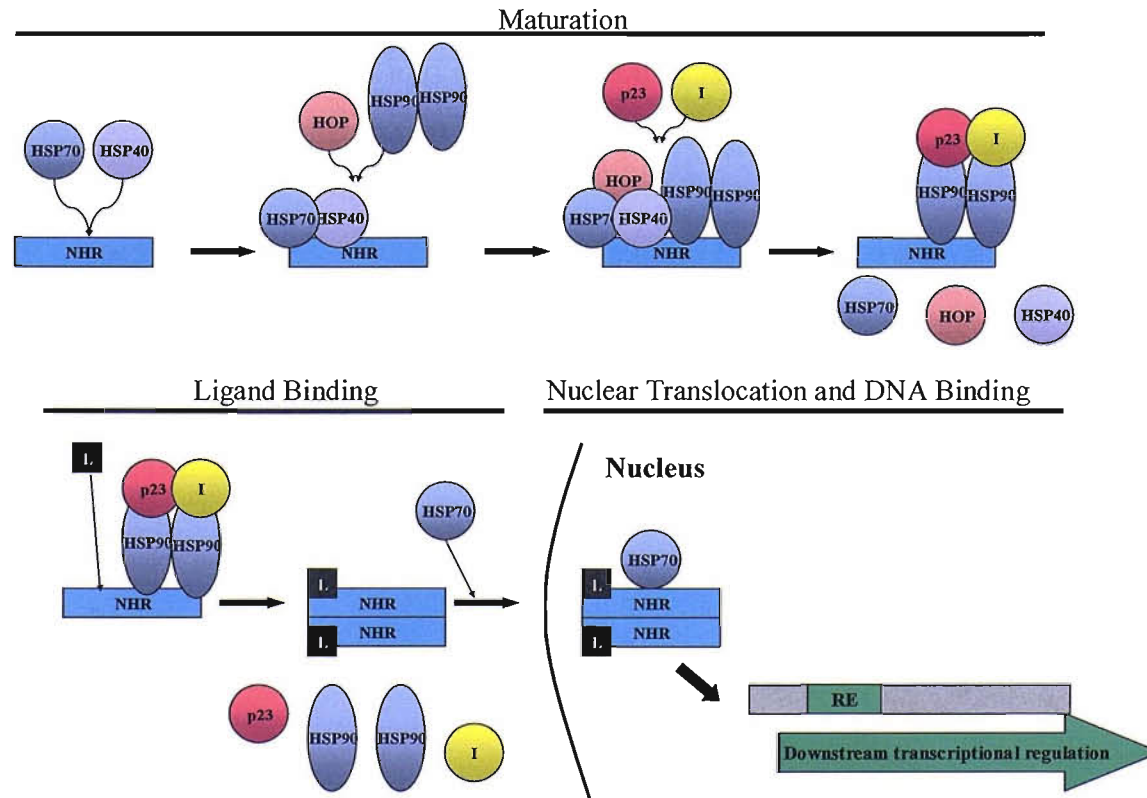


**Figure 1-4 Generalised mechanism for chaperone function in NHR maturation, activation and downstream transcriptional modulation of target genes**

See text for details and references. (I – immunophilin, L – hormone ligand, RE – DNA response element to NHR)

Receptor	BAG-1 Effect	Active Isoforms	Active BAG-1 Mutants	Inactive BAG-1 Mutants	C-Terminal Mutants	Reference
AR	Activated	BAG-1L (Not S or M)	NLS-BAG-1L NLS-BAG-1M BAG-1L $\Delta$ 1-16 NLS-BAG-1L $\Delta$ 1-16 NLS-BAG-1L $\Delta$ 1-50	NLS-BAG-1S NLS-p29-BAG-1 BAG-1L $\Delta$ 1-50 BAG-1L $\Delta$ C	Inactive (trans-dominant)	52,76,77
ER $\alpha/\beta$	Activated	BAG-1L (Not S or M)		NLS-BAG-1S	Unknown	4
GR	Inhibited	BAG-1L BAG-1M (Not S)	BAG-1M $\Delta$ 11-67 BAG-1M $\Delta$ 1-40 BAG-1M -T5 BAG-1M +A5 BAG-1M +2A5	BAG-1M $\Delta$ 1-10 BAG-1M $\Delta$ 1-70 BAG-1M $\Delta$ C47 BAG-1M K(2-4)A	Inactive	33,75,78
RAR	Inhibited	BAG-1S (L and M unknown)			Unknown	79
TR	Inhibited	BAG-1S (L and M unknown)			Unknown	79
RXR	No Effect	No effect			N/A	79
MR	No Effect	No effect			N/A	79
VDR	Activated/inhibited	BAG-1L (Not S or M)	BAG-1L $\Delta$ C47 (Dominant inhibitor)		Inactive (Trans-dominant?)	80,81

**Table 1-3 The interaction of BAG-1 isoforms and mutants with NHRs based on reporter construct assays**

NLS – nuclear localisation sequence,  $\Delta$  - deletion of the indicated BAG-1 isoform amino-terminal amino acids



### **1.3.2 Specific Examples of BAG-1 NHR Interaction and Relevance to Malignancy**

#### **1.3.2.1 BAG-1 Enhances Oestrogen Receptor (ER $\alpha/\beta$ ) Activity in Breast Cancer Cell Lines**

Recent evidence has indicated a clear interaction between ER $\alpha$  and ER $\beta$  mediated downstream transcriptional activation and BAG-1 which may go some way to explaining a mechanism for the role of BAG-1 as a molecular marker for disease behaviour. BAG-1 has been shown to bind the ER in a HSP dependant manner.<sup>44</sup> Subsequently, in MCF7 human breast cancer cells transfected with ER response elements linked to a luciferase reporter construct, transcription stimulated by 17 $\beta$ -oestradiol was enhanced by co-transfection with BAG-1L in a specific and dose dependant manner. This effect did not occur with transfection of the shorter isoforms BAG-1M or S. Co-immunoprecipitation experiments confirmed interaction between BAG-1L (but not M or S), with both ER $\alpha$  and ER $\beta$  as well as the chaperone HSC70. Furthermore, nuclear localisation of the BAG-1L isoform in itself does not seem to explain the lack of enhancement seen with the other isoforms, as a BAG-1S expression construct linked to an NLS did not allow for enhancement of ER $\alpha$  or ER $\beta$  dependant transcription despite the mutant protein being localised to the nucleus. This might be explained by nucleolar localisation characteristics found with BAG-1L but not mimicked by the NLS tagged BAG-1S in this experiment, or alternatively by other actions of the amino terminal domains present only in the larger BAG-1L isoform.<sup>4</sup>

#### **1.3.2.2 BAG-1 Enhances Androgen Receptor (AR) Function and Inhibits Prostate Cancer Hormonal Therapy Agents**

Similar results to those seen for the ER $\alpha/\beta$  are seen with the androgen receptor. BAG-1L has been shown in human prostate and monkey kidney cancer cell lines, to

enhance AR mediated transcription in response to hormone. Again the shorter BAG-1M and S isoforms did not have this activity.<sup>76</sup> Also in this study, transfection of BAG-1L was shown to reduce inhibition of AR mediated transcription by cyproterone acetate, an anti androgen used in prostate cancer therapy. Furthermore, a C-terminal mutated form of BAG-1L failed to interact with the AR in co-immunoprecipitation experiments whereas the full BAG-1L isoform did, and instead acted as a trans-dominant inhibitor of BAG-1L. Thus the C-terminal of BAG-1L seems to be required for interaction and activity in this system, potentially via HSP70/HSC70 interaction. (This differs from the effect seen with the thyroid and retinoic acid receptor.<sup>79</sup>) Therefore levels of BAG-1 activity might be relevant in prostate cancer in modulating sensitivity both to endogenous hormonal ligand and for hormonal intervention agents which are a mainstay of current therapy. Over expression of BAG-1 might conceivably provide a mechanism to explain development of hormone insensitive disease which can develop despite the AR still being expressed.

### **1.3.2.3 BAG-1 Effect On Vitamin D Receptor (VDR) May Depend On Cell Or Tumour Type**

The published data regarding the interaction of BAG-1 with the VDR are conflicting. On the one hand Guzey et al<sup>80</sup> have shown BAG-1L, but not the shorter BAG-1M or S isoforms, to enhance VDR mediated transactivation in human embryonal kidney 293T and COS-7 monkey kidney cell lines. A C-terminal deletion mutant of BAG-1L acted as a dominant inhibitor of BAG-1L in this system, again suggesting a dependence on HSP interaction in a similar manner to the AR. In BAG-1L over expressing PC3 human prostate cancer cells, ligand induced expression of the VDR cell cycle regulator target gene p21<sup>(WAF1/Cip1)</sup> was enhanced, with suppression of DNA synthesis. Also in PC3 cells, BAG-1L over expression increased the growth suppression induced by VDR stimulation. These results suggest that BAG-1L may be important in enhancing the growth suppressive effect of VDR stimulation which is at odds with the notion that BAG-1 is predominantly anti-apoptotic in its activity. However in a separate study Witcher et al<sup>81</sup> have shown

BAG-1L, but not its shorter isoforms, binds the VDR using a GST binding assay and Far Western blot analysis. They also show that stable transfection of BAG-1L blocked VDR binding to its response element in U87 glioblastoma cells. Finally they show that forced over-expression of BAG-1L in U87 cells inhibited the 1,25(OH) vitamin D<sub>3</sub> growth suppressive effect in cell growth assays.

Thus BAG-1 modulation of VDR control on cell proliferation may vary in different cell, tissue or tumour types (or experimental systems). It is possible that these differences are mediated through interaction of chaperone molecules<sup>81</sup> such as HSPs or perhaps through competitive interactions with other molecules such as RAF1. It is unclear to what degree BAG-1 has such variation in effect in-vivo depending on tissue or tumour type. Better understanding might allow explanation of the apparent conflict in published data regarding the role of BAG-1 in breast cancer.

#### **1.3.2.4 BAG-1 Inhibition Of The Thyroid (TR), Retinoic acid (RAR) and Retinoid X Receptors (RXR) Depends On Dimerisation Partner**

Liu et al <sup>79</sup> have looked at these three receptors together, and shown that BAG-1S in in-vitro gel retardation assays will block binding of RAR/RXR or TR/RXR heterodimers but not RXR/RXR homodimers to their respective response elements. These interactions were maintained with a C-terminal BAG-1S deletion mutant implying that this interaction is independent of the HSP interacting BAG domain (in distinction to the effect seen with the AR and VDR). Using reporter assays they found that BAG-1S will inhibit response to ATRA following RAR transfection but does not inhibit RXR homodimers in the same system. In growth inhibition and apoptosis assays, stably transfected BAG1-S inhibited the effect of ATRA in MCF7 and ZR-75-1 breast cancer cell lines. Therefore BAG-1 expression patterns and activity might be relevant to the role of retinoids as a therapeutic modality in cancer, with increased BAG-1 expression being detrimental. This possibility warrants further investigation. Finally this study shows BAG-1S inhibition of the TR.

### 1.3.3 Peroxisome Proliferator Activated Receptor $\gamma$ (PPAR $\gamma$ )

One of the focus points for this thesis is the potential relationship between BAG-1 and PPAR $\gamma$ . The reasons for focussing on this possible interaction are two fold. Firstly the PPAR $\gamma$  receptor has represented a research interest for potential modulation in malignancy as a means to induce differentiation and cell death. Evidence discussed in the following sections indicates it is over-expressed in breast cancer and that its synthetic ligands might be active therapeutically although data are inconclusive. BAG-1 is known to be over-expressed in breast cancer also, and to potentiate the ER in this disease. Separately, in prostate cancer cells, BAG-1 has been shown to limit the efficacy of cyproterone acetate. This model for blockade by BAG-1 of therapeutic benefit through the AR in prostate cancer might also apply to the putative role for PPAR $\gamma$  ligands in breast cancer. This made it important to understand whether BAG-1 has an interaction with PPAR $\gamma$  in breast cancer cells. Secondly, BAG-1 interacts with most other NHRs with the exception of the MR and RXR. A potential interaction between BAG-1 and PPAR $\gamma$ , which would be predicted to be opposing based on their known functions, would provide a useful model for investigation of BAG-1 NHR interactions generally.

PPAR $\gamma$  belongs to the PPAR family of NHRs of which there are three isotypes -  $\alpha$ ,  $\beta$ , and  $\gamma$ . PPARs are involved in lipid metabolism and their ligands are usually fatty acids and eicosanoids. PPAR isotypes each function according to the general mechanistic model for NHRs. Following ligand binding, heterodimerisation occurs with the retinoid X receptor. This leads to downstream transcriptional modulation via a specific response element (PPRE). Binding of either receptor's ligand is adequate for activation of the heterodimer complex but dual ligand binding has greater potency.

The PPAR $\gamma$  gene comprises nine exons on chromosome 3p25. In the human, three isoforms are described, PPAR $\gamma$ 1, 2 and 3 generated by differential splicing and

alternative promoters. PPARs exhibit a modular structure similar to other NHRs (Figure 1-5). Firstly in the N-terminus A/B domain lays a ligand independent activation domain, AF1. Next a DNA binding domain consists of two zinc fingers that bind to specific response elements (PPRE) and thus allow transactivation of PPAR responsive genes followed by a hinge region important for cofactor docking. In the C terminal a ligand binding domain (LBD) exists consisting of 13  $\alpha$ -helices and a single  $\beta$ -sheet. The subsequent large size of the ligand binding pocket has been proposed to allow for a wide range of potential endogenous ligands to activate the receptor. Also within the C-terminus region, lies a ligand dependant activation domain, AF2, which modulates a co-activator binding pocket and a dimerisation interface region.<sup>82-85</sup>

PPAR $\gamma$  was initially discovered as an orphan receptor but was subsequently found to be the receptor for a comparatively new class of drugs used widely in type II diabetes, the thiazolidinediones (TZD). A range of TZDs exist with variable specificity and potency profiles. Endogenous ligands include arachidonic acid and linoleic acid derivatives including eicosanoids such as 15-deoxy- $\Delta^{12,14}$ -prostaglandin J<sub>2</sub> (PGJ<sub>2</sub>) and polyunsaturated fatty acids such as 15-HETE and 13-HODE. PGJ<sub>2</sub> is commonly used for in-vitro investigation, although its exact role and degree of PPAR $\gamma$  specificity in-vivo remains uncertain which should be borne in mind when interpreting apparent PPAR $\gamma$  effects from its use in the literature. In addition PPAR $\gamma$  antagonists such as bisphenol A diglycidyl ether (BADGE) and GW9662, and constitutively active and dominant negative PPAR $\gamma$  constructs have been developed to allow investigation of its function.<sup>6</sup> PPAR $\gamma$  expression is found in adipose tissue, large bowel, and haemopoietic tissue, and at lesser levels in kidney, liver and small intestine. It functions to regulate the storage of fatty acids in adipose tissue and to stimulate maturation and differentiation of adipocytes. Adipose tissue target genes for PPAR $\gamma$  are directly linked to lipogenesis including lipoprotein lipase, adipocyte fatty acid binding protein, acyl-CoA synthase and fatty acid transport protein.<sup>84,86</sup> PPAR $\gamma$  null mice die as embryos but if rescued to term are found to have no detectable white adipose tissue and a fatty liver.<sup>87</sup>

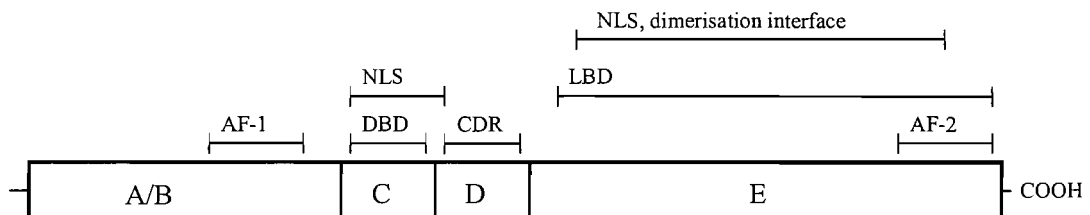


**Figure 1-5 Structural organisation of the PPAR $\gamma$  receptor.**

The A/B amino region contains a constitutively active ligand-independent transactivation domain, (AF-1). The C region contains a DNA response element binding domain, (DBD) and NLS. The D region is involved in cofactor docking allowing modulation of receptor activity, (CDR). Finally the carboxy terminal E region contains a dimerisation interface, an NLS, a ligand binding domain (LBD) and a ligand-dependant transactivation domain, AF-2.

#### 1.3.4 In-Vitro and Animal Data To Support The Role Of PPAR $\gamma$ In Cancer

Evidence points to PPAR $\gamma$  having a possible role in malignancy, and that it is a potential target for therapeutic intervention. TZD exposure has been shown to cause differentiation, growth inhibition and apoptosis in MCF7 and MDA-MB-231 breast cancer cell lines. These effects were found to be synergistic when combined with ATRA exposure (an RAR specific ligand) and were shown to be associated with suppression of Bcl2 protein expression. Forced expression of Bcl2 was found to counteract apoptosis in response to combined PPAR $\gamma$  and RAR stimulation.<sup>88,89</sup>

Cross talk occurs between PPAR $\gamma$  and the ER. Firstly PPAR $\gamma$  can interact with oestrogen response elements (ERE) and cause transactivation of certain ER transcriptional targets but inhibit ER activation of others.<sup>90</sup> Conversely ER $\alpha$  and  $\beta$  can block PPAR $\gamma$  mediated transcriptional activity in breast cancer cell lines.<sup>91</sup> Finally PPAR $\gamma$  is able to block aromatase activation and thus inhibit local oestrogen production in cultured breast adipose stromal cells.<sup>92</sup> Thus PPAR $\gamma$  and the ER interact bidirectionally in ways that might impact on current hormonal therapy for breast cancer, and possibly for the potential as PPAR $\gamma$  as a therapeutic target. It is unknown whether PPAR $\gamma$  activation can modulate the BAG-1/ER interaction.

Another important therapeutic target in breast cancer, the HER2 receptor (ErbB2), has been shown to be inhibited by PPAR $\gamma$  stimulation. In MCF7 cells, the PPAR $\gamma$  ligand PGJ<sub>2</sub> was shown to inhibit neuregulin induced tyrosine phosphorylation of ErbB2 and ErbB3. This blocked both PI3 kinase and ERK signalling and inhibited downstream effects including proliferation, cell survival and anchorage independent growth otherwise mediated by the ErbB proteins.<sup>93</sup>

At the level of animal experiments, it has been shown that PPAR $\gamma$  ligands will inhibit MCF7 tumour growth in triple immuno deficient mice and decrease the

tumour incidence, number and weight in a nitrosomethylurea breast carcinogen model in rats.<sup>89,94</sup>

Finally in human thyroid follicular carcinoma a t(2;3)(q13;p25) translocation has been detected that forms a fusion protein with PAX8 (a thyroid specific transcription factor) and PPAR $\gamma$ 1. The fusion oncogene is found in up to 50% of thyroid follicular carcinomas and promotes accelerated cell growth, reduced apoptosis and contact/anchorage independent growth in thyroid cell lines probably in part by competitive inhibition of wild type PPAR $\gamma$ .<sup>95,96</sup>

### **1.3.5 Human and Clinical Data Regarding PPAR $\gamma$ and Cancer**

Two studies have looked at mRNA expression in breast cancer resection specimens. In one study, COX2 and PPAR $\gamma$  mRNA expression were found to be increased and decreased respectively in cancer samples compared to uninvolved breast tissue or compared to tissue from healthy patients. In addition, PGJ2 levels were decreased in malignant compared to normal tissues.<sup>97</sup> In the other study, decreasing levels of PPAR $\gamma$  were found to correlate with increasing disease stage, risk of local recurrence and disease specific mortality (but did not correlate with tumour grade or nodal status).<sup>98</sup>

One interesting aspect of the early stage development of PPAR $\gamma$  agonists as potential anti-neoplastic therapies is that they are already widely used in routine clinical practice for diabetes. As such a large, unplanned, chemo-prevention trial is in effect underway for which we have extremely limited data on outcome. One retrospective study has been presented in abstract form to address this issue looking at 127658 male diabetics of whom 25% were found to taking a TZD. In this group, the use of these drugs was associated with a decreased risk of lung cancer by 15%, an increased risk of prostate cancer by 8% but no change in risk of colorectal cancer.<sup>99</sup> Further data is required to elucidate what effect this form of treatment might be having, if any, as a chemo-modulator of cancer incidence. Specifically with regard



to this thesis, there is no data on routine TZD use in diabetics and subsequent effect on breast cancer incidence.

Early phase clinical investigation of PPAR $\gamma$  agonists in different cancers has produced conflicting and mixed results at best.<sup>6</sup> In breast cancer, a phase II study using troglitazone that was terminated prematurely due to hepatic toxicity concerns relating to this drug, detected no objective tumour responses in twenty two patients with advanced refractory disease.<sup>100</sup> In prostate cancer, limited phase II data exists to suggest that PPAR $\gamma$  stimulation with troglitazone can induce stabilization or reduction in prostate specific antigen levels as a surrogate marker for disease progression.<sup>101,102</sup> Liposarcoma has generated interest as a disease in which PPAR $\gamma$  agonists might be useful because cell lines have been shown to express high mRNA levels of PPAR $\gamma$  in all histologic subtypes compared both to normal tissues and other soft tissue sarcomas. These cell lines have been shown to undergo terminal differentiation in response to TZDs.<sup>103</sup> Subsequently a study by the same group, in which biopsies of liposarcomas from three patients pre and post therapy with troglitazone showed cellular lipid accumulation, differentiation and reduction in cellular proliferation markers.<sup>104</sup> However in a phase II study using rosiglitazone in 12 liposarcoma patients, no evidence of a differentiating effect or clinical response was seen.<sup>105</sup> Finally in colorectal cancer where PPAR $\gamma$  agonists show activity against xenograft, a phase II study of troglitazone resulted in progressive disease for all of 25 chemotherapy refractory patients.<sup>106</sup> In each of these studies toxicity was generally very good aside from concerns regarding hepatic transaminitis.

### **1.3.6 Evidence Regarding Interaction Of BAG-1 With PPAR $\gamma$**

No published evidence exists to show a direct link between PPAR $\gamma$  with BAG-1 function. However in one study, Clay et al have shown that early de-novo gene expression is required for apoptosis to occur following exposure to PGJ<sub>2</sub>. As part of

this study they performed a cDNA array experiment following RT-PCR in MDA-MB-231 breast cancer cells exposed to  $\text{PGI}_2$ , and showed mRNA expression changes in a range of critical cell cycle and apoptosis genes. Amongst these BAG-1 and the heat shock proteins HSP70, HSP40 and HSC70 showed increased expression by 2 to 4.6 fold.<sup>107</sup>

As discussed already,  $\text{PPAR}\gamma$  stimulation is known to induce cell cycle arrest and differentiation leading to inhibition of malignant cell proliferation and cell death via apoptosis. Therefore interaction and potential opposition of  $\text{PPAR}\gamma$  action by BAG-1, in a manner analogous to its known interactions with other NHRs, might represent an obstacle to its use as a cell cycle and differentiating therapeutic target in hormone sensitive cancers. The potential interaction between BAG-1 and  $\text{PPAR}\gamma$  in breast cancer is one of the areas addressed in this work with particular emphasis placed on addressing the relevance of BAG-1 activity in the processes of cell cycle progression and differentiation.

## **1.4 Histone Deacetylase Inhibitors**

### **1.4.1 Acetylation Is An Epigenetic Control Mechanism Of Gene Expression**

One of the hallmarks of the malignant cell is that the normal control of differentiation, cell cycle progression and appropriate entry into apoptosis becomes deranged. The existence of this abnormal phenotype occurs from patterns of protein expression which result from a variety of genetic abnormalities. One area of increasing interest in basic and clinical research, relevant to malignant cell growth, are the epigenetic control mechanisms, focusing on the modulation of DNA packaging as a means of gene expression regulation.

Genomic DNA is packaged in the higher order structure of chromatin which comprises histones, non-histone proteins and DNA. These components come together in a tightly packed and organised structure which is dynamic in its nature. Regulation of this structure is a means of gene expression control. The basic repeating unit of such chromosomal organisation is the nucleosome. Nucleosomes occur approximately every 200 DNA base pairs, consisting of 146bp of DNA wrapped left handed twice around an octamer core of paired histones H3, H4, H2A and H2B as successive 'beads on a string'. Nucleosomes are then usually further packed together via the linker histone H1 allowing condensation of this fundamental unit into higher order structures visible as chromosomes at metaphase. Histones are rich in lysine and arginine and the positive charges on these amino acids counteract the negative charge of DNA to allow DNA coiling around it. Histones exist as globular domains with long amino terminal tails making up 25% of their structure which are open to several covalent modifications which change chromatin structure and so alter transcriptional patterns. Post translational covalent modification of histone tails is known to occur by several mechanisms. These include methylation of lysine and arginine residues by histone methyltransferases, phosphorylation of serine and threonine residues by histone kinases, and acetylation of lysine residues by

histone acetyltransferases (HAT) and can occur at specific residues resulting in variation of both expression and silencing of specific gene targets. Further histone modifications include attachment of ubiquitin groups, small ubiquitin like modifiers (SUMOs) and poly-ADP ribose (PAR) units. Different patterns of histone modification have been hypothesised to represent a 'histone code' for determining gene expression patterns for surrounding DNA regions.<sup>12-14,108-110</sup> The complexity of this code remains to be fully elucidated but some aspects are understood. An example to highlight this code are the variable effects of phosphorylation at serine 10 of histone H3, which in addition to possible phosphorylation at serine 28, can lead to chromosome condensation during mitosis. By contrast, the simultaneous phosphorylation of serine 10 and acetylation at lysine 14 respectively instead promotes de-condensation and transcription. Epigenetic modifications of this code are known to be 'read' by interactions with certain protein motifs such as the bromodomain found in proteins such as the HAT enzyme PCAF (p300/CBP associated factor). Thus, histone tails, via modification through such changes as acetylation and phosphorylation, can function as specific 'receptors' depending on modification status to interacting protein modifiers many of which have modifying function including those with HAT activity.<sup>6</sup>

As an example of such epigenetic control through histone modification, it was discovered in the 1960s that histone acetylation results in increased transcriptional activity.<sup>111</sup> Acetylation of histones is controlled by two competing groups of enzymes and is summarised in figure 1-6. Histone deacetylases (HDAC) are an evolutionarily conserved group of enzymes which remove acetyl groups on chromatin and other proteins. Such deacetylation of histones tends to lead to a more tightly bound and transcriptionally silenced state. The HAT enzymes catalyse the opposing reaction leading to histone acetylation and a more open chromatin structure with increase in active transcriptional expression.<sup>12,13,112-114</sup> In general, transcriptional activators can bind and recruit HATs while transcriptional repressors and co-repressors interact with HDACs. Acetylation of conserved lysine residues on histones by HATs causes neutralisation of the positive charge associated with the  $\epsilon$ -

amino groups in the amino domains of core histones. It is thought that this makes nucleosomal DNA more accessible for transcription by masking of the amino terminal domains and destabilizing higher order folding of nucleosomal contacts caused by electrostatic interactions. HDACs restore the positive charge on  $\epsilon$ -amino acetyl moieties and reverse this process.<sup>113-115</sup> This mechanism is conceptually helpful for understanding the action of HATs and HDACs, however it is clear that it represents a simplistic and incomplete explanation for the way in which these enzymes control gene expression. In fact it is known that inhibition of HDAC function leads to both increased and decreased expression of a comparatively narrow band of transcriptional targets. The complexities of the histone code including other modifications such as serine/threonine phosphorylation are likely to underlie this. Furthermore as already discussed, it is also the case that 'histone' acetyltransferases and deacetylases act on other transcription factors, instead or as well as histones. For example, regulation of transcription may also be affected through acetylation of regulatory proteins which bind histones themselves.<sup>110,114</sup> Thus inhibitors of HDACs will target modification by acetylation both of histones but a range of other protein targets.

HDACs are grouped into three classes based on structure and functional characteristics (Table 1-4). Class I enzymes (HDACs 1, 2, 3, 8 and 11) have homology in their catalytic sites to the yeast HDAC Rpd3. They have a ubiquitous distribution and are localised to the nucleus. Class II enzymes (4, 5, 6, 7, 9 and 10) are restricted in their tissue distribution, have the ability to shuttle between the cytoplasm and nucleus and are homologous to the yeast HDAC HdaI. Class I and class II HDACs each have a highly conserved catalytic domain of 390 amino acids but differ in overall size and composition and utilise a charge relay system for which a zinc ion at the base of the catalytic pocket is crucial. The zinc ion is the site of activation of a water molecule to induce hydrolytic cleavage of an acetyl group. HDAC6 and 10 contain two catalytic domains, one of which is specific for tubulin and not histones.<sup>116</sup> They may be considered as a subclass of class II enzymes (class IIb).<sup>12</sup> The formation of multi-protein complexes is critical to HDAC functions. For

example HDACs 4, 5, 7 and 9 bind MEF family transcription factors which interact with specific promoters and thus target deacetylase activity. In the case of the HDAC4:MEF2 interaction, HDAC4 and the HAT enzyme p300 compete for the same binding site for MEF2 and determine whether this transcription factor exerts a repressive or an activating effect on gene transcription respectively in a calcium dependant manner.<sup>108,117</sup> Class III enzymes (sirtuins) are a conserved nicotinamide adenine dinucleotide dependant family of deacetylases with a common 275 amino acid catalytic site and homology to yeast Sir2 (silent information regulator 2). The NAD<sup>+</sup> group acts as an acetyl acceptor following hydrolysis of the nicotinamide moiety.

HATs are grouped into several families based on conserved structural motifs and include the GNAT, MYST, PCAF, SRC and p300/CBP families.<sup>115</sup> They are divided into type A HATs which acetylate chromosomal histones/proteins, whilst type B HATs are cytoplasmic and acetylate free histones prior to chromatin assembly and other proteins. As with HDACs they generally function as components of large multi-protein complexes, commonly including transcription factors that alter specificity for lysine residues often by recognition of adjacent histone modifications such as methylation and phosphorylation. It has been suggested that acetylation cascades may exist leading to complex signal transduction mechanisms similar to phosphorylation cascades. For example, ACTR a member of the SRC family of HATs, undergoes acetylation.<sup>110,118,119</sup>

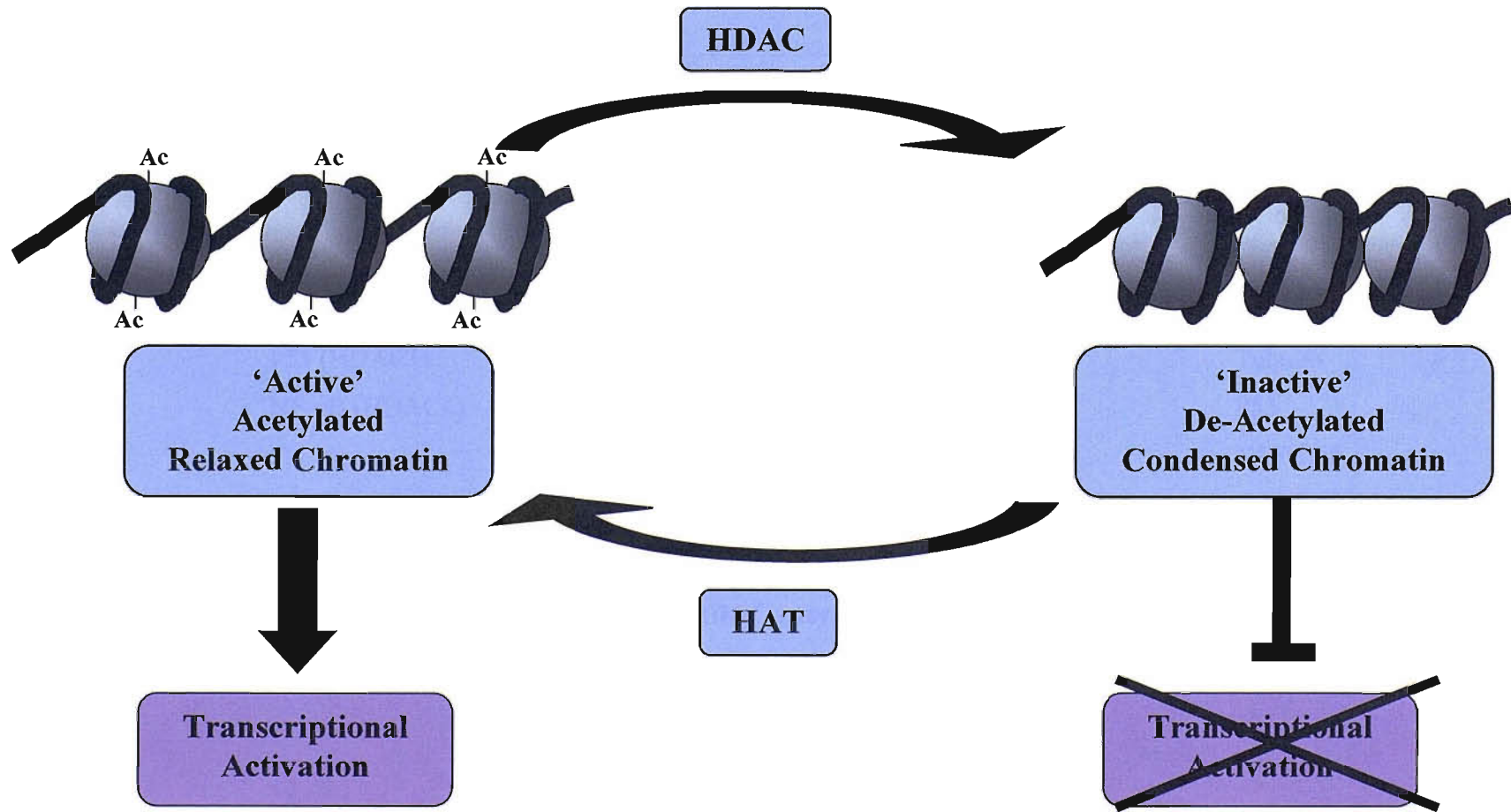


Figure 1-6 Schematic representation of histone acetylation as a model for transcriptional control by epigenetic mechanisms

See text for discussion. HAT – histone acetyl transferase, HDAC – histone deacetylase

	Class I	Class IIa	Class IIb	Class III
Members	HDAC 1, 2, 3, 8, 11	HDAC 4, 5, 7, 9	6, 10	SIRT 1, 2, 3, 4, 5, 6, 7
Distribution	Ubiquitous	Tissue restricted	Tissue restricted	Unknown
Cellular localisation	Nucleus	Nuclear/cytoplasmic shuttling	Nuclear/cytoplasmic shuttling	Nuclear Cytoplasmic Mitochondrial
Targets	Histones P53 (HDAC1) NF-κB (HDAC4)	Histones	Histones Tubulin	Histones Tubulin P53 TAF(I)68
Enzymatic co-factors	Zinc ion	Zinc ion	Zinc ion	NAD <sup>+</sup>

**Table 1-4 Characteristics and classification of the human HDAC enzymes<sup>12,112</sup>**



### **1.4.2 HDAC And HAT Activity Are Aberrant In Malignancy**

There are increasing strands of evidence from different malignancies that one method for abnormal transcriptional regulation is via alteration in HDAC and HAT activity.<sup>114</sup> For example in acute promyelocytic leukaemia, where the associated PML-RAR $\alpha$  and PLZF-RAR $\alpha$  chromosomal translocations produce fusion oncoproteins that act via transcriptional repression in part through recruitment of HDACs, leading to abnormal gene regulation via chromatin modification. Such repression of otherwise active genes leads to a block in differentiation and contributes to tumour progression. In the in-vitro setting, inhibition of HDAC activity potentiates the response to retinoic acid of responsive APL cell lines and restores responsiveness of resistant cell lines.<sup>120,121</sup> In melanoma and other solid tumours, recruitment to methylated cytosine residues of multifactor co-repressor complexes containing DNA methyltransferase and HDACs may lead to silencing of tumour suppressor genes such as p16<sup>INK4a</sup>.<sup>12</sup> Finally in non Hodgkin's lymphoma, the transcriptional repressor LAZ/Bcl6 is over expressed and recruits a co-repressor complex containing SMRT, mSIN3A and HDAC1 resulting in aberrant acetylation patterns.<sup>122</sup>

HAT activity has also been found to be modified in a variety of cancers through translocation, amplification, over-expression or mutation. One example is loss of function mutations in p300, identified in colorectal, breast and other epithelial cancers suggesting it may have a role as a tumour suppressor in certain circumstances.<sup>123</sup>

### **1.4.3 HDACs And HATs Also Target Non-Histone Proteins**

Both the HDAC and HAT group of enzymes are able to modify acetylation of an ever-increasing range of target enzymes involved both in transcriptional regulation

as well as a range of other processes including cell cycle regulation, apoptosis, nuclear transport, cytoskeletal structure and signal transduction.<sup>12,13,124</sup> Transcription factors dominate the list of proteins regulated by acetylation with over 40 documented. Acetylation modifies their DNA binding affinity, co-regulator association, nuclear localisation, phosphorylation ubiquitylation and stability. Proteins known to be modified by acetylation are summarised in table 1-5 and three examples are expanded upon below.

During G1 phase of the cell cycle E2F in complex with Rb, causes repression of transcription in association with HDAC activity. Phosphorylation of Rb subsequently releases free E2F which stimulates transcription of S-phase genes. Free E2F has been shown to undergo acetylation via the P/CAF and p300/CBP HATs at conserved lysine residues close to the E2F DNA binding domains leading to increased DNA binding, activity and protein stability. Thus acetylation status is a control mechanism for E2F activity and cell cycle progression<sup>125</sup>

The Rb protein is also acetylated by p300/CBP. Acetylation of Rb hinders its phosphorylation by the cyclin dependant kinases and acetylated Rb binds more strongly to the MDM2 oncoprotein. Thus Rb acetylation may represent a level in post-translational control of its activity, in addition to mechanisms such as phosphorylation, and so effect cell cycle progression.<sup>126</sup>

Finally p53 has also been shown to undergo acetylation by both p300 and PCAF at conserved C-terminal sites leading to the augmentation of p53 DNA binding and ubiquitylation as well as the generation of docking sites for bromodomain containing co-activators.<sup>124,127</sup>

Function	Acetylation Targets
Transcription factor	p73, TCF, GATA-1, RelA, E2F, UBF, EKLF, NF-Y, STAT6, CREB, c-Jun, C/EBP $\beta$ , E2A, HMGI (Y), UBF, NF- $\kappa$ B p65/Rel A, NF- $\kappa$ B p50, YY1, Bcl6, Cart-1, HIV-1 Tat, Brm, MyoD, TAL1/SCL, E2A, HIF-1 $\alpha$ , TFIIE, TFIIF, PC4, TFIIB, TAFI68
Tumour suppressor	p53
Cell cycle	Rb
Cell adhesion	$\beta$ catenin
Nuclear hormone receptor	AR, ER $\alpha$
Nuclear import factor	Importin $\alpha$ , Reh1
Cytoskeleton protein	$\alpha$ -Tubulin
Chaperone protein	HSP90
Signalling regulation	Smad7
Apoptosis regulator	Ku70
Non histone chromatin protein	HMGB1/HMG1, HMGB2/HMG2, HMGN1/HMG14, HMGN2/HMG17
DNA metabolism	Flap endonuclease-1, Thymine DNA glycosylase, Werner DNA helicase
DNA replication factor	PCNA, MCM3
Chromatid cohesion protein	San, Cohesion subunits
Viral protein	Adenoviral E1A, Large T antigen, HIV Tat, s-HDAg
Bacterial protein	Alba, CheY, Acetyl CoA synthetase
Histone acetyl transferase	PCAF, p300, CBP

**Table 1-5 Non-histone proteins regulated by acetylation status<sup>12,13,124</sup>**

#### 1.4.4 HDACs Can Be Inhibited By Compounds Targeted To Their Active Sites

In recent years increasing pre-clinical and early phase clinical trial data have appeared regarding compounds capable of inhibiting HDAC activity. The understanding that epigenetic control mechanisms such as histone (and non-histone protein) acetylation may be an attractive mechanism for modification of malignant cell progression makes this an interesting area for cancer therapy and potentially in other diseases. The majority of work to date has focused on compounds inhibitory to class I and II HDACs. A variety of classes of such inhibitors exist based on chemical structure with variability seen in HDAC class selectivity and potency (Table 1-6 and Figure 1-7). The characteristic feature of these compounds is an ability to induce acetylation at specific lysine residues on histones as well as an ever increasing list of other protein targets.<sup>12,13,128-131</sup>

One of the first compounds shown to have HDAC inhibitory activity, is the naturally occurring anti-fungal antibiotic trichostatin A (TSA). TSA is a hydroxamic acid compound which has inhibitory effects on HDACs in the low nanomolar range. It has been shown to induce hyper-acetylation of histone lysine residues and to inhibit proliferation in a range of breast cancer cell lines. Using an *N*-methyl-*N*-nitrosourea carcinogen-induced rat mammary carcinoma model, TSA has been shown to produce a pronounced anti-tumour activity, with histological characteristics suggesting this was at least in part attributable to a differentiating effect of the drug.<sup>131</sup> TSA can be considered a reference compound for validating both the HDAC enzymes and other HDAC inhibitory compounds but has not progressed in clinical trials due to toxicity. Its mechanism of HDAC inhibition has been determined by Finnin et al using the mammalian HDAC homologue HDLP.<sup>132</sup> This paper showed the elucidation of the crystal structure for HDLP with predictions for the interaction with TSA and a second hydroxamate inhibitor SAHA (suberoylanilide hydroxamic acid, vorinostat). The active site of the enzyme consists of a deep narrow tube like

pocket lined with hydrophobic aromatic residues. The zinc ion critical to enzymatic activity of class I and II HDACs is situated near the bottom and beyond the narrowest part of this pocket in a polar region at the active site for the enzyme. TSA binds the active site by inserting its aliphatic chain 'spacer' through the hydrophobic section of the pocket to allow the hydroxamic acid 'functional group' at one end to bind the zinc ion. The aromatic dimethylamino-phenyl group at the other end interacts with the pocket entrance acting as a 'cap' to it. This basic premise for HDAC inhibitor interaction with the class I and II HDAC enzymatic sites is shown as a diagrammatic model in figure 1-8. The residues that are relevant to interactions with lysine side chains (and HDAC inhibitors) are conserved across HDAC family members. Other HDAC inhibitors are thought to act in a similar manner to this model with a functional group, a 5-6 carbon aliphatic chain spacer which mimics a lysine side chain and a cap component. Variability in potency and possibly class selectivity of HDAC inhibitors, are felt to be explained by structural variability of these inhibitor compounds, particularly with respect to the cap group.<sup>112,132,133</sup> Other hydroxamic acid based HDAC inhibitors include PXD101, LBH589 and LAQ824 which are each in early phase clinical trials.<sup>130,134-136</sup>

Less potent than the hydroxamates with millimolar inhibitory levels, are the aliphatic acids valproic acid and phenylbutyrate. This is reflected in simpler structure compared to the hydroxamates which allows for interaction with the zinc ion but not with the rest of the catalytic pocket in the way proposed for other more complex inhibitor classes. Valproic acid, although in clinical trials for cancer is also a widely used anti-epileptic therapy and effects a range of cellular processes.<sup>12,112,137</sup> Whether this broader range of interactions limits its usefulness as a specific HDAC inhibitor remains to be determined.

The cyclic tetrapeptides include depsipeptide (also known as FK228 or FR901228), apicidin and cyclic hydroxamic acid containing peptides (CHAP) are the most structurally complex group of HDAC inhibitors. Like the hydroxamates they have inhibitory potency in the nanomolar range. In the case of FK228 reduction of an

internal disulphide bond is required to produce the cap, spacer and functional group structure proposed for other potent HDAC inhibitors (discussed further in section 1.4.8).<sup>133,138-142</sup>

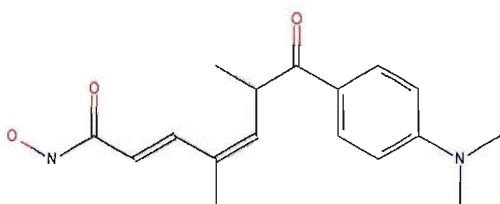
The benzamides include MS-275 and CI-994 and are less potent than the hydroxamates and cyclic tetrapeptides. Finally the electrophilic ketones include the trifluoromethyl ketone and  $\alpha$ -ketoamides and like the benzamides have micro molar inhibitory levels.<sup>112,135,143</sup>

Aside from class I/II HDAC inhibitors, both inhibitors and activators of sirtuins and HATs have been described.<sup>144-146</sup>

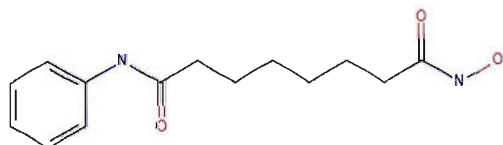
Class	HDAC Inhibitory Potency	Examples	Clinical Trial Status
Hydroxamate	Nanomolar	Trichostatin A (TSA)	-
		Suberoylanilide hydroxamic acid (SAHA, Vorinostat)	Phase III
		CBHA	-
		PXD101	-
		Pyroxamide	Phase II
		LAQ-824	Phase I
		Sulphonamide hydroxamic acid	Phase I
		Oxamflatin	-
		Scriptaid	-
		LBH589	-
Aliphatic acid	Millimolar	Valproic acid	Phase I/II
		Phenyl butyrate	-
		Butyrate	Phase I/II
Benzamide	Micro molar	MS-275	Phase II
		CI-994	Phase II
Electrophilic ketone	Micro molar	Triflouromethyl ketones	-
		$\alpha$ -ketoamides	-
Cyclic tetrapeptide	Nanomolar	Depsipeptide	Phase II
		Apicidin	-
		Cyclic hydroxamic acid containing peptides (CHAP)	-

**Table 1-6 HDAC inhibitor classes, examples and clinical trial status**

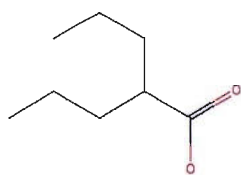
Clinical trial status relates to published (discussed in section 1.4.7) and registered ongoing trials (accessed at [www.clinicaltrials.gov](http://www.clinicaltrials.gov))



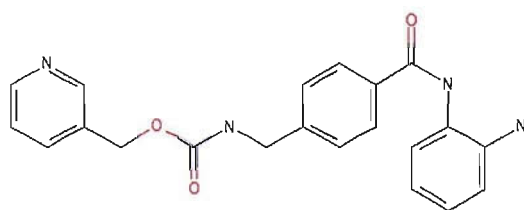
TSA (Hydroxamate)



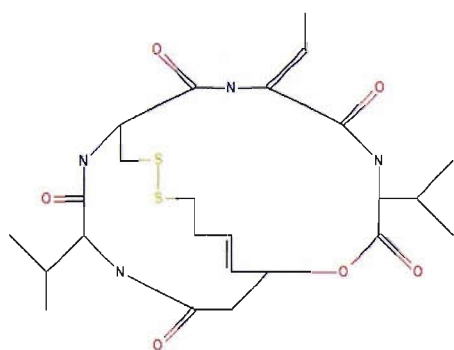
SAHA (Hydroxamate)



Valproic acid (Aliphatic acid)



MS-275 (Benzamide)

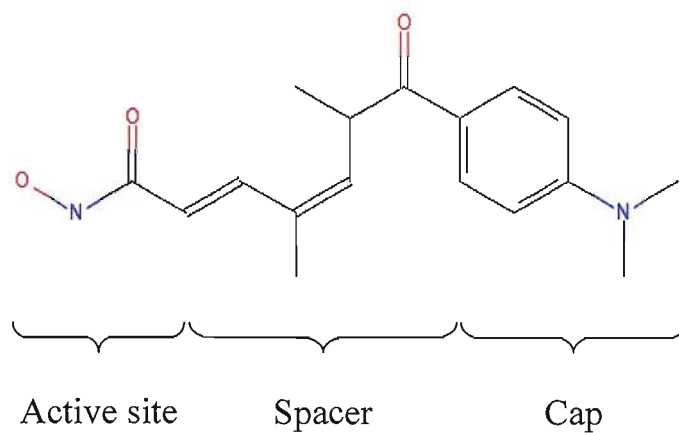


FK228 (Cyclic tetrapeptide)

**Figure 1-7 Selected HDAC inhibitor structures**



A



B

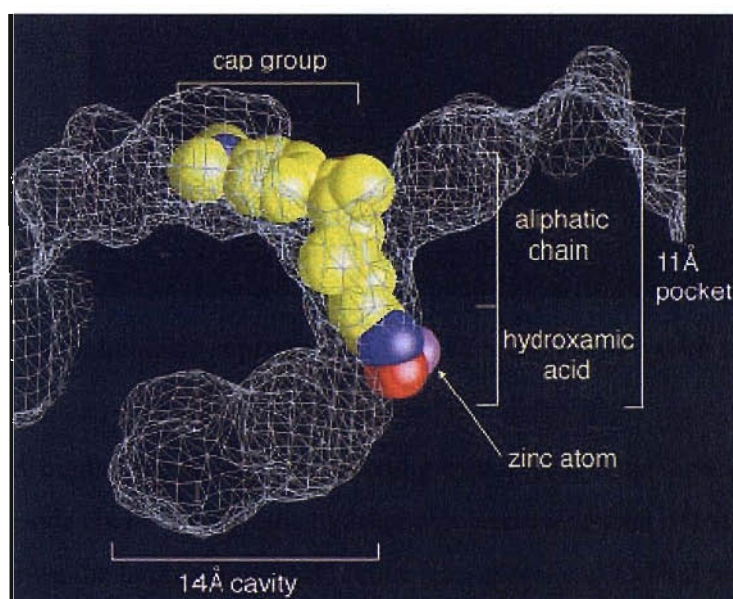


**Figure 1-8 Schematic representation of TSA interaction with the HDAC active site**

(A) TSA binds the active site by inserting its aliphatic chain ‘spacer’, which mimics a lysine side chain, through the hydrophobic narrow section of the enzyme pocket. This allows the hydroxamic acid ‘active site’ at one end to bind the zinc atom at the enzyme active site. The aromatic dimethylamino–phenyl group at the other end interacts with the pocket entrance acting as a ‘cap’ to it. (B) Space filling representation of TSA in the active-site pocket of the HDAC homologue HDLP.<sup>132</sup>

#### 1.4.5 Biological Effects Of HDAC inhibitors

A large volume of data exists to show that HDAC inhibitors are able to inhibit cancer cell proliferation in the in-vitro setting.<sup>120,128-131,134,139,140,147,148</sup> Cell types that are susceptible to growth inhibition are extensive and include carcinoma, sarcoma and haematological malignancies including multiple breast cancer cell lines. Sensitivity appears not to correlate with total HDAC activity of a particular cell line or with the extent of HDAC inhibition induced in any particular cell line.<sup>130,131</sup> In one study using the hydroxamate PXD101, sensitivity did not correlate with sensitivity to DNA damaging agents such as cisplatin, and there was low cross resistance in doxorubicin and cisplatin resistant cell lines.<sup>130</sup> These compounds might potentially be of use therefore in combination with other therapeutic modalities.

Gene expression profiling of HDAC inhibition has been assessed in a number of studies. One clear message from these studies, is that alteration in genetic expression is restricted to a limited number of core genes in response to these drugs in the range of 1-2%. These genes were mostly involved in cell cycle control, apoptosis and DNA synthesis. This indicates that relaxation of chromosomal structure by histone acetylation does not result in a blanket alteration in gene expression that a simple increase in accessibility of transcriptional machinery might imply. In addition, as many genes are down regulated as up regulated, suggesting that increased expression of negative regulatory transcription factors may be important to the ultimate proteomic alteration induced by these compounds. Although the general profile of expression is similar between different HDAC inhibitors, cluster analysis has been able to show distinction between MS-275 (a benzamide) and TSA and SAHA (hydroxamates).<sup>135,149</sup> HDAC structural classes are likely to have different biological effects although these differences are in the main not well defined. For example, HDAC5 or 9 knockout mice are known to develop cardiac hypertrophy in response to specific stress responses.<sup>150</sup> This raises the question as to whether

HDAC class selectivity for HDAC inhibitors would confer benefits in terms of efficacy or toxicity of these compounds as drugs in the clinical setting. As discussed in later sections, the bicyclic tetrapeptide FK228 has been shown to exhibit HDAC class I selectivity and is one of the more extensively developed compounds.

Multiple studies have confirmed that HDAC inhibitors induce cell cycle arrest and apoptosis.<sup>120,128,130,134,135,151</sup> Apoptosis can be seen to occur from 24 hours and exhibits both dose and time dependence. Apoptosis is at least partially inhibited by caspase inhibition with one study finding caspase 9 to be critical, and Bcl-2 antagonistic, to apoptosis. The fact that caspase inhibition does not completely abrogate apoptosis suggests both caspase dependant and independent mechanisms may be involved.<sup>134,151,152</sup> Indeed it has been shown that HDAC inhibitors can induce caspase independent autophagic cell death in addition to apoptosis which might be important in targeting cancers with apoptotic defects.<sup>153</sup> Cell cycle arrest is also a feature of HDAC inhibitor action. Most studies show G2M arrest, as assessed by FACS analysis, to occur in a dose and time dependant manner in response to these drugs. However some studies also indicate that G1 arrest can occur.<sup>134,136,147,148,154-156</sup> In three studies involving SAHA in various breast cancer cell lines it was possible to show that G1 arrest occurred at low doses (<1-2.5µM in MCF7 cells) but that both G1 and a dose dependant G2M arrest occurred at higher doses with G2M arrest appearing as a dominant feature.<sup>136,147,148</sup> HDAC inhibition is able to alter expression of a range of proteins involved in cell cycle arrest including p21<sup>(WAF1/Cip1)</sup>, p27 and gelsolin which is compatible with such effects. Beyond this, direct acetylation of proteins such as p53, E2F and Rb which are also involved in cell cycle control, means that acetylation beyond that occurring at the level of histones is likely to be relevant.<sup>13,125-127,147</sup>

HDAC inhibitors are able to induce differentiation in addition to cell cycle arrest. In one study, MCF7 cells treated with SAHA were shown to undergo morphological change (flattening, increased cytoplasmic:nuclear ratio), accumulation of Nile Red stained intracellular lipid droplets and accumulation of milk fat globule protein and

milk fat membrane globule protein indicating differentiation. These effects were reversible on washout of drug and appeared to be independent of ER, Rb or HER-2 status.<sup>136</sup> Induction of differentiation might provide one mechanism by which HDAC inhibition would target malignant cells in preference to normal ones and allow for therapeutic benefit.

A number of papers have assessed the effect of HDAC inhibitors in the in-vivo setting. These papers have used a range of animal, tumour type and HDAC inhibitors but a majority have assessed human tumour xenografts in murine systems. A universal finding of tumour growth inhibition and/or increased animal survival has been shown with generally no or minimal adverse effects described at therapeutic doses. In those that have assessed tumour effects on ex-vivo tissue samples, histone acetylation, differentiation and apoptosis have been confirmed.<sup>120,128-131,138-140,151,157</sup> In one study of FK228 where differences in efficacy between tumour line types was observed (PC3 pheochromocytoma > DU145 prostate > AHCN renal) a correlation of response to increased p21<sup>(WAF1/Cip1)</sup> and decreased c-myc mRNA expression was described.<sup>138</sup>

#### **1.4.6 Differences Between HDAC Inhibitor Effects In Normal Versus Malignant Cells**

Clinical trial and animal data suggests that HDAC inhibitors are comparatively tolerable with respect to adverse effects compared to, for example, conventional cytotoxics. They are not without toxicity however as discussed in the following section. This may relate in part to an apparent difference in the effects of these compounds on malignant compared to normal cells, although most in-vitro studies have examined the effects of these drugs only on malignant cell lines without comparisons to normal tissues. Therefore our understanding of why normal cells might be less sensitive or even resistant to HDAC inhibitors is limited. Huang and

Pardee have described cell death in response to SAHA to be increased in MCF7 breast cancer cells compared to MCF10A normal breast epithelial cells or normal human dermal fibroblasts by trypan blue exclusion assay. They also describe increased cell death in MCF7 cells as judged by floating cells on microscopy.<sup>147</sup> This may seem initially surprising in that HDAC inhibitors disrupt a transcriptional control mechanism that is part of normal cellular mechanisms. It has been suggested that the narrow range of gene expression changes induced by HDAC inhibition may in part explain this phenomenon. In a gene expression profiling experiment, changes seen with SAHA in fibroblasts differed from that in T24 bladder carcinoma cells. For example at 5 $\mu$ M doses, p21<sup>(WAF1/Cip1)</sup> induction occurred in the malignant cells but not the fibroblasts but histone H4 acetylation was seen for both. At 50 $\mu$ M fibroblasts did however show increased p21<sup>(WAF1/Cip1)</sup> expression and so some differences between normal and malignant cells may be of relative rather than absolute susceptibility to the downstream consequences of HDAC inhibition.<sup>135</sup> More recently it has been shown that in acute myeloid leukaemia HDAC inhibition induces p53 independent apoptosis in leukaemic cells, which depends in-vitro and in-vivo upon activation of TRAIL and Fas death receptor pathways which was not seen in normal haematopoietic progenitors.<sup>158,159</sup> In another study, HDAC inhibition was shown to increase thioredoxin, a major cellular reducing protein in normal but not transformed cells which was associated with an increase of reactive oxygen species and cell death in transformed cells.<sup>160</sup> These studies are beginning to elucidate the differences between malignant and normal cellular response to HDAC inhibition.

#### **1.4.7 Clinical Trials Involving HDAC Inhibitors**

A number of HDAC inhibitors are in early phase clinical trials. Of these a number of phase I studies are published, and are summarised in table 1-7. These studies indicate that the main toxicities of these drugs are fatigue, nausea and myelo-suppression. Early canine toxicology studies have raised concerns regarding cardiac

and catheter related toxicity with the cyclic tetrapeptides but it remains unclear from clinical studies how significant this will be to their potential use in man. By their nature these studies were not designed to assess response as a primary endpoint and typically treated refractory or multiply relapsed patients; however occasional objective responses and more frequently minor responses have been seen. Phase II data is not available except in conference abstract form but this suggests initially encouraging results. FK228 may be particularly effective in cutaneous T cell lymphoma, where in case reports of four patients with refractory or relapsed disease, a complete response and three partial responses were seen.<sup>161</sup>

It may be the case that traditional phase I design, defined by dose limiting toxicity, may not be the optimal method to assess administration of these drugs. In addition the cytotoxic effect which they may induce in malignancy might lend these drugs to combination therapy with drugs having other modes of action. There is no clinical data in this area as yet but in HER2 over-expressing breast cancer cell lines HDAC inhibition with SAHA has been shown to exert a synergistic cytotoxic effect both in combination with and chemotherapy using docetaxel and with the HER2 monoclonal antibody trastuzumab.<sup>162</sup>

Source	Drug	Design	n	ORR	Toxicity	Comments
Marshall et al <sup>163</sup>	FK228	Phase I Advanced malignancy	33	None	Nausea, vomiting, fatigue, anorexia, thrombocytopenia	
Piekarz et al <sup>161</sup>	FK228	Case report Cutaneous T cell lymphoma	4	1 CR 3 PR	Itching, erythema	
Sandor et al <sup>164</sup>	FK228	Phase I Advanced solid malignancy	37	1 PR	Fatigue, nausea/vomiting, atrial fibrillation, thrombocytopenia, neutropenia	First order two compartment kinetics Histone acetylation seen in peripheral blood mononuclear cells Patient serum ex-vivo to PC3 cells induced histone acetylation/cell cycle arrest
Byrd et al <sup>165</sup>	FK228	Phase I CLL and AML	20	None	Tumour lysis, fatigue, nausea, diarrhoea	Histone acetylation, HDAC inhibition and p21 <sup>(WAF1/Cip1)</sup> increased expression seen at 4 hours and diminishing at 24 hours
Kelly et al <sup>166</sup>	SAHA	Phase I Advanced cancer	37	4 Minor 0 PR/CR	Leucopaenia, thrombocytopenia, fatigue, tumour flare pain	Histone acetylation confirmed in tumour and mononuclear cells
Gore et al <sup>167</sup>	Phenyl butyrate	Phase I MDS/AML	13	None	Fatigue, neurocortical toxicity	
Gilbert et al <sup>168</sup>	Phenyl butyrate	Phase I Advanced solid tumours	28	None	Fatigue, dyspepsia	

Source	Drug	Design	n	ORR	Toxicity	Comments
Ryan et al <sup>169</sup>	MS-275	Phase I Advanced solid tumours and lymphoma	28	15 Stable disease 0 PR/CR	Anorexia, nausea, vomiting, fatigue	Histone H3 acetylation demonstrated on peripheral blood mono-nuclear cells
Prakash et al <sup>143</sup>	CI-994	Phase I Advanced solid tumours	15	1 PR	Thrombocytopenia, fatigue, nausea, gastrointestinal	
Undevia et al <sup>170</sup>	CI-994 and capecitabine	Phase I Advanced solid tumours	54	1 PR	Thrombocytopenia (DLT), fatigue, gastrointestinal	Platelet nadir predicted by maximal CI-994 concentration
Bug al <sup>171</sup>	Valproic acid and ATRA	Phase I Poor risk AML	26	2 PR	Fatigue, petechiae, vasculitis, hypocalcaemia, hyponatraemia	
Kuendgen et al <sup>172</sup>	Valproic acid +/- ATRA	Phase I AML unfit for intensive treatment	58	3 PR	Thrombocytopenia, fatigue, tremor	
Kuendgen et al <sup>173</sup>	Valproic acid and ATRA	Phase I Myelodysplastic syndrome +/- secondary AML	18	7 Minor 1 PR	Thrombocytopenia, fatigue, tremor	

**Table 1-7 Clinical trials using HDAC inhibitors**

ORR - Objective response rate, CR - complete response, PR - partial response



#### 1.4.8 Spiruchostatin A Is A Homologue Of FK228 Amenable For Chemical Synthesis

One of the more potent examples of HDAC inhibitors are the cyclic tetrapeptides including FK228 (depsipeptide, formally known as FR901228), Apicidin and the cyclic hydroxamic acid containing peptides (CHAP). FK228 is the most widely studied of these compounds and was originally identified as a natural product of the organism *Chromobacterium Violaceum*. It induces histone and non-histone protein acetylation, cell cycle arrest and inhibition of cancer cell proliferation in-vitro and in murine xenografts.<sup>133,139,140,174-177</sup> It is currently in phase II clinical trials for cancer having shown early promise of therapeutic efficacy in lymphoproliferative and solid malignancies with a manageable toxicity profile. FK228 received orphan drug status from both the Food and Drug Administration (FDA) and European Agency for the Evaluation of Medicinal Products (EMEA) as monotherapy in relapsed or refractory cutaneous T-cell lymphoma. In addition the FDA has granted fast track designation for this setting.

FK228 has been shown to exhibit potent HDAC inhibitory activity, but has a bicyclic ring structure which would not be expected at first sight to interact with HDAC active sites in the model outlined in section 1.4.4.<sup>133,175</sup> It has been shown however that this drug undergoes reduction of its internal disulfide bond to allow an active sulfhydryl group to interact with the HDAC enzymatic active site. This reduction step makes it markedly more active in inhibiting HDAC enzymes in-vitro. FK228 is far more stable in medium and serum before undergoing this reduction and so acts as a prodrug with activation after entry into the cell by reduction.<sup>133</sup> This process is shown diagrammatically in figure 1-9.

One point of particular interest with regards to FK228 is that it appears to exhibit selectivity for class I HDACs. Furumai et al were able to show strong inhibition of HDAC1 and HDAC2 class I enzymes but weak inhibition of HDAC4 and HDAC6

class II enzymes.<sup>133</sup> Koeller et al have shown differential effects on protein acetylation that correlates with this finding in that TSA but not FK228 produced tubulin acetylation which is an HDAC6 class II effect.<sup>178</sup> It is likely that this is due to the large cap structure which the FK228 ring structure generates following internal reduction of its disulfide bond to the active state. This comparatively large cap group (by comparison to other non HDAC class selective HDAC inhibitor structural types) may allow for interaction with a wider or more variable range of HDAC enzyme amino acids leading to this HDAC class selectivity. This is an important point because it raises the implication that this HDAC inhibitor structural class might show useful selectivity in HDAC enzyme class effects. This might allow for their use as chemical tools to address the role of histone/protein acetylation in malignancy and also hold potential benefit for therapeutic utilisation. At present it remains unknown if selectivity for HDAC enzyme class inhibition by these compounds would be useful clinically either in terms of efficacy or toxicity profiles. The initial clinical data regarding FK228 is encouraging but the same can be said for SAHA which is a pan class I and II HDAC inhibitor.

A related natural compound to FK228, Spiruchostatin A (figure 1-10), has been described following isolation from *Pseudomonas* sp. The original description was of biological activity of TGF- $\beta$  induced gene expression which could result from a variety of mechanisms. However the close structural similarity to FK228 suggested that it might in fact have HDAC inhibitory activity. Recently a total synthesis of Spiruchostatin A has been described as part of a collaborative effort between the author's laboratory and Dr A Ganesan's group in the Department of Chemistry at Southampton University.<sup>141</sup> In addition an inactive epimer of Spiruchostatin A has been produced. The potential to subsequently create structural variants of Spiruchostatin A, and so allow for its use as a tool to address structure function relationships, makes it an attractive target for investigation as an HDAC inhibitor. The in-vitro characterisation of Spiruchostatin A and its use in comparative investigation of cyclic tetrapeptide to hydroxamate HDAC inhibitors in breast cancer cells is detailed in this work.

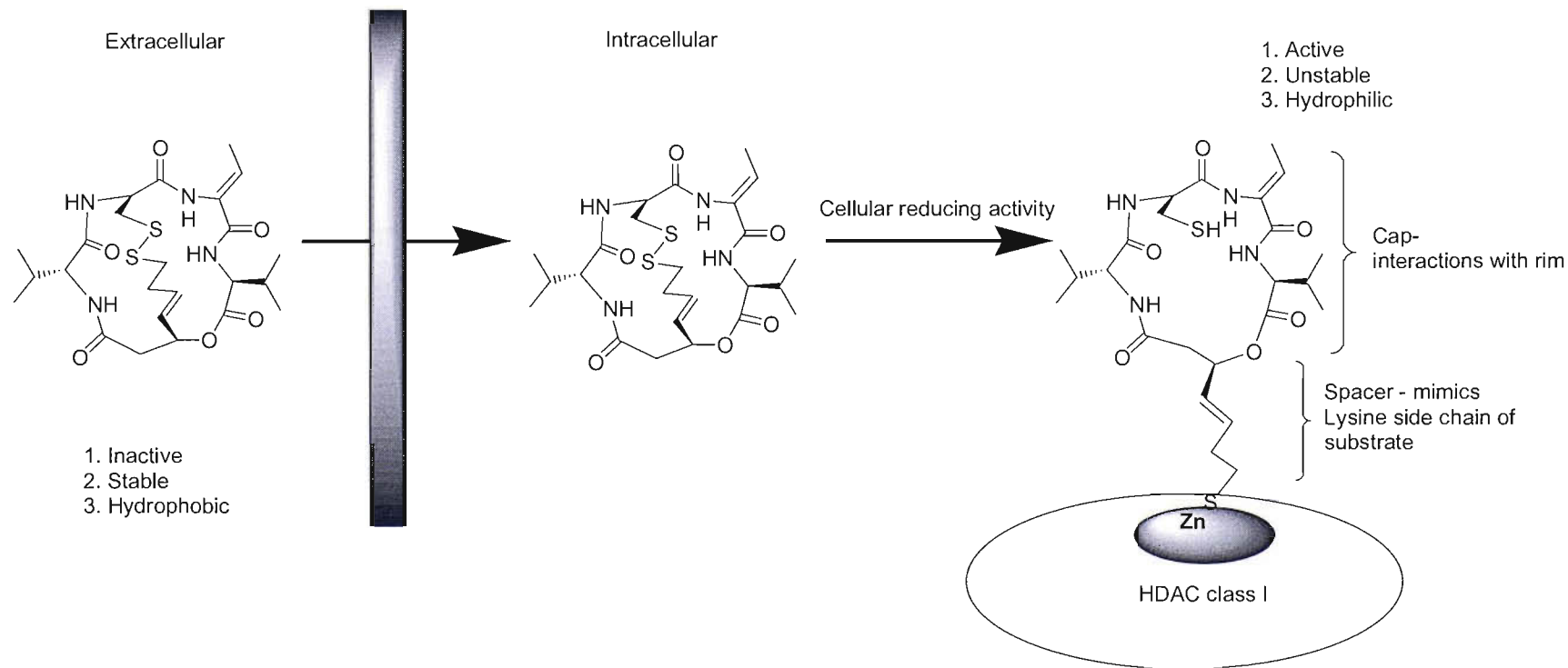
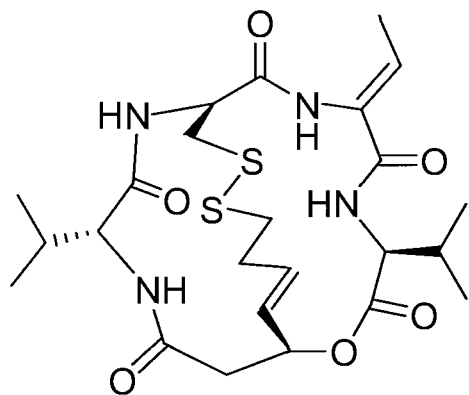
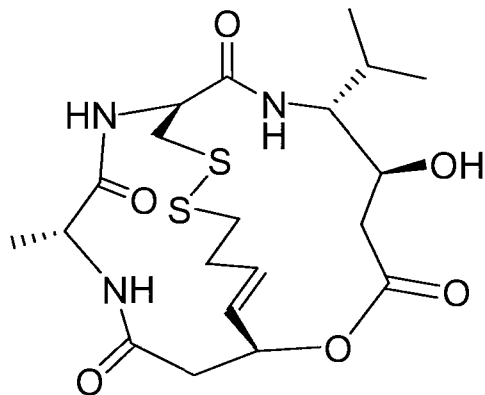


**Figure 1-9 Activation of FK228 by reduction of the internal disulfide bond**

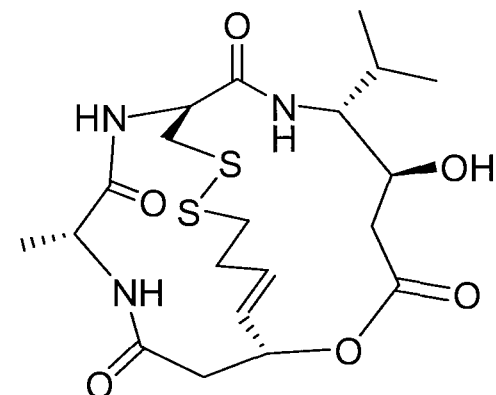
Entry of the inactive, stable, hydrophobic FK228 into the cell leads to reduction of the internal disulfide bond resulting in an active, unstable, hydrophilic conformation with the sulfhydryl active group able to access the HDAC enzymatic cleft. Taken from Furumai et al.<sup>133</sup>



FK228



Spiruchostatin A



Epi-Spiruchostatin A

**Figure 1-10 Structures of FK228 and Spiruchostatin A and its inactive epimer**

## **2 Project Aims and Outline of Investigation**

This thesis details investigation surrounding a central theme of the therapeutic manipulation of cell cycle progression and differentiation as means to induce to malignant cell death through apoptosis in breast cancer. With the basic premise that improvement in therapeutic options for this disease will require treatments that directly target these key underlying biological processes, work has been conducted to investigate two such approaches as detailed below.

### **2.1 Interaction Between BAG-1 and PPAR $\gamma$**

Firstly, interaction between the anti-apoptotic protein BAG-1 and PPAR $\gamma$  was investigated. The central hypothesis was that the known over expression of BAG-1 in a proportion of breast cancers might be a direct negative regulator of PPAR $\gamma$  that would compromise the potential for PPAR $\gamma$  ligands as a potential therapeutic modulator of cell cycle, apoptosis and differentiation in breast cancer. This starting point was based on the proven interaction of BAG-1 with a range of NHRs including the known potentiating interaction with the ER in breast cancer, and data that BAG-1 blocks the cyproterone acetate effect on the AR. In addition the putative BAG-1:PPAR $\gamma$  interaction might provide a useful model for basic research into BAG-1 function in breast cancer and other malignancies. Investigation was performed in the following areas.

1. Transcription reporter assays were performed in breast cancer cell lines using co-transfection of response elements to PPAR $\gamma$  (and subsequently the vitamin D receptor for comparative validation of results) and BAG-1 isoforms.
2. Flow cytometry experiments were performed in breast cancer cells to investigate effects on cell cycle progression and apoptosis in response to PPAR $\gamma$  stimulation, and to assess the effect on these outcomes following forced over expression of BAG-1 isoforms by stable transfection.

3. Differentiation experiments were performed using Nile Red staining for milk fat and lipid accumulation as a marker for breast cancer cell differentiation, again with assessment of the effect of forced over expression of BAG-1 isoforms.

## **2.2 Characterisation of the Novel HDAC Inhibitor Spiruchostatin A**

As a further means of manipulating breast cancer cell proliferation and differentiation status, investigation was performed of a novel HDAC inhibitor. Spiruchostatin A has close structural similarity with the potent class I HDAC selective inhibitor FK228. Work was performed to characterise Spiruchostatin A in terms of its effects on cell cycle, induction of cell death and differentiation using the following techniques.

1. The ability of Spiruchostatin A to induce histone acetylation and to mediate the expression of key target proteins such as p21<sup>(WAF1/Cip1)</sup> was determined by Western blot analysis in breast cancer cell lines.
2. Subsequently the ability of this compound to produce downstream biological endpoints that would be predicted as effects of histone acetylation including inhibition of cell proliferation, cell cycle arrest and differentiation were assessed.
3. Having addressed the in-vitro effects of inhibiting HDAC activity on breast cancer cells, comparative experiments were performed to determine relative effects on normal non-malignant cells with respect to histone acetylation, inhibition of cell proliferation and cell cycle progression.
4. Finally, work was done to assess cell adhesion characteristics in breast cancer cell lines, which were noticed to be modified by this compound.

## **2.3 Comparisons Between Cyclic Tetrapeptide and Hydroxamate HDAC Inhibitors**

Following on from work to characterise Spiruchostatin A with respect to its HDAC inhibitory characteristics and patterns of biological activity in breast cancer cell lines, investigation was performed together with the analogue FK228 compared to the

hydroxamate HDAC inhibitors TSA and SAHA. This provided comparison of the biological activity of these compounds to assess differences between the class I selective cyclic tetrapeptides and the pan HDAC I and II inhibitory hydroxamates.

1. Firstly proliferation, mRNA expression and cell cycle progression characteristics were compared for each of these four drugs.
2. Secondly work was performed looking at tubulin acetylation characteristics to address the class I selectivity that is known to exist for FK228 and predicted for Spiruchostatin A but not for the hydroxamates.
3. Finally, comparisons were made to assess the pharmacodynamic differences seen between these drugs with regards to histone acetylation and subsequent cell cycle progression characteristics.

### 3 Materials and Methods

#### 3.1 Reagents

Unless otherwise stated, chemicals were supplied by Merck Ltd (BDH Laboratory Supplies, UK).

TSA, troglitazone and 1,25(OH) vitamin D<sub>3</sub> were sourced from Sigma, UK. PGJ2 and SAHA were from Alexis Biochemicals, UK. Spiruchostatin A was a kind gift from Dr G Packham having been synthesised by Dr A Ganesan in the Department of Chemistry, University of Southampton. FK228 was a kind gift from Dr Minoru Yoshida, RIKEN, Japan.

##### 3.1.1 General Buffers and Solutions

Phosphate buffered saline (PBS)

125mM Sodium Chloride  
16mM Na<sub>2</sub>HPO<sub>4</sub>  
10mM NaH<sub>2</sub>PO<sub>4</sub>  
HCl to pH 7.2

Tris buffered saline (TS)

10mM Tris-hydrochloric acid pH 8  
150mM Sodium chloride

ONPG (o-nitrophenyl-beta-D-galactopyranoside) reagent

120mM Na<sub>2</sub>HPO<sub>4</sub>.12H<sub>2</sub>O  
80mM Na<sub>2</sub>H<sub>2</sub>PO<sub>4</sub>.2H<sub>2</sub>O  
2mM MgCl<sub>2</sub>.6H<sub>2</sub>O  
pH to 7.5 with 10 N NaOH then add  
100mM 2 Mercaptoethanol



1.33 g/L ONPG

Luciferase/ $\beta$ -galactosidase lysis buffer

10mM Tris-HCl  
1mM EDTA pH8  
150mM NaCl  
0.65% (v/v) Nonidet P40

Lysozyme solution

50mM Glucose  
10mM EDTA  
25mM Tris-HCl pH 8

**3.1.2 Protein Manipulation Solutions And Buffers**

RIPA lysis buffer

150mM Sodium Chloride  
1% (v/v) IPEGAL (Nonidet P-40)  
0.5% (w/v) Sodium deoxycholate  
0.1% (w/v) Sodium dodecyl sulphate  
50mM Tris-HCl pH 8.0

SDS-PAGE sample buffer

50mM Tris-hydrochloric acid pH 6.8  
200mM Glycine  
0.1% (w/v) Sodium dodecyl sulphate

Protein running buffer

25mM Tris Base  
200mM Glycine

0.1% (w/v) Sodium dodecyl sulphate

#### Protein transfer buffer

25mM Tris Base

200mM Glycine

0.1% (w/v) Sodium dodecyl sulphate

25% (v/v) Ethanol

#### Tris buffered saline-tween (TST)

TS with 0.05% (v/v) Tween 20

#### Phosphate buffered saline – tween (PBS-T)

PBS with 0.05% (v/v) Tween 20

### 3.1.3 DNA Electrophoresis Reagents

#### Agarose gel loading buffer (6X)

0.25% (w/v) Bromophenol blue

0.25% (w/v) Xylene cyanole

15% (w/v) Ficoll 400

#### Tris-Borate-EDTA buffer (TBE)

80mM Tris base

80mM Orthoboric acid

1mM EDTA

### 3.1.4 Bacterial manipulation reagents

#### Luria Bertani (LB) media

10g/L Tryptone (Becton Dickinson, UK)

5g/L Yeast Extract (Becton Dickinson, UK)

10g/L Sodium chloride

pH to 7.4 with 4M Sodium hydroxide  
Where indicated: 100µg/ml Ampicillin

#### LB plate media

10g/L Tryptone  
10g/L Yeast Extract  
5g/L Sodium chloride  
pH to 7.4 with 4M Sodium hydroxide  
15g/L Agar (Becton Dickinson, UK)  
Where indicated: 100µg/ml Ampicillin

### **3.1.5 Mammalian Cell Culture**

All tissue culture plastic ware was supplied by Grenier, UK. Dulbecco's Modified Eagles Medium (DMEM) and trypsin were supplied by Invitrogen, UK.

DMEM:Hams F12 1:1 nutrient mix medium and Fibroblast Basal Medium were supplied by Cambrex, UK. Foetal calf serum (FCS) was supplied by PAA laboratories, Austria for all cell lines except Normal Human Dermal Fibroblasts (NHDF) for which foetal bovine serum from Cambrex was used. G418 antibiotic was from Promega, UK.

#### Penicillin/Streptomycin/L-Glutamine 100X concentrate (PSG)

10mg/ml Penicillin G  
10mg/ml Streptomycin  
29.2mg/ml L-glutamine

#### Mammalian cell line freeze media

50% (v/v) DMEM  
10% (v/v) Dimethyl sulfoxide  
40% (v/v) FCS

NHDF freeze media

80% (v/v) Fibroblast Basal Medium

10% (v/v) Dimethyl sulfoxide

10% (v/v) Foetal bovine serum

## **3.2 In-vitro Cell Culture Techniques**

### **3.2.1 Cell Lines**

Table 3-1 shows the cell lines used for this work. MCF-7 cell lines stably transfected to over express the pcDNA3 based BAG-1S or BAG-1L expression vectors, or the empty pcDNA3 vector as a control, were a kind gift from Dr G. Packham.

### **3.2.2 Cell Culture and Cryopreservation Techniques**

MCF7, MDA-MB-231, BT474 and HEK293 cells were maintained in DMEM with 10% (v/v) FCS and PSG at 37°C and 10% (v/v) CO<sub>2</sub>. For MCF7 stably transfected clones, G418 antibiotic was added to culture medium. NHDF cells were maintained in Fibroblast Basal Medium and 10% foetal bovine serum supplemented with hFGF-B, insulin and gentamicin/amphotericin-B aliquots (Cambrex, UK) at 37°C and 5% (v/v) CO<sub>2</sub>. H376 cells were maintained in DMEM:Hams F12 1:1 nutrient mix medium with 10% (v/v) FCS and 0.5µg/ml hydrocortisone at 37°C and 5% (v/v) CO<sub>2</sub>. Media and other reagents were warmed to 37°C prior to use and medium was changed every 48 to 72 hours. Cell passage was performed by removing existing culture medium and washing with trypsin followed by incubation with trypsin for 1 to 10 minutes depending on cell line and gentle tapping until cells had detached. Fresh growth medium was then added to neutralise trypsin, prior to plating of cells at the required density.

For cell line cryopreservation, cell mono-layers were grown to confluency, trypsinised and centrifuged at 1000rpm for 2 minutes (Sorvall RT6000B centrifuge, H1000B rotor). After removal of the supernatant, cells were resuspended in the appropriate freeze media and aliquoted in cryovials. Samples were frozen in a Nalgene Cryo 1° freezing container at -80°C overnight and then transferred to liquid

nitrogen for long term storage. Cell samples were subsequently thawed for use to 37°C and added drop wise to 10ml of growth medium. Following centrifugation at 1000rpm for 2 minutes at room temperature (Sorvall RT6000B centrifuge, H1000B rotor), cells were re-suspended in growth medium, plated, and incubated at 37°C.

Cell type	Source	Notes
MCF-7	Dr G. Packham	Human breast adenocarcinoma expressing oestrogen receptor $\alpha$ and oestrogen receptor $\beta$ (weakly).
MDA-MB-231	Dr G. Packham	Human breast adenocarcinoma. Oestrogen receptor negative.
BT474	Dr J. Blaydes, Southampton University	Human breast carcinoma. HER2 over expressing
HEK293	Dr G. Packham	Transformed human embryonal kidney cell line
H376	Dr A. Hague, Bristol University	Human oral carcinoma
NHDF	Cambrex, UK	Normal human dermal fibroblast (adult)

**Table 3-1 Cell lines used for this work**

Cell lines were sourced as indicated. Those from individual investigators were kind gifts, having been sourced originally from the European Collection of Cell Cultures (ECACC) or the American Type Culture Collection (ATCC).

### **3.3 Protein Manipulation Techniques**

#### **3.3.1 Protein Quantification**

Samples were assessed for protein quantification by the addition of 2 $\mu$ l to 1ml of a 1 in 5 dilution of Bio-Rad Protein Assay Reagent (Bio-Rad, UK) in PBS, followed by measuring of absorbance at 595nm using a UV-1700 PharmaSpec spectrophotometer (Shimadzu, UK). This product utilises the standard Bradford method for protein concentration analysis using the differential colour change of Coomassie Blue dye on binding basic and aromatic amino acid residues. Protein concentration calculations were then performed by comparison to a standard curve from samples containing known concentrations of bovine serum albumin (Promega).

#### **3.3.2 Sodium Dodecyl Sulphate Polyacrylamide Gel Electrophoresis (SDS-PAGE)**

Protein expression and acetylation status was determined by SDS-PAGE and Western blot analysis. Cell mono-layers were first washed in PBS and detached by scraping in fresh PBS. Cells were then collected as a pellet by centrifugation at 5000 rpm for 2 minutes at 4°C in a micro-centrifuge (Heraeus Biofuge) followed by removal of the supernatant. Sample pellets were then lysed immediately for sample production or snap frozen in liquid nitrogen and stored at -80°C for subsequent analysis. Cell lysis was routinely performed by the addition of 100 $\mu$ l RIPA lysis buffer to the pellet supplemented by 1% (v/v) mammalian protease inhibitor cocktail (Sigma, UK) and 1% (v/v) phosphatase inhibitor cocktail 2 (Sigma, UK), vortexing briefly and incubating for 30 minutes on ice. Cell debris was then removed by centrifugation for 20 minutes at 13000rpm at 4°C in a micro-centrifuge (Heraeus Biofuge) with retention of the supernatant. Protein sample buffer (New England Biolabs, UK) supplemented with 0.1M Dithiothreitol (DTT, New England Biolabs, UK) was added to protein extracts normalised to a final concentration of 1 $\mu$ g/ $\mu$ l. Samples were heated for 3 minutes at 95°C and 15 $\mu$ g of sample was loaded onto a pre-cast 4-15% gradient Tris HCl SDS-polyacrylamide gel (Bio-Rad, UK). Protein

markers were used as molecular weight standards (New England Biolabs, UK). Electrophoresis was performed in Mini-Protean III cells (Bio-Rad, UK) in Protein Running Buffer at 200 volts for 45 minutes.

### **3.3.3 SDS-PAGE Sample Preparation For Histone Acetylation Experiments**

Sample preparation for Western blot analysis in experiments to assess histone acetylation differed from SDS-PAGE sample preparation described in section 3.3.2 in the following ways. Sample growth medium containing floating detached cells was retained on ice. Adherent cells were washed with 1ml of trypsin and then adherent cells were detached by trypsinisation. The retained growth medium, trypsin wash and trypsinised cells were combined on ice. The combined cell sample was centrifuged at 1000rpm for 2 minutes (Sorvall RT6000B centrifuge, H1000B rotor), the supernatant was removed and then resuspended in 1ml of ice cold PBS. Cells were then collected as a pellet by centrifugation at 5000 rpm for 2 minutes at 4°C in a micro-centrifuge (Heraeus Biofuge) followed by removal of the supernatant. Sample pellets were then lysed immediately for sample production or snap frozen in liquid nitrogen and stored at -80°C for subsequent analysis. Cell pellets were lysed by resuspension in 75µl protein sample buffer (New England Biolabs, UK) supplemented with 0.1M Dithiothreitol (DTT, New England Biolabs, UK) followed by sonication (MSE Soniprep 150) on ice, three times at 23kHz and approximately 100W for 15 seconds. Samples were then run in 15µl volumes by SDS-PAGE without protein quantification and normalisation.

### **3.3.4 Western Blot Analysis**

Following SDS-PAGE, transfer of the protein to nitrocellulose membrane (Protran, Schleicher and Schuell, Germany) was performed using a Mini-Protean III transfer unit (Bio-Rad, UK) in Protein Transfer Buffer at 100 volts for one hour. Non specific protein binding was then blocked by washing the nitrocellulose membrane in TS or PBS with 3% (w/v) non-fat milk (Marvel) for 90 minutes. The membrane was then incubated with the primary antibody at the appropriate concentration in TS



or PBS with 3% (w/v) non-fat milk at 4°C overnight unless otherwise stated. The membrane was then washed three times in TST or PBST for five minutes followed by incubation with the appropriate horseradish peroxidase conjugated secondary antibody (Amersham, UK) for a minimum of one hour at room temperature. A further three washes in TST or PBST were performed and the membrane was then incubated for five minutes at room temperature with Supersignal West Pico Chemiluminescent Substrate (Pierce, UK) which provides a luminous peroxide containing substrate. Subsequent chemiluminescence was visualised with a Flour-S-Multi-imager (Bio-Rad, UK) and Quantity One software (Bio-Rad, UK). The antibodies used for western blot analysis during this study are summarised in table 3-2.

Antibody to	Name/Clone	Source	Type	Dilution	Antigen
PCNA	PC10	Cancer Research UK	Mouse monoclonal	Ascites at 1/1000	Rat PCNA
Human BAG-1	3.10 G3E2	Dr G. Packham	Mouse monoclonal	Hybridoma supernatant	GST-BAG-1S
Human BAG-1	TB2, TB3	Dr G. Packham	Rabbit polyclonal	1/1000	GST-BAG-1S
HSP70	C92F3A5	Stressgen	Mouse monoclonal	1 µg/ml	Recombinant HSP70
HSC70	B6	Santa Cruz	Mouse monoclonal	0.2 µg/ml	Human HSC70 C-terminus
HSP40	SPA-400	Stressgen	Rabbit polyclonal	1/10000	Recombinant human HSP40
β catenin	C-18	Santa Cruz	Goat polyclonal	1 µg/ml	Human β catenin C-terminus
p21 <sup>(WAF1/Cip1)</sup>	SX118	Pharmingen	Mouse monoclonal	1/1000	GST- p21 <sup>(WAF1/Cip1)</sup>
EGFR	1005	Santa Cruz	Goat polyclonal	1/1000	Human EGFR C-terminus
Neu (HER2)	C-18	Santa Cruz	Rabbit polyclonal	1/1000	Human Neu C-terminus
α-Tubulin	TAT-1	Cancer Research UK	Mouse monoclonal	1/2000	T. brucei cytoskeletal extraction
Tubulin (acetylated lysine 40)	6-11B-1	Sigma	Mouse monoclonal	Ascites at 1/2000	Sea urchin acetylated tubulin
Histone H3 (acetylated lysine 9)	-	Upstate	Rabbit polyclonal	1 µg/ml	KLH-H3 amino acids 1-12 (Ac-K9)
Histone H3 (acetylated lysine 14)	-	Upstate	Rabbit polyclonal	1 µg/ml	KLH-H3 amino acids 7-17 (Ac-K14)
Histone H4 (acetylated lysine 8)	-	Upstate	Rabbit polyclonal	1/1000	KLH-H4 amino acids 1-12 (Ac-K8)

**Table 3-2 Antibodies used in this study**

Antibodies were either kind gifts from Dr G. Packham or sourced from either Cancer Research UK or commercially as indicated.

## **3.4 DNA Manipulation Techniques**

### **3.4.1 Bacterial Transformation**

1  $\mu$ l of DNA was added with gentle mixing to 50  $\mu$ l of JM109 competent bacterial cells (Promega). After 30 minutes on ice, the mixture was heat shocked for 45 seconds at 42°C and then placed on ice for 5 minutes. 250  $\mu$ l LB medium was added and cells were incubated for 1 hour at 37°C with horizontal shaking. Finally the bacterial suspension was spread on LB agar plates with the appropriate selection antibiotic and incubated overnight at 37°C prior to colony selection.

### **3.4.2 DNA Purification Methods**

#### **3.4.2.1 Small Scale (Miniprep) DNA Plasmid Purification**

Transformed bacterial colonies were individually selected from LB media plates and grown up overnight in LB media supplemented with ampicillin. Small and medium scale preparation of DNA from colonies following transformation was performed using the Wizard Plus Miniprep DNA Purification System (Promega) according to the manufacturer's instruction. This utilises a proprietary alkaline lysis technique followed by purification by resin binding and elution. Purification was followed by verification by endonuclease digestion and DNA sequencing analyses.

#### **3.4.2.2 Large Scale (Maxiprep) DNA Plasmid Purification**

Transformed bacteria were grown in 500ml LB culture medium overnight at 37°C together with ampicillin. Cells were then collected by centrifugation at 6500 rpm for 10 minutes (Sorvall RC5C centrifuge, F-16/250 rotor), followed by resuspension and gentle mixing in 20ml of lysozyme solution, supplemented with lysozyme at 1mg/ml. Following 5 minutes for lysis to occur, 40ml of freshly made 0.2M sodium hydroxide in 1% SDS (w/v) was added, the mixture was mixed gently, and left for a further 5 minutes to allow protein and DNA denaturation. Protein and DNA precipitation was then performed by the addition of 20ml 3M sodium acetate pH4.8

with gentle mixing followed by the removal of cell debris by centrifugation at 7000rpm for 20 minutes (Sorvall RC5C centrifuge, F-16/250 rotor). The supernatant was filtered through muslin and 50ml propan-2-ol was added followed by centrifugation at 7000rpm for 20minutes (Sorvall RC5C centrifuge, F-16/250 rotor). The supernatant was discarded and the DNA resuspended in 20ml of water. 25g caesium chloride and 0.7ml of 10mg/ml ethidium bromide were added followed by centrifugation at 10000rpm for 10 minutes (Sorvall RC5C centrifuge, SS34 rotor). The subsequent supernatant was then concentrated by ultra-centrifugation at 40000 rpm for a minimum of 40 hours (Sorvall OTD55B ultra-centrifuge, TFT50.38 rotor). The lower DNA containing band was then collected using a peristaltic pump and an equal volume of water saturated butan-1-ol was added and thoroughly mixed. Samples were centrifuged for 5 minutes at 2000rpm and the upper phase discarded. This was repeated until the upper phase became completely clear to completely remove the ethidium bromide.

The resultant purified plasmid DNA was then concentrated by ethanol precipitation. First an equal volume of water was added to the sample and two times the total volume of 100% ethanol and the resultant mixture stored at -20°C for one hour. The sample was then spun at 10000rpm for 20 minutes (Sorvall RC5C centrifuge, SS34 rotor). The pellet was resuspended in 6ml of 70% ethanol and centrifuged again at 10000rpm for 10minutes. The pellet was air dried overnight followed by resuspension in water and measurement of concentration by absorbance at 260nm using a UV-1700 PharmaSpec spectrophotometer (Shimadzu, UK).

#### **3.4.2.3 DNA Sequence Analysis**

Sequencing of plasmids following manipulation and purification was performed commercially by MWG (UK).

#### **3.4.3 Restriction Endonuclease Digestion**

A typical restriction enzyme digestion reaction would contain

DNA 1  $\mu$ g  
Restriction endonuclease 0.5  $\mu$ l  
10x BSA (1mg/ml) 1.5  $\mu$ l  
10x Buffer 1.5  $\mu$ l  
Water to 15  $\mu$ l

Reactions were incubated at the appropriate temperature for a minimum of three hours or overnight to ensure complete digestion (such as for linearization of vectors prior to ligation). Subsequent restriction fragments were assessed by agarose gel electrophoresis.

#### **3.4.4 Agarose Gel Electrophoresis**

Agarose gels were made using TBE and 0.5  $\mu$ g/ $\mu$ l ethidium bromide at 1.5% (w/v) agarose (Invitrogen). Samples were made up with 6x agarose gel loading buffer and electrophoresis was performed in TBE at 10 V/cm. Promega DNA ladders were used as standards for DNA fragment size estimation. Gels were visualized using long wave ultraviolet light with a digital camera (Kodak DC 120, Kodak UK) and Kodak KDS 1D software.

#### **3.4.5 Summary of DNA Plasmid Constructs Used**

Plasmids used in this study are summarised in table 3-3.

Plasmid	Source	Notes
pcDNA3	Invitrogen, UK	
pcDNA3-BAG-1S	Dr G. Packham	Optimised to express human BAG-1S <sup>4</sup>
pcDNA3-BAG-1M	Dr G. Packham	Optimised to express human BAG-1M <sup>4</sup>
pcDNA3-BAG-1L	Dr G. Packham	Optimised to express human BAG-1L <sup>4</sup>
CMV- $\beta$ -Gal	Invitrogen, UK	$\beta$ -galactosidase reporter plasmid expression construct under constitutive control of the CMV IE promoter
pRL-tk-luc	Promega, UK	Renilla luciferase reporter plasmid expression construct under constitutive control from the HSV tk promoter
PPRE-tk-luc	Dr K. Lillycrop, University of Southampton	Contains three copies of a PPAR response element consensus sequence upstream of a tk promoter and firefly luciferase expression gene <sup>179</sup>
pGL2-DR3-luc	Dr A. Hague, University of Bristol	Contains four copies of a DR3 response element to the vitamin D receptor upstream of a firefly luciferase expression gene

**Table 3-3 DNA expression plasmids used in this work**

### **3.5 Transcription Reporter Assays**

Assays to assess transcriptional activity via the PPAR $\gamma$  and VDR receptors in cell culture systems were performed using luciferase reporter construct assays. Cells were transfected using either the TransFast (Promega, UK) or FuGENE 6 (Roche, UK) reagents according to the respective manufacturers' instructions. Each utilises a cationic liposomal lipid bilayer as a means of transporting DNA into cells for subsequent analysis of gene expression.

#### **3.5.1 tk.luc Control Reporter Construct For PPRE-tk-luc**

A plasmid construct containing response elements to PPAR $\gamma$  receptor was a kind gift from Dr K. Lillycrop. This plasmid contains three copies of a rat PPAR $\gamma$  response element TGACCTTTGTCCT sequence upstream of a tk promoter and firefly luciferase gene. To obtain a control expression plasmid for this reporter construct, the response elements were excised by endonuclease digestion with Sal I which removes a 108 base pair fragment (and retains the tk.luc component). The remaining plasmid was purified using the 'High Pure PCR Product' purification kit (Boeringer Mannheim) according to the manufacturers instructions followed by ligation of the Sal I digested ends using T4 DNA ligase (Promega, UK) according to the manufacturers instructions. The resulting plasmid was first transformed into competent bacteria, purified by miniprep purification and confirmed first by agarose gel electrophoresis and then commercial sequencing. The plasmid was then bulked up by maxiprep purification.

#### **3.5.2 Transcription Reporter Assays For PPAR $\gamma$**

MCF7, MDA-MB-231 and HEK293 cells were used for these experiments. Typically  $3 \times 10^5$  cells were plated per 35mm well. Transfection was performed the following day using Transfast reagent (Promega, UK). A typical transfection mixture would contain 1  $\mu$ g PPRE.luc, 2  $\mu$ g of pcDNA3 based BAG-1 expression plasmid and 1  $\mu$ g of  $\beta$ -galactosidase to act as an internal control for transfection efficiency applied to each 35mm sample well. Cells were transfected using a 3  $\mu$ l:1  $\mu$ g ratio of transfection reagent to total transfected

DNA per sample, in serum free medium. Exposure to the transfection mixture was for one hour. The transfection mixture was replaced by fresh medium and samples were then exposed to the PPAR $\gamma$  ligand PGJ2 typically to a concentration of 10 $\mu$ M or an equivalent concentration of dimethyl sulfoxide (DMSO) vehicle. After 16 hours samples were washed once in PBS, scraped in fresh PBS to detach cells followed by centrifugation at 5000rpm for 2 minutes at 4 $^{\circ}$  in a micro-centrifuge (Heraeus Biofuge). The pellet was re-suspended in 100 $\mu$ l of luciferase/ $\beta$ -galactosidase lysis buffer, vortexed, rested for 5 minutes and then re-centrifuged at 12000rpm for 5 minutes. The supernatant was retained for sample analysis. 20 $\mu$ l was assessed for luciferase activity in a Sirius single tube luminometer (Berthold Detection Systems, UK) according to the manufacturer's instructions following the (automatic) addition of 100 $\mu$ l luciferase assay reagent (Promega, UK).  $\beta$ -galactosidase assay samples were prepared in a 96 well plate with each well containing 50 $\mu$ l ONPG, 10 to 50 $\mu$ l of sample (depending on the transfection efficiency of the cell type used) and luciferase/ $\beta$ -galactosidase lysis buffer to a final volume of 100 $\mu$ l. Samples were then analysed for  $\beta$ -galactosidase activity on a BioRad 550 microplate reader using Microplate Manager 5.0 software (BioRad, UK). Results were analysed as luciferase activity divided by  $\beta$ -galactosidase activity for each individual sample to control for inter-sample variations in transfection activity and cell number.

### **3.5.3 Transcription Reporter Assays For VDR and VDR/PPAR $\gamma$ Comparisons**

H376 and H400 oral carcinoma cells were used for these experiments. Typically 5x10<sup>3</sup> cells per well were plated per well in a 24 well plate. Transfection was performed two days later using Fugene reagent (Roche). A typical transfection mixture would contain 2 $\mu$ g pGL2-DR3.luc, 2 $\mu$ g pcDNA3 based BAG-1 isoform expression plasmid or pcDNA3 control and 0.5 $\mu$ g pRL-tk-luc to act as an internal control for transfection efficiency applied in cell culture medium with 1% FCS and Fugene reagent, using a 3 $\mu$ l:1 $\mu$ g ratio of transfection reagent to total transfected DNA per sample, in serum free medium. Exposure to the transfection mixture was for six hours to six wells per pcDNA3 based BAG-1 plasmid or mutant. This provided triplicate samples with or without drug



treatment. Transfection mixture was replaced by fresh cell culture medium at 6 hours containing either DMSO vehicle or  $1\alpha,25$  dihydroxyvitamin D<sub>3</sub> at a concentration of  $10^{-7}$  M for 24 hours. Cells were then lysed and analysed for firefly and renilla luciferase activity using the Dual Luciferase Assay System (Promega, UK) and a Sirius single tube luminometer (Berthold Detection Systems, UK) each according to the manufacturer's instructions. Briefly this system uses utilises the fact that Firefly and Renilla luciferase enzymes have dissimilar enzyme structures and substrate requirements allowing for discrimination between their respective bio-luminescent reactions. Thus a sample can be assayed for both enzymes with the firefly reaction quenched in the luminometer before addition of the renilla substrate. Results were analysed as firefly luciferase activity divided by renilla luciferase activity to control for inter-sample variations in transfection activity and cell number, and were expressed as the mean for triplicate samples.

### **3.6 Cell Cycle and Cell Death Analysis by FACS**

Cell cycle progression and cell death were assessed by Fluorescent Activated Cell Sorter analysis (FACS). Flow Cytometry is a means of measuring certain chemical and physical characteristics of cells as they travel in suspension past a sensing point. This can be applied to cell cycle and cell death analysis by the use of dyes such as propidium iodide which fluoresces on DNA binding. This allows determination of cell count with respect to cell DNA content which varies as cells pass through the cell cycle or into apoptosis.

Cells were plated typically at a density of  $3-5 \times 10^5$  per 35mm well, prior to application of the appropriate drug. At the appropriate time point, samples were washed twice in Hanks modified salt solution without calcium or magnesium (GIBCO, UK) and then trypsinised for 5 minutes until cells became detached. The original cell culture medium, trypsinised cells and each wash solution were combined and the resultant mixture centrifuged at 1000rpm for 2 minutes at room temperature (Sorvall RT6000B centrifuge, H1000B rotor). The cell pellet was washed twice by re-suspension in 5ml PBS and repeat centrifugation, before re-suspension in 3ml cold 70% (v/v) ethanol to permeablise cells (prior to subsequent propidium iodide staining) and incubation at 4°C for a minimum of

24 hours. Following centrifugation at 1500rpm for 5 minutes, the cell pellet was re-suspended in 500µL PBS supplemented with propidium iodide (Sigma, UK) at 80µg/ml and ribonuclease A (Sigma, UK) at 10µg/ml and incubated at room temperature in the dark for 30 minutes. Samples were then analysed on a FACScaliber FACS counter (Becton Dickenson, UK) using CellQuest software. Cell counts were gated to exclude doublet and higher cell counts to leave single cell counts only. Cell cycle fractions were assessed as percentages of total gated cells in cell cycle. Dead cell fraction was assessed as the percentage of cells in the hypodiploid pre-G0 region of total gated cells.

### **3.7 Nile Red Fluorescence Microscopy**

One feature of breast cancer cell differentiation in-vitro is the accumulation of fat and lipids which exist as droplets within the cytoplasm. Nile Red is a selective fluorescent stain for intracellular lipid droplets which can be used to detect this. The method used is based on that described by Greenspan et al.<sup>180</sup> Cells were plated typically at a density of  $3-5 \times 10^5$  per 35mm well, each containing a microscope cover slip. Appropriate application of drug was performed the following day. Slide preparation was performed by washing twice with PBS and then fixing with PBS containing 4% (w/v) para-formaldehyde for 20 minutes at room temperature. Cover slips were then washed twice again in PBS followed by incubation in the dark for 5 minutes in freshly made PBS supplemented with 100ng/ml Nile Red (Sigma, UK) from a 1mg/ml stock solution in 100% ethanol. Cover slips were then washed twice again in PBS prior to mounting on microscope slides with DAKO Fluorescent Mounting Medium. Slides were stored in the dark at 4°C overnight and then visualised.

Slides stained for Nile Red were visualised by fluorescent microscopy using a Zeiss Axiovert 200 microscope and Openlab 3.0.8 software (Improvision, UK). Objective assessment of differentiation was performed by determination of the average number of lipid droplets per cell on each slide. For each slide fields were selected at random and five adjacent cells were selected for manual counting of lipid droplets. This was

performed twice for each slide and the average lipid droplet count (of ten counted cells) was thus determined.

### **3.8 Cell Proliferation Assays for HDAC Inhibitors**

Cell proliferation assays following HDAC inhibition were performed using the CyQuant assay system (Molecular Probes, Inc. USA) according to the manufacturer's instructions. Briefly this system utilises a proprietary green fluorescent dye which undergoes strong fluorescent enhancement on binding cellular nucleic acids with a linear detection range between 50 to 250000 cells. Thus fluorescence may be used as a surrogate for cell number.

Cells were plated at a density of 1000 cells, in 100 $\mu$ L of cell culture medium per well, in a 96 well plate. Drugs were added a minimum of 5 hours later, in serial dilutions in cell culture medium, in 100 $\mu$ L volumes at 2x concentrations. Six days later cell culture medium was removed by inversion of the plate onto blotting paper and cells were gently washed once with 200 $\mu$ L PBS. Plates were frozen immediately for a minimum of one hour at -80°C and thawed to aid cell lysis. 200 $\mu$ L of 1x CyQuant cell lysis buffer supplemented with dye, made according to the manufacturer's instruction, was added immediately to each well and incubated at room temperature for 3-5 minutes. Sample fluorescence was then measured for each well using a CytoFluor II Fluorescence Multiwell Plate Reader and CytoFluor II software with filters at 480nm for excitation and 520nm for emission maxima. Cell proliferation was determined for mean values of duplicate samples as percentages relative to untreated cell samples.

### **3.9 RNA Gene Expression Analysis**

#### **3.9.1 RNA Isolation and Purification**

Typically  $8 \times 10^5$  adherent cells were plated in 35mm wells and treated with HDAC inhibitors as appropriate. After the relevant duration of exposure samples were harvested

for purification of total RNA. First 1ml of TRIzol reagent (a monophasic phenol/guanidine isothiocyanate solution, Invitrogen, UK) was added to cells which were incubated for 5 minutes at room temperature. Samples were then mixed by pipette 5 times, transferred to micro-centrifuge tubes and 200 $\mu$ l of chloroform was added. Samples were shaken for 15 seconds, incubated for 3 minutes at room temperature and centrifuged for 15 minutes at 12000g and 4°C. The RNA containing aqueous upper phase was transferred to a new tube and 500 $\mu$ l isopropanol was added with incubation for 10 minutes at room temperature, to induce RNA precipitation. The sample was then spun at 12000g for 10 minutes at 4°C and the supernatant discarded. 500 $\mu$ l of 75% ethanol was added to the pellet which was vortexed and centrifuged at 7500g for 5 minutes at 4°C. The supernatant was discarded and the sample re-centrifuged and any remaining supernatant removed prior to air drying the pellet for 5-10minutes. The RNA sample was then resuspended in 50 $\mu$ l RNase free water, incubated at 55°C for 10 minutes and stored at -70°C. RNA purity and concentration was then determined on an Agilent 2100 Bio analyzer according to the manufacturers instructions.

### 3.9.2 cDNA Production

First strand cDNA synthesis from RNA samples was performed using M-MLV reverse transcriptase as follows using reagents from Promega, UK. Firstly 1 $\mu$ g total RNA was combined with 1 $\mu$ l oligo(dT)<sub>15</sub> primer (which hybridizes to the poly(A) tail of mRNA) and water to 15 $\mu$ l and heated to 70°C for 5 minutes to melt secondary structure. Working on ice, the following components were added in the order shown.

MMLV 5x Reaction Buffer	5 $\mu$ l
dATP, 10mM	1.25 $\mu$ l
dCTP, 10mM	1.25 $\mu$ l
dGTP, 10mM	1.25 $\mu$ l
dTTP, 10mM	1.25 $\mu$ l

Recombinant RNasin Ribonuclease Inhibitor	25units
Nuclease free water	to 25 $\mu$ l final volume

The sample was heated to 42°C for 60 minutes, then 95°C for 5 minutes and then cooled immediately to 4°C. Samples were made up to a final volume of 100 $\mu$ l with water and finally stored at -70°C.

### 3.9.3 RNA Expression Analysis

Gene expression analysis was performed on cDNA samples from purified RNA by real time PCR (polymerase chain reaction) using TAQMAN Gene Expression Assays (Applied Biosystems). PCR was performed in reactions containing 5 $\mu$ l cDNA, 10 $\mu$ l 2x Universal Taqman PCR master mix and 1 $\mu$ l of the TAQMAN gene expression assay of interest to a final volume of 20 $\mu$ L. All reactions were performed in triplicate on a 384 well plate using a Dual 384-Well GeneAmp® PCR System 9700 sequence detection system (Applied Biosystems) using a thermal cycle protocol of 94°C for 10 minutes followed by forty cycles of 94°C for 15 seconds followed by 60°C for one minute. Control reactions containing no cDNA were run on each plate for each gene assay and no gene expression was detected in any of these controls. GAPDH expression was assessed in triplicate for each RNA sample on each plate run and expression profiles for other genes of interest were expressed relative to this. Expression assays were obtained from Applied Biosystems and are listed in table 3-4.

### 3.10 Statistical Analysis

Statistical analysis was performed using GraphPad Prism4 (GraphPad Software Inc, USA). Unpaired t tests and ANOVA tests were used for analysis of differences between means for results of two and multiple means respectively.

Gene	Assay ID	Accession Number	Comments
GAPDH	Hs99999905	NM_002046	Glyceraldehyde-3-phosphate dehydrogenase
ICB-1	Hs00191466	NM_004848	Basement membrane induced gene
RAB33A	Hs00191243	NM_004794	RAS oncogene family
ABCB1	Hs00184491	NM_000927	ATP-binding cassette, sub-family B (MDR/TAP) member 1, P glycoprotein
CTGF	Hs00170014	NM_001901	Connective tissue growth factor
SIRT4	Hs00202033	NM_012240	Sirtuin silent mating type information regulation 2 homolog 4
RGL1	Hs00248508	NM_015149	RalGDS-like gene
FOXC2	Hs00270951	NM_005251	Forkhead transcription factor
CDKN1A	Hs99999142	NM_078467	Cyclin dependant kinase inhibitor 1A (p21 <sup>(WAF1/Cip1)</sup> )
HDAC5	Hs00608357	NM_139205	Histone deacetylase 5

**Table 3-4 Gene expression assays used for real time PCR for results presented in this thesis**

## **4 Interaction Between BAG-1 and PPAR $\gamma$**

### **4.1 Introduction**

Data suggest a potential therapeutic role for PPAR $\gamma$  agonists in breast cancer, although this currently remains a research question with contradictory evidence regarding whether they will prove to be useful clinically.<sup>6</sup> In addition, a large amount of data exists surrounding the regulatory role for BAG-1 for other NHRs, including the ER in breast cancer where it is over expressed.<sup>4,10</sup> This led to the hypothesis that BAG-1 might influence PPAR $\gamma$ , which could be important clinically with respect to its potential as a therapeutic modality and interfere with its ability as a novel means to induce cell cycle arrest and differentiation. To explore this, investigation was performed in breast cancer cell lines to address the relevance of BAG-1 on the transcriptional activity, cell cycle and differentiating characteristics and cell proliferation control of PPAR $\gamma$ . In addition the ability of PPAR $\gamma$  to modify BAG-1 and HSP expression was addressed. The results are presented in this chapter.

### **4.2 PPAR $\gamma$ Stimulation Increases HSP40 And HSP70 But Not BAG-1 Protein Expression**

Data from Clay et al<sup>107</sup> using micro-array analysis indicates that PPAR $\gamma$  stimulation in MDA-MB-231 cells leads to increases in BAG-1, HSP70, HSC70 and HSP40 RNA expression. Experiments were performed therefore, to determine if PPAR $\gamma$  stimulation would induce increases in protein expression of these genes in breast cancer cells. Experiments were performed using Western Blot analysis to assess the effect of PPAR $\gamma$  activation on the protein expression of BAG-1 isoforms and heat shock chaperones in MCF-7 and MDA-MB-231 breast cancer cells. Cell mono-layers were exposed to a medium supplemented with PGJ2 at a concentration of

10 $\mu$ M over a time-course out to 16 hours. As shown in figure 4-1, none of the three main isoforms of BAG-1 exhibited altered protein expression induced by PPAR $\gamma$  stimulation in MCF7 cells (or in MDA-MB-231 cells, data not shown). However expression of the heat-shock proteins HSP40 and HSP70 was up regulated from as early as 8 hours in both cell lines, with a dose response effect to PGJ2 exposure. By contrast, HSC70 protein expression was not altered in response to PGJ2, reflecting its constitutive expression patterns. Band quantitation from similar experiments showed a consistent rise of HSP40 and HSP70 expression of between 5 and 10 times

Therefore PPAR $\gamma$  activity does not modulate BAG-1 protein expression in these breast cancer cell lines. However heat-shock protein expression is increased in response to PPAR $\gamma$  stimulation. This might constitute a mechanism by which interaction could occur in an indirect manner between PPAR $\gamma$  and BAG-1 as BAG-1 is known to exert multiple functions through HSPs.



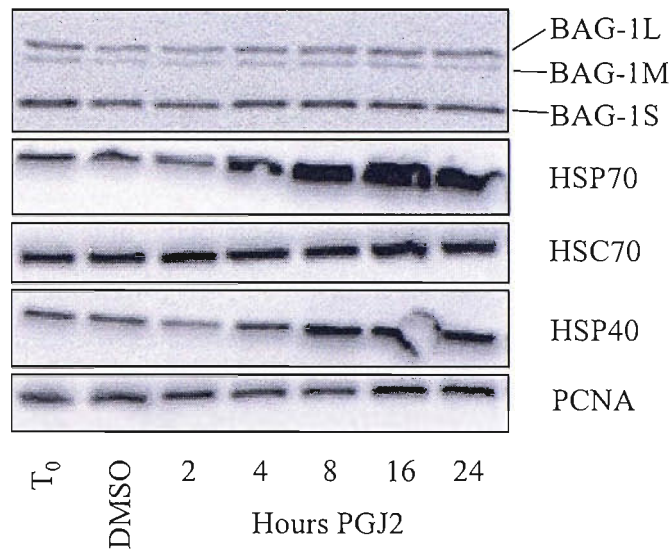


**Figure 4-1 BAG-1 and HSP protein expression following PPAR $\gamma$  stimulation in MCF7 breast carcinoma cells**

MCF7 cell mono-layers were harvested at time zero (T<sub>0</sub>) or exposed to culture medium supplemented with 10 $\mu$ M PGJ2 for the durations indicated or DMSO vehicle for 24 hours at an equivalent dilution. Samples were then processed for Western blot analysis using the indicated antibodies. PCNA is shown as a control for sample loading. Results are representative of three similar experiments.

### 4.3 BAG-1 Does Not Modulate Downstream Transcriptional Effects Of PPAR $\gamma$

BAG-1 has been shown to modulate trans-activation by a range of (but not all) NHRs in response to ligand, based on DNA response element reporter assays.<sup>10</sup> Therefore experiments were carried out to investigate the ability of BAG-1 to alter PPAR $\gamma$  activity patterns based on expression of target proteins. Cells were transfected with a reporter plasmid construct containing PPAR $\gamma$  response elements upstream of a minimal HSV-1 tk promoter and firefly luciferase gene. Initial dose response experiments confirmed activation of the PPRE reporter construct after transfection into breast cancer cell lines in response to the PPAR $\gamma$  ligand PGJ2 as shown in figure 4-2. Based on these results a concentration of 10 $\mu$ M PG2 was selected for further investigation of PPAR $\gamma$  induced activity in breast cancer cells.

Having established the ability to detect PPAR $\gamma$  activity using this system co-transfection in subsequent experiments was performed with pcDNA3 based expression plasmids containing BAG-1 isoforms (or empty pcDNA3 vector as a control) and a constitutively active  $\beta$ -galactosidase reporter as a control for transfection efficiency. The conclusion from these experiments is that BAG-1 isoforms do not alter PPAR $\gamma$  induced transcription in breast cancer cells. This is shown in figure 4-3, using BAG-1L in MCF-7 breast cancer cells after stimulation with PGJ2. This lack of BAG-1:PPAR $\gamma$  interaction was confirmed for each of the three major isoforms of BAG-1 (data not shown). This assay system was subsequently modified to address a range of factors that might have been relevant to detecting an interaction between PPAR $\gamma$  and BAG-1. Firstly, experiments confirmed a lack of BAG-1 interaction with PPAR $\gamma$  in a range of different cell lines that included two breast cancer cell lines (MCF-7 and MDA-MB-231) as well as HEK 293 transformed human embryonal kidney cells (chosen as they exhibit high transfection efficiency) and H376 oral carcinoma cells (discussed subsequently). PPAR $\gamma$  ligand dose and BAG-1 co-transfection 'dose' were modified and confirmed

a lack of effect for BAG-1 on reporter activity despite increasing the extent of BAG-1 over expression or the use of a wide range of PGJ2 dosages. The TZD troglitazone was assessed as an alternative PPAR $\gamma$  ligand to PGJ2, as PGJ2 has been shown to have some non-PPAR $\gamma$  mediated effects.<sup>181</sup> Use of the more PPAR $\gamma$  specific TZD however did not alter the results regarding a lack of interaction with BAG-1. Finally, PPAR $\gamma$  reporter plasmid experiments were also carried out in MCF7 clones that had been stably transfected to over express BAG-1L or BAG-1S isoforms. These cells were assessed in part, to be clear that efficiency of BAG-1 isoform transfection in partial transfection experiments, had not been the reason for failing to detect an effect on PPAR $\gamma$  activity. Again no BAG-1 modulation of PPAR $\gamma$  function was detected. In the case of each of these experimental modifications to PPAR $\gamma$  reporter assays, experiments were performed a minimum of twice and differences in reporter activity augmentation by PPAR $\gamma$  ligand showed no statistically significant difference with respect to increased BAG-1 isoform expression. These experimental modifications each supported the central finding that BAG-1 isoforms do not modulate the induction of PPAR $\gamma$  downstream transcription in response to ligand.

In experiments to provide a positive control to confirm a lack of BAG-1 modulating effect on PPAR $\gamma$  induced transcription, parallel co-transfection reporter assay experiments were performed using BAG-1L together with either vitamin D receptor or PPAR $\gamma$  response elements. Using VDR response element reporter plasmids, BAG-1L potentiates VDR activity in H376 or H400 oral carcinoma cell lines (Dr A. Hague, personal communication). Therefore this system was utilised for confirmatory evidence that BAG-1L fails to modulate PPAR $\gamma$  activity. This is shown in figure 4-4. PPAR $\gamma$  and VDRE reporter plasmids were separately co-transfected with or without BAG-1 followed by exposure to either PGJ2 or vitamin D3 respectively. Over expression of the BAG-1 isoform in the appropriate samples was confirmed by Western blot. The VDR is clearly potentiated by BAG-1L by over 2 fold in response to stimulation and this acts as a positive control to confirm BAG-1 failing to modulate PPAR $\gamma$ . Similar results were performed using MCF7 breast cancer cells. The VDR activation in this cell line was modest and in the region of

50% in response to vitamin D stimulation. The effect of BAG-1 co-transfection again potentiates this VDR activity but the effect is again modest at around 25% increase which failed to reach statistical significance compared to pcDNA3 control transfected cells. PPAR $\gamma$  activity again failed to show potentiation in response to BAG-1 co-transfection. Thus, the results of these comparative experiments when performed in MCF7 cells are less impressive in magnitude, and are not statistically robust, but are entirely consistent in the basic trends seen with those shown here in H376 cells.

In conclusion therefore, PPAR $\gamma$  can be placed together with the retinoid X and mineralocorticoid receptors in that it is resistant to the modulating effect on transcription which BAG-1 exerts on other NHRs.

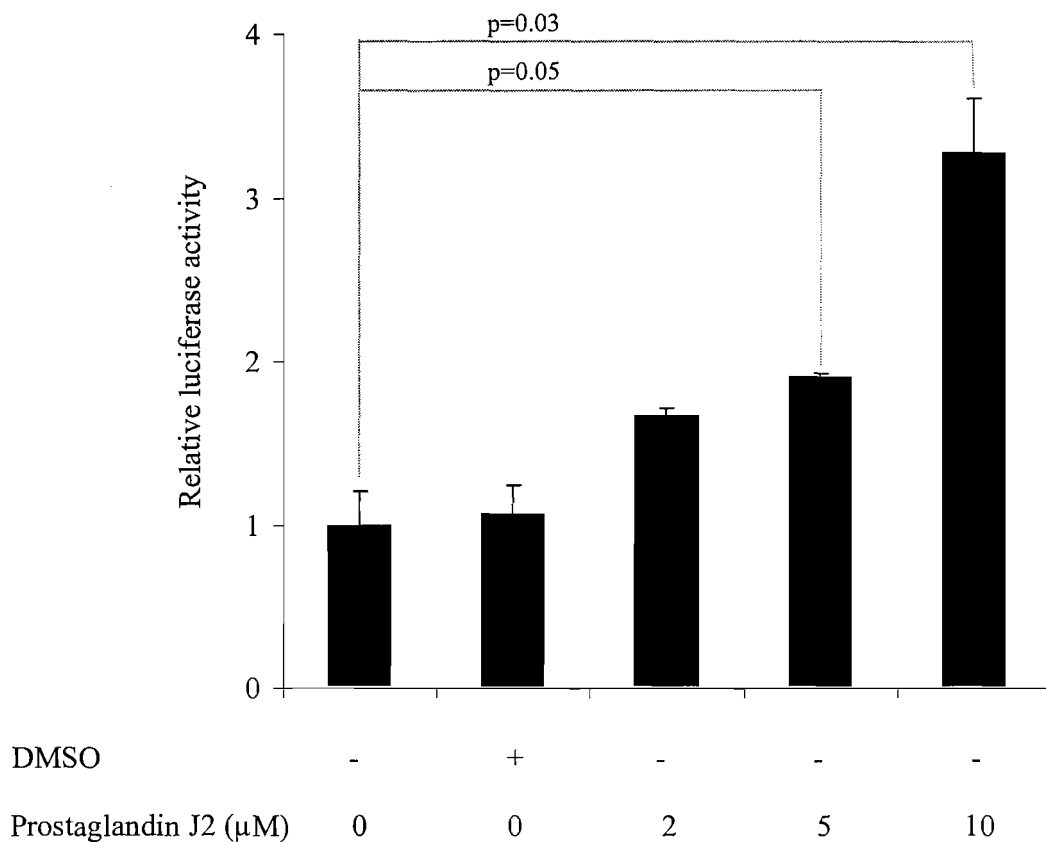


**Figure 4-2 Analysis of PPAR $\gamma$  activity with PGJ2 stimulation with respect to dose, in MCF7 breast cancer cells**

Cells were co-transfected with a PPAR $\gamma$  response element luciferase reporter plasmid (PPRE-tk-luc) and a constitutively active CMV- $\beta$ -galactosidase reporter. Samples were then exposed to medium supplemented with PGJ2 (or DMSO vehicle) at the indicated concentrations for 16 hours. Luciferase activity for cell lysates has been corrected for transfection efficiency with respect to  $\beta$ -galactosidase activity for each sample. Results show mean values +/- standard deviation (sd) for duplicate samples with respect to untreated samples which are normalised to one. Results are representative of two separate experiments and similar results were obtained in experiments performed in MDA-MB-231 breast cancer cells. Results reaching statistical significance ( $p < 0.05$ ) are indicated.

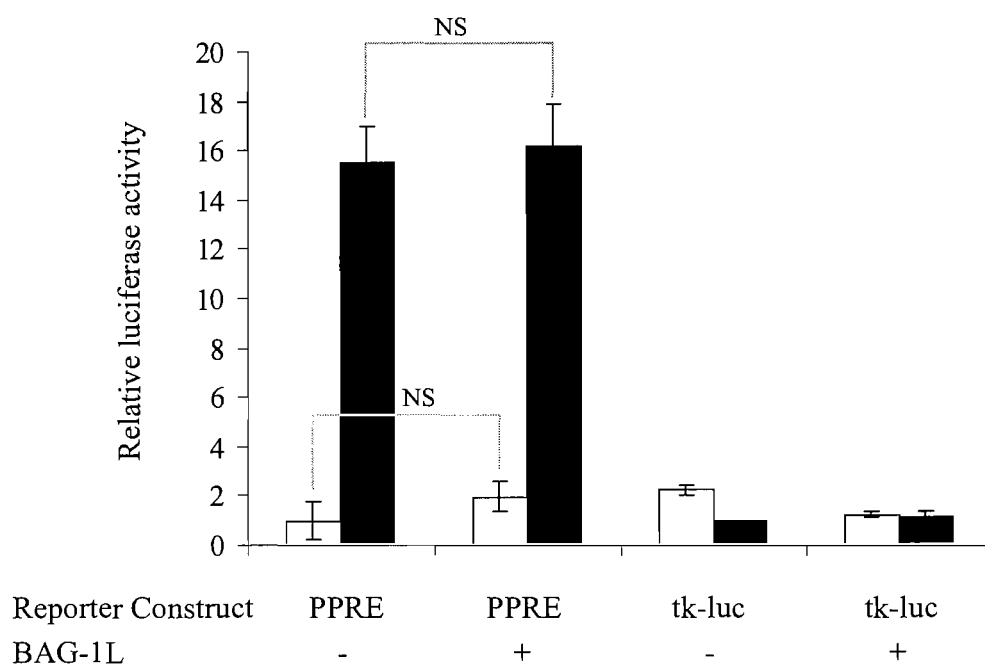


**Figure 4-3 Effect of BAG-1L co-transfection on PPAR $\gamma$  stimulated downstream transcription in MCF7 breast cancer cells**

Cell mono-layers were co-transfected with expression plasmids for BAG-1L or pcDNA3, together with PPRE-tk-luc or empty tk-luc control vector together and the constitutively active CMV- $\beta$ -galactosidase expression plasmid. Cells were either exposed to DMSO (solvent control, open bars) or underwent PPAR $\gamma$  stimulation (closed bars) with 10 $\mu$ M PGJ<sub>2</sub> as indicated for 16 hours. Results show luciferase activity of cell lysates corrected for  $\beta$ -galactosidase activity as mean values  $\pm$  sd for duplicate samples. Results are shown relative to un-stimulated PPRE/pcDNA3 samples which have been normalised to one and are representative of multiple experiments. BAG-1 co-transfection does not alter results for PPRE transfected samples as indicated (NS indicates  $p > 0.05$ ).

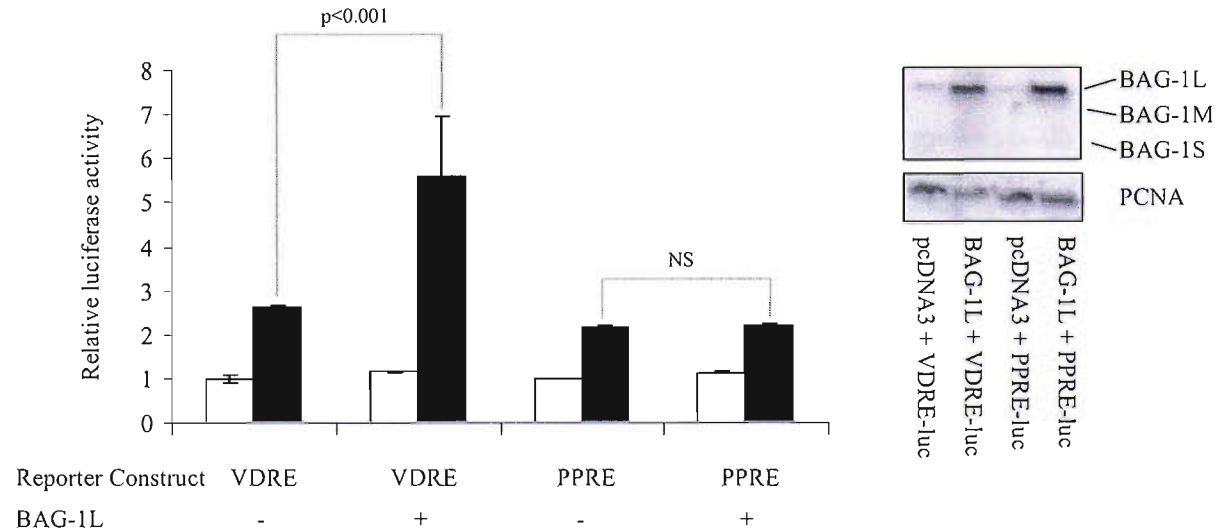


**Figure 4-4 Comparison of BAG-1L co-transfection in H376 cells on either VDR or PPAR $\gamma$  downstream transcription**

Cell mono-layers were co-transfected with expression plasmids for either pcDNA3 or BAG-1L, together with either pGL2-DR3-luc (VDRE) or PPRE-tk-luc firefly luciferase response elements, and with a constitutively active renilla luciferase plasmid. Cells were either untreated with DMSO vehicle (open bars), or treated (closed bars) with 100nM 1,25(OH) vitamin D3 for VDRE transfected cells, or 10 $\mu$ M PGJ<sub>2</sub> for PPRE transfected cells for 24 hours. Results show firefly luciferase activity of cell lysates, corrected for renilla activity as a control for transfection efficiency and are mean values +/- sd for triplicate samples. Results are shown relative to either the un-stimulated pcDNA3/VDRE or pcDNA3/PPRE samples that have each been normalised to one and are representative of two separate experiments. Western blots of parallel samples transfected with the same transfection mixture are shown for BAG-1 with PCNA as a control for sample loading. Results reaching statistical significance (p<0.05) by ANOVA are indicated.

#### **4.4 The Influence of BAG-1 Isoforms on PPAR $\gamma$ Mediated Differentiation in Breast Cancer Cells**

PPAR $\gamma$  is recognised to cause differentiation of breast cancer cell lines following stimulation by ligand. In keeping with its role as a key regulator of lipids and glucose one of the characteristic effects of the differentiation process, as a result of PPAR $\gamma$  stimulation, is the development of lipid droplets within cells. Initial experiments showed that this effect could be seen clearly within breast cancer cell mono-layers on light microscopy. As shown in figure 4-5, stimulation of MDA-MB-231 cells with 10 $\mu$ M PGJ2 produced clear morphological change after 16 hours which included the production of intra-cytoplasmic vacuoles and flattening out of the typically spindle shaped cells. To further utilise this approach for assessing differentiation, experiments were performed to assess lipid droplet accumulation directly by staining with the dye Nile Red using the method developed by Greenspan et al<sup>180</sup>. As shown in figure 4-6, PGJ2 induces differentiation of MCF7 cells with development of intra-cytoplasmic lipid droplets from 24 hours exposure onwards by comparison to DMSO vehicle controls. MCF7 cells are shown here as their morphology lends itself to appreciation of this effect, however similar effects were seen with MDA-MB-231 cells.

To investigate the ability of BAG-1 expression levels to modulate these responses, subsequent experiments were carried out in MCF7 cells which had been stably transfected to over express either the BAG-1S or BAG-1L isoforms or empty pcDNA3 vector as a control. Confirmation of over expression of the relevant BAG-1 isoform was obtained by Western blot analysis (figure 4-7A). These comprised three separate clones for each isoform, and were a kind gift from Dr G. Packham having been made previously by Dr R.C. Cutress in the author's laboratory. Clear increase in expression can be seen for the respective isoform above wild type levels which is of broadly similar extent for each individual clone. The Nile Red staining experiments were then repeated using these clones to assess the ability of forced



BAG-1 over expression to modulate the induction of differentiation in response to PPAR $\gamma$  stimulation following exposure to PGJ2. Figure 4-7B shows that BAG-1 isoform over expression in these cells did not effect PPAR $\gamma$  stimulated differentiation as determined by the formation of lipid droplets.

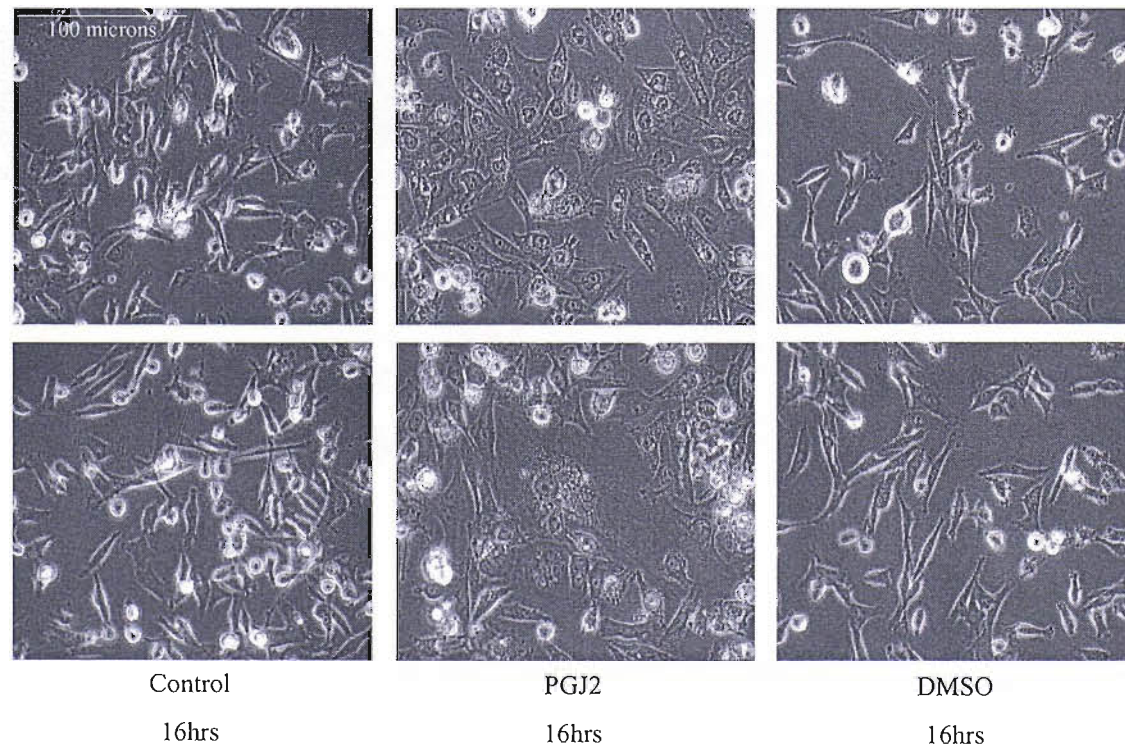


**Figure 4-5 Effect of PPAR $\gamma$  stimulation on MDA-MB-231 breast cancer cell morphology**

Cell mono-layers were grown on microscope cover slips in culture medium supplemented with either the PPAR $\gamma$  ligand PGJ2 at a concentration of 10 $\mu$ M for 16 hours (middle two images) or DMSO vehicle (right two images) or left untreated as controls (left two images). Samples were then fixed and visualised by light microscopy at 40x magnification. In the PGJ2 treated cells, flattening of cells and intra-cytoplasmic accumulation of lipid droplets can be seen. Results are representative of two separate experiments.

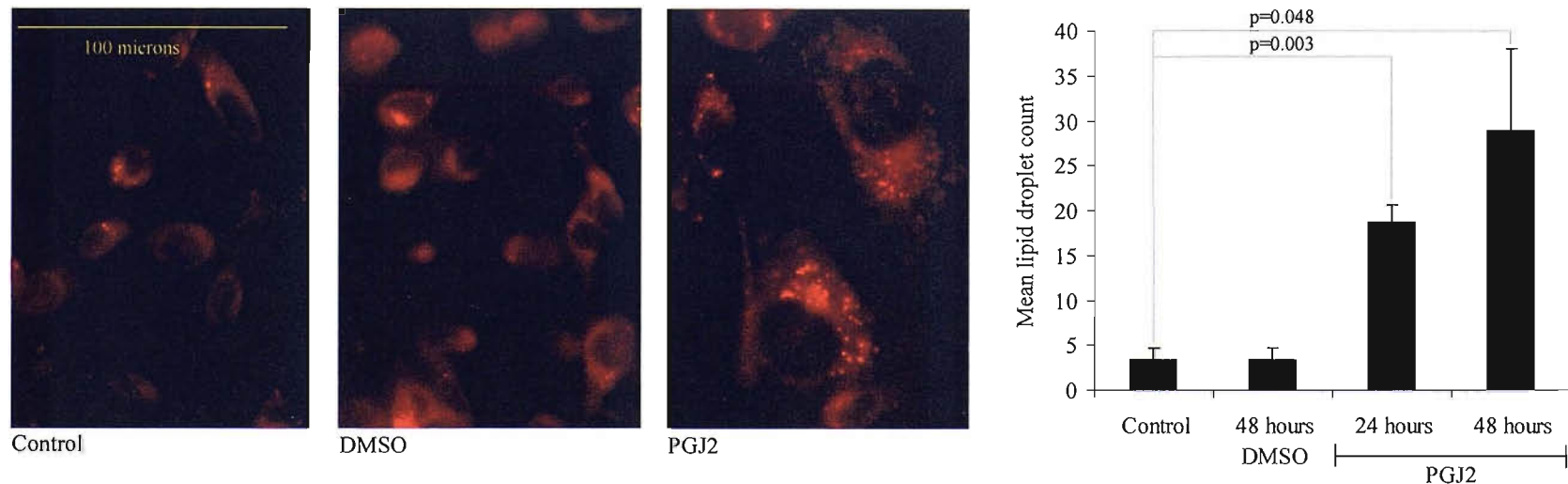


**Figure 4-6 Effect of PPAR $\gamma$  stimulation on average cell lipid droplet count assessed by Nile Red staining in MCF7 cells**

Cell mono-layers were exposed for the indicated durations to medium supplemented with either 10 $\mu$ M PGJ2 or DMSO vehicle or were left untreated as indicated. Samples were then stained for lipid droplet accumulation with Nile Red and imaged by fluorescence microscopy with representative images shown at 40x magnification. Results of mean lipid droplet count per cell are shown graphically and indicate mean lipid droplet counts per cell  $\pm$  SEM from two separate counts of five cells each and are representative of three separate experiments. Results reaching statistical significance ( $p < 0.05$ ) compared to controls are indicated.

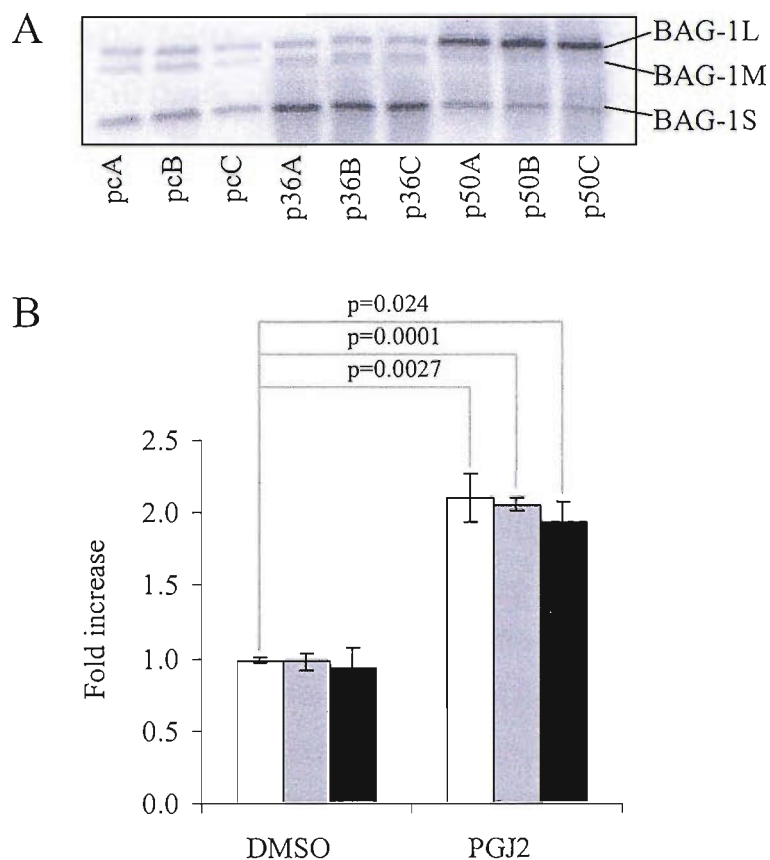


**Figure 4-7 The effect of BAG-1 over expression on differentiation induced by PPAR $\gamma$  stimulation in MCF7 stably transfected clones**

(A) Cells were stably transfected to over express pcDNA3 empty vector (pcA, pcB, pcC) or BAG-1S (p36A, p36B, p36C) or BAG-1L (p50A, p50B, p50C) and protein expression was confirmed by Western blot. (B) Cell mono-layers were stained for lipid droplet content with Nile Red and visualised by fluorescence microscopy at time zero or following exposure to medium supplemented with 10 $\mu$ M PGJ2 or DMSO vehicle for 16 hours. Mean cell lipid droplet count was determined for each sample from two separate counts of five cells each. Results indicate mean increase in lipid droplet count per cell  $\pm$  SEM for DMSO or PGJ2 treated cells compared to untreated samples as combined results for pcDNA3 clones (open bars), for BAG-1S over expressing clones (grey bars) or BAG-1L over expressing clones (black bars), representative of three separate experiments. (Statistically significant results ( $p < 0.05$ ) compared to pcDNA3 samples treated with DMSO are indicated.)

#### **4.5 Effect of BAG-1 Isoforms on PGJ2 Induced Breast Cancer Cell Cycle Arrest and Cell Death**

PPAR $\gamma$  activity induces apoptosis and alters cell cycle progression in breast cancer cells lines. Therefore experiments were performed to investigate the ability of BAG-1 isoforms to modulate these effects. Initial experiments were carried out to characterise the effect of PPAR $\gamma$  stimulation on cell death and cell cycle progression in MCF7 breast cancer cells by flow cytometry. Cells were treated for a varying durations to medium supplemented with the PPAR $\gamma$  ligand PGJ2, and then analysed, after propidium iodide staining, by FACS analysis. The percentage of cells in the respective points of the cell cycle, and of those in the sub-G0 phase indicative of cell death, was subsequently determined. As shown in figure 4-8 in MCF7 cells, the proportion of cells in the sub-G0 phase is increased from 48 hours onwards reaching an increase of over five fold at 72 hours, in cells exposed to PGJ2 compared to DMSO exposed controls. Thus cell death occurs in these cells in response to PPAR $\gamma$  stimulation. Analysis of the varying percentage of cells in cycle shows reproducible increases in the proportion of cells in G2M phase following PPAR $\gamma$  stimulation and a corresponding reduction of those in G0/G1. Therefore these experiments show the ability of the PPAR $\gamma$  ligand PGJ2 to cause cell cycle arrest in G2M and to induce cell death. Similar results were obtained in experiments using MDA-MB-231 cells (data not shown).

To determine the effect of BAG-1 isoforms on PPAR $\gamma$  induced cell cycle progression and induction of cell death, this experimental system was applied to the same MCF-7 clones that had been used previously in differentiation experiments, over expressing BAG-1S, BAG-1L or pcDNA3 empty vector as a control. Cells were exposed to PGJ2 for 96 hours followed by FACS analysis to determine cell cycle characteristics. (Figure 4-9A and see figure 4-7A for confirmation of BAG-1 expression status of MCF7 clones.) Results for flow cytometry experiments were averaged for each BAG-1 isoform type. As shown in figure 4-9B, over-expression of either the BAG-1S or BAG-1L isoforms does not affect cell cycle progression in

these experiments. Thus G2M arrest is shown with a corresponding decrease in G0/G1 cell fraction following PPAR $\gamma$  stimulation, regardless of the over-expression of either BAG-1S or BAG-1L. The degree of G2M arrest seen is the same as for pcDNA3 in extent to that seen in the preparatory experiments described in figure 4-8.

When considering the ability of PGJ2 to induce cell death however, differences were detected based on BAG-1 isoform expression status. This is shown in figure 4-9C based on the proportion of cells entering the pre-G0 fraction by flow cytometry. The MCF7 clones over expressing BAG-1S and BAG-1L were protected from progressing to cell death following PGJ2 exposure by comparison to those expressing pcDNA3.

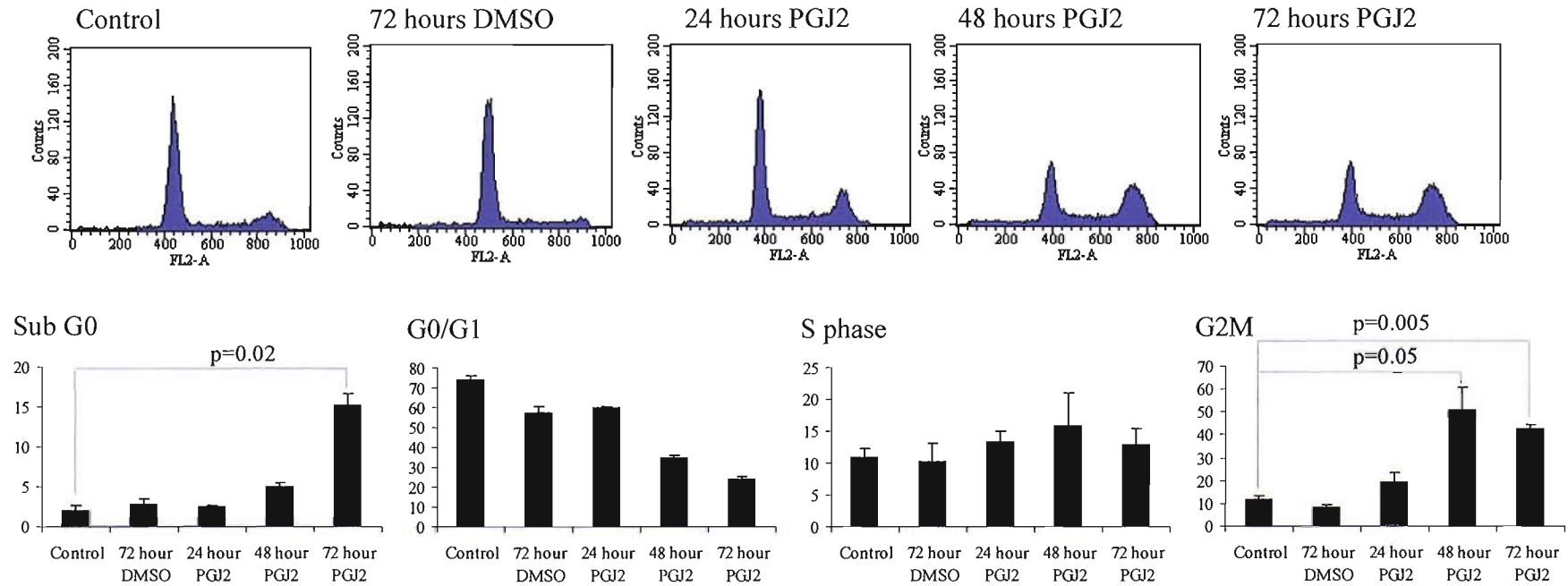
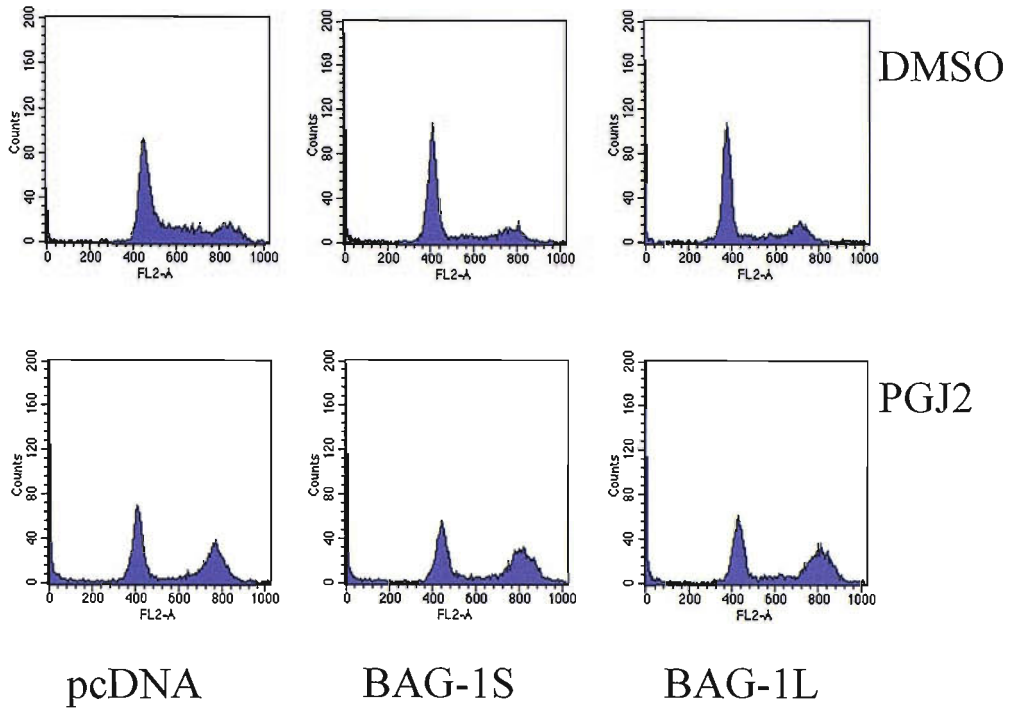


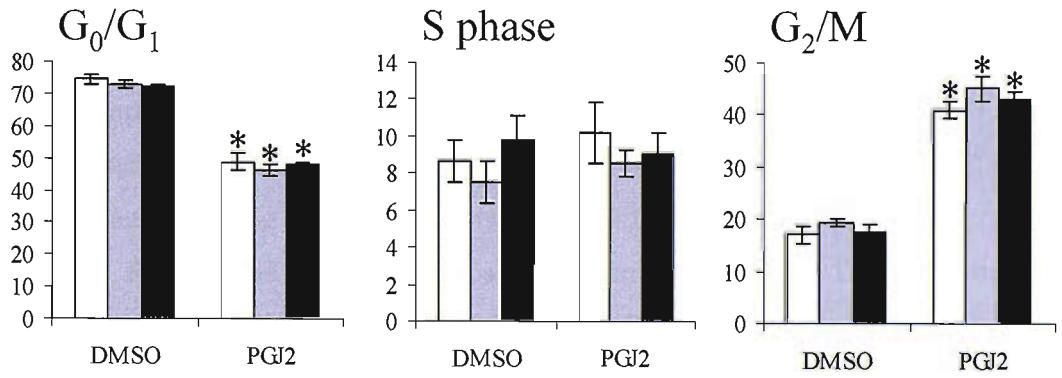
**Figure 4-8 Cell cycle analysis of MCF7 cells by flow cytometry following PPAR $\gamma$  stimulation**

Cell mono-layers were stained with propidium iodide and analysed by FACS at time zero (controls) or after exposure for the stated durations to culture medium supplemented with 10 $\mu$ M PGJ2 or with DMSO vehicle. Representative histograms obtained from FACS analysis of individual samples are shown (top panel) followed by graphs showing percentages of total cells in the indicated cell cycle divisions (bottom panel) with mean values +/- SEM of duplicate samples shown, representative of two separate experiments. Results reaching statistical significance relative to controls are indicated (p<0.05).

A



B





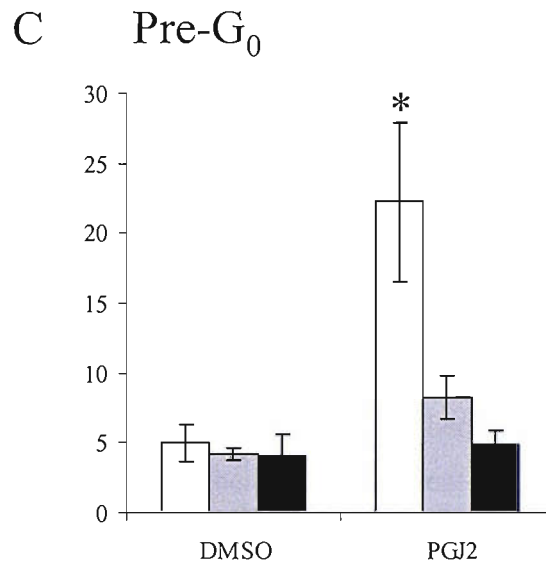


**Figure 4-9 Cell cycle analysis in BAG-1 over expressing MCF7 clones following PPAR $\gamma$  stimulation**

(A) Mono-layers of each clone were stained with propidium iodide and analysed by flow cytometry after exposure for 96 hours to 10 $\mu$ M PGJ2 or DMSO vehicle. Representative histograms are presented for clones transfected for the indicated BAG-1 isoform or pcDNA3, and treated with DMSO or PGJ2 as shown. Results express the mean percentage of cells (B) in the respective cell cycle phases or (C) in the pre-G<sub>0</sub> dead cell fraction averaged separately for pcDNA3 clones (open bars), for BAG-1S over expressing clones (grey bars) or BAG-1L over expressing clones (black bars). Results which reach statistical significance compared to DMSO treated pcDNA3 transfected cells are indicated ( $p < 0.05$ , ANOVA). Results are representative of four separate experiments. (See figure 4-7A for confirmation of BAG-1 isoform expression status.)

## 4.6 Discussion

Data presented in this chapter confirm that BAG-1 does not directly regulate PPAR $\gamma$  in breast cancer cells in-vitro. Specifically increased BAG-1 expression levels failed to impact on a number of key effects of PPAR $\gamma$  action including PPAR $\gamma$  mediated transcription. Attempts to address the effect of BAG-1 on transcriptional regulation via PPAR $\gamma$  included an extensive range of experimental approaches. Each of the three main BAG-1 isoforms was assessed, as it is known that for all other NHRs that are regulated by BAG-1, effects are isoform specific (albeit with significant inconsistencies between different NHRs). Other factors such as the PPAR $\gamma$  ligand (PGJ2 or TZD) and the breast cancer cell line used were addressed also. Finally, to provide a positive control for NHR modulation by BAG-1 in light of these negative results, investigation turned to the VDR using an oral carcinoma cell line where BAG-1 potentiated the VDR as predicted but had no effect on PPAR $\gamma$ . The failure therefore of BAG-1 to modulate PPAR $\gamma$  function at the transcriptional level, allows us to categorise it together with the mineralocorticoid and retinoid X receptors which are also impervious to BAG-1 interaction.

Having confirmed that BAG-1 fails to modulate transcriptional activity, work proceeded to address important downstream biological effects of PPAR $\gamma$ , including differentiation, cell cycle arrest and the induction of cell death. Results presented here show that BAG-1 does not modify differentiation or cell cycle arrest induced by PPAR $\gamma$ . This may be important, as these are biological processes that would be expected to be key in the potential use of PPAR $\gamma$  ligands, such as the TZDs, as a differentiating anti-cancer therapy. In contrast, using stably transfected MCF7 clones, over-expression of BAG-1S or BAG-1L was able to block the induction of cell death seen with PPAR $\gamma$  stimulation. In light of the other data presented here it is proposed that this is a non-specific generalised effect of BAG-1 as an anti-apoptotic molecule, rather than a specific interaction with PPAR $\gamma$  itself. This is consistent with data produced by the author's laboratory, which has shown BAG-1 to block apoptosis by a chaperone dependant pathway in response to a diverse range of pro-apoptotic stimuli including heat shock, radiation and conventional

cytotoxics.<sup>38</sup> Interestingly in the data presented in that work, BAG-1 isoforms were found not to be increased in response to the apoptotic stimuli used but the shortest isoform BAG-1S re-localised from the cytoplasm to the nucleus. Clay et al had shown mRNA levels of a variety of genes that were increased or decreased in MDA-MB-231 breast cancer cells in response to two hours exposure to PGJ2. The genes with increased mRNA expression included HSPs and BAG-1 (perhaps counter intuitively as an anti-apoptotic protein). They did not confirm alterations at the protein level for these genes or investigate them further in this paper. In addition they confirmed the induction of genes critical to cell cycle arrest and apoptosis, including the cyclin-dependent kinase inhibitor p21<sup>(WAF1/Cip1)</sup> as well as the induction of caspase activation.<sup>107</sup> Work presented here has confirmed that BAG-1 expression at the protein level is not altered in response to PPAR $\gamma$  stimulation in breast cancer cells using PGJ2. Re-localisation of the short BAG-1 isoform was not addressed in response to PPAR $\gamma$  stimulation but would be predicted to also induce this sub-cellular re-localisation.

One aspect of the data regarding PPAR $\gamma$  activity that complicates much of the literature surrounding its relevance to cancer is the choice of ligand to investigate its actions. PGJ2 is most commonly used; however data exists to show that some of its actions are likely to occur through mechanisms independent of PPAR $\gamma$ .<sup>181</sup> This includes the fact that PPAR $\gamma$  is required for the induction of apoptosis in breast cancer cells by TZDs but not for PGJ2. Data presented here confirm certainly that transcriptional activation through the PPRE reporter is not modulated by BAG-1 using either PGJ2 or TZDs. Thus we can be confident that regardless of the ligand used, BAG-1 is not a modulator of PPAR $\gamma$ . Other potential mechanisms for PGJ2 induced apoptosis may include the NF- $\kappa$ B pathway, inhibition of the ubiquitin proteasome system and induction of reactive oxygen species (ROS). The finding in this work that BAG-1 exerts a non-specific block on PGJ2 induced apoptosis, suggests that it's over expression in breast cancer cells may be able to abrogate PPAR $\gamma$  dependant effects of PPAR $\gamma$  ligands as well as other potential non-PPAR $\gamma$  mediated effects of arachidonic acid metabolites.

In attempting to understand why BAG-1 fails to interact with PPAR $\gamma$ , we are hampered by the lack of a cohesive mechanistic explanation for the differences described in the literature, of patterns of interaction between other NHRs and BAG-1 isoforms. The majority of the available data surrounds the GR where it is known that the BAG-1M and BAG-1L isoforms will down regulate receptor activity. This inhibitory activity of BAG-1 on the GR is likely to be multi-factorial. Data suggests both the ability of BAG-1 to inhibit GR:HSP90 heterocomplex assembly through HOP release from the receptor chaperone complex, but in addition BAG-1 can reduce GR ligand binding at higher expression levels including those induced through transfection.<sup>74</sup> However in separate work BAG-1 has been shown to co-localise with the GR:HSP70 complex to the nucleus and inhibit DNA binding.<sup>33,75</sup> Data to elucidate whether the mechanisms of BAG-1 potentiation (ER, AR, VDR) or inhibition (RAR, TR, VDR) of some NHRs and the lack of interaction with others (MR, RXR and now PPAR $\gamma$ ) is mediated by these same mechanisms of receptor complex assembly, ligand binding and DNA binding does not exist.

Data regarding the maturation and co-activator and repressor mechanisms for PPAR $\gamma$  are less well understood compared to the well-defined model for the GR. The lack of information regarding the requirement for molecules such as HSP70 and HSP90 to take part in receptor maturation processes prior to and following ligand binding, as seen with the GR makes it impossible to know if this is the reason for BAG-1 failing to interact with PPAR $\gamma$ . BAG-1:HSP interactions may therefore remain the explanation for these observed effects. Equally however it remains unclear if BAG-1 fails to bind the PPAR $\gamma$  molecule directly as shown for receptors such as the GR, ER TR and AR.<sup>4,16</sup> Such interactions have been shown for example with the ER using co-immunoprecipitation experiments.<sup>4</sup> This approach was not attempted for the investigation of a potential BAG-1:PPAR $\gamma$  interaction. Such an experiment would be hampered if, as would be predicted, it were negative based on the other work presented here, by the need for some form of positive control although the ER:BAG-1 interaction would provide a potential means for doing this.

Where does this leave us in addressing the relevance of BAG-1 expression status for the still experimental and unproven approach of the use of PPAR $\gamma$  ligands in breast cancer? If increased BAG-1 expression does exert a non-specific block on PPAR $\gamma$  induced apoptosis, this might provide a mechanism to explain the negative clinical data in breast cancer seen in the trial by Burstein et al where clinical benefit from PPAR $\gamma$  stimulation was not seen in patients with advanced disease.<sup>100</sup> No attempt was made in this study to determine hormonal or PPAR $\gamma$  expression status which, along with the treatment refractory advanced disease in this cohort, may have limited the opportunity to detect clinical benefit. The BAG-1 expression status of this cohort is of course also unknown. This raises the point that, as with other therapies targeting specific mechanisms that underlie cancer proliferation, knowledge of the expression status of the target is likely to be key to detecting and potentiating therapeutic benefit. In terms of BAG-1 expression, it remains unclear which effect might be more important to tumours treated with PPAR $\gamma$  ligands: differentiation and cell cycle arrest on the one hand (not BAG-1 susceptible according to data presented here) or cell death via apoptosis (BAG-1 inhibited based on this study, via mechanisms which are proposed to be indirect). If the anti-apoptotic effects of BAG-1 are able to counteract PPAR $\gamma$  benefits in breast cancer albeit via a non-specific mechanism, one could perhaps envisage combination treatment with agents able to specifically block the action of BAG-1 in breast cancers where it is over-expressed. The in-vitro data presented here is consistent with the hypothesis that this would be required for optimal tumour cell kill. Cell culture and breast cancer cell xenografts would be the obvious way forward to begin to test this if BAG-1 attenuating therapies could be developed. Furthermore, it remains unclear what the effect might be of BAG-1/PPAR $\gamma$  opposing actions in the poor prognostic setting of ER negative breast cancer where we do not have as clear an idea for a potential BAG-1 role and where we remove the potential of PPAR $\gamma$ /ER interaction.

In summary therefore the evidence presented here is conclusive in demonstrating that BAG-1 and PPAR $\gamma$  do not interact. It would seem therefore that BAG-1 over-expression is not likely to be a barrier to the development of PPAR $\gamma$  agonists such as TZDs as potential modulating agents of cell cycle progression and differentiation processes in

breast cancer. In light of this data, work then proceeded to a second potential modality for breast cancer therapy, regarding inhibitors of histone deacetylase enzymes. Like PPAR $\gamma$  agonists, these compounds have also been shown to have interesting effects on cancer cell lines, including those of the breast, which include both cell cycle arrest and differentiation. This work is the subject of the following two chapters.

## **5 Characterisation of a Novel HDAC Inhibitor Spiruchostatin A**

### **5.1 Introduction**

HDAC inhibitors show promise as a potential novel therapy for malignant disease. The ability of FK228 to exhibit selectivity for class I HDAC enzymes compared to other non-HDAC selective structural classes of inhibitors raises the possibility of the development of improved efficacy/toxicity relationships for these compounds. The natural compound Spiruchostatin A represents a potential new HDAC inhibitor and was produced synthetically by the Department of Chemistry in Southampton University. It was first necessary to characterise its biological activity and determine whether it functioned as an HDAC inhibitor. Having done so, investigation was performed to assess its ability to produce the range of biological effects characteristic of HDAC inhibitors including modulation of gene expression profiles, induction of cell cycle arrest and cell death, inhibition of cell proliferation and induction of differentiation. Following on from this, experiments were performed to investigate whether Spiruchostatin A affects normal and malignant cells *in vitro*. This section describes results that characterise the biological activity of Spiruchostatin A with respect to these outcomes.

### **5.2 Spiruchostatin A Induces Histone Acetylation**

The bicyclic compound Spiruchostatin A is structurally similar to FK228 and would therefore be predicted to induce acetylation of lysine residues on histones as well as other proteins and to alter gene expression patterns. To investigate this, MCF7 and BT474 breast carcinoma cell mono-layers were exposed to Spiruchostatin A in dose

response studies. These samples were processed for Western blotting following SDS-PAGE to assess acetylation of specific lysine residues of nucleosomal histones, and expression status of proteins previously shown to be regulated by histone acetylation (HER2 neu and EGFR), and a protein not previously documented to be regulated by HDAC inhibition,  $\beta$ -catenin. Results are shown in figure 5-1.

Acetylation was seen in response to nanomolar concentrations of Spiruchostatin A at specific lysine residues on histones H3 and H4. A dose response effect was apparent in both cell lines and was broadly of similar potency in each. This confirms that Spiruchostatin A is indeed an inhibitor of histone deacetylation as predicted from its structural similarity to FK228. All histone lysine specific residues assessed to date have undergone induction of acetylation in response to Spiruchostatin A at doses of 10nM and above in MCF7 cells. Furthermore all cell lines assessed to date have shown histone acetylation to be induced by Spiruchostatin A including MCF7 and BT474 breast cancer cells and normal human dermal fibroblasts.

With respect to gene expression, a number of genes were seen to exhibit altered expression either at the protein level (shown here in figure 5-1 and for p21<sup>(WAF1/Cip1)</sup> in section 6.3) or at the level of mRNA expression (shown in section 6.2) in response to Spiruchostatin A exposure. For example the tyrosine kinase cell signalling receptors EGFR and HER2 were reduced in HER2 over-expressing BT474 cells. These receptors were assessed as both are relevant to breast cancer cell proliferation, and in the cases of HER2 as both a prognostic indicator and an established therapeutic target. Interestingly SAHA has been shown to induce acetylation of the chaperone HSP90 leading to its reduced association with HER2 and subsequent ubiquitylation dependant degradation of HER2.<sup>162</sup> This may represent a mechanism for the HER2 depletion seen here following HDAC inhibition. The same may be true for the EGFR which is also an HSP90 'client' protein. Increased p21<sup>(WAF1/Cip1)</sup> expression is commonly used as a key example of HDAC inhibitor downstream effect and this was also shown to be reduced following Spiruchostatin A exposure. (These results are presented later in chapter 6 as part of



comparative work with other HDAC inhibitors.) A further gene assessed at the protein level was  $\beta$ -catenin whose levels were reduced in both cell lines tested (figure 5-1), which may have significance in cell signalling as well as the cell adhesion characteristics following treatment explored in section 5.7.  $\beta$ -catenin has been shown to undergo acetylation in response to HDAC inhibition, but at the time these experiments were performed was not known to have expression altered in response to HDAC inhibitor exposure.

Therefore, the bicyclic tetrapeptide compound Spiruchostatin A is a potent inducer of histone acetylation at nanomolar concentrations in breast cancer cell lines. It is also able to effect expression of protein targets known to be altered by this class of drugs and alter protein expression targets relevant to cell signalling and adhesion.

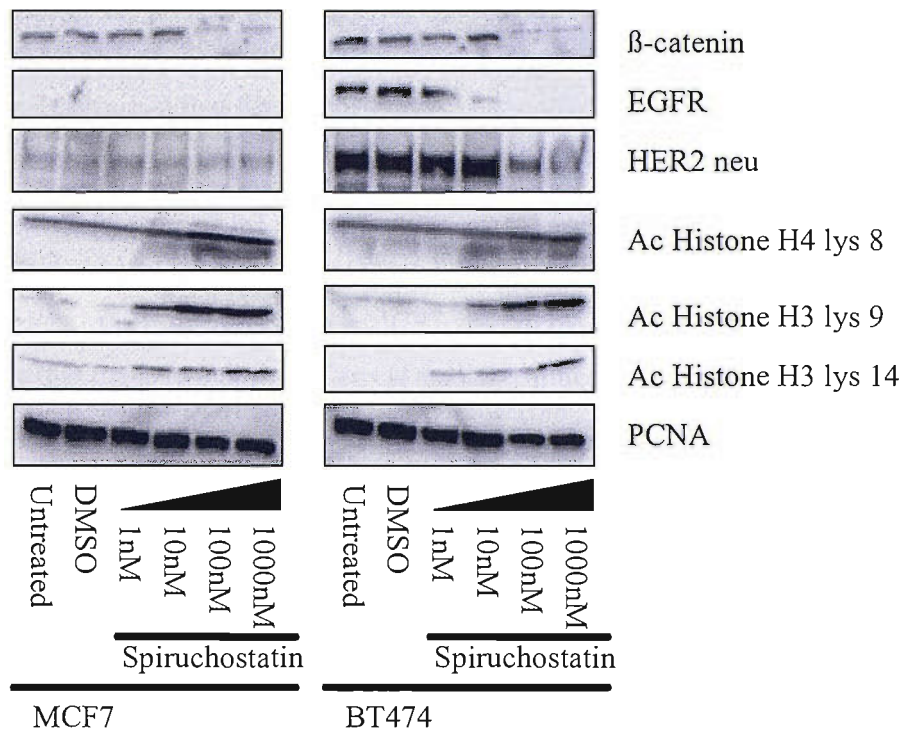


**Figure 5-1 Protein acetylation and expression with respect to Spiruchostatin A dose in MCF7 and BT474 breast cancer cells**

MCF7 and BT474 cell mono-layers were exposed to culture medium supplemented with the indicated concentrations of Spiruchostatin A, or DMSO vehicle, and harvested at 24 hours for Western blot analysis using the indicated antibodies. PCNA is shown as a control for sample loading. All protein or acetylation targets shown were assessed in a minimum of two separate experiments and representative examples are shown.

### 5.3 Spiruchostatin A Induces Cell Cycle Arrest and Cell Death

Having determined that Spiruchostatin A is an inducer of histone acetylation, experiments were performed to assess its effects on cell cycle progression and apoptosis as key examples of known biological effects of HDAC inhibition. Cell cycle arrest has been shown to occur in both G1 and G2M phases of the cell cycle, in a variety of cell lines including MCF7 and MDA-MB-231 breast cancer cells. It appears that these two points of arrest are determined in dose and time dependant ways, and may of course coexist. Broadly speaking the available evidence suggests that G1 arrest occurs at earlier time points and lower doses in response to HDAC inhibition but that G2M arrest is seen at later time points and higher doses. In many studies G2M arrest is the predominant effect elicited. From around 24 hours onward cells enter an irreversible apoptotic pathway.<sup>136,147,148,154-156</sup>

To assess the ability of Spiruchostatin A to produce these effects, MCF7 cells were treated in dose response experiments for 72 hours. Samples were then analysed by flow cytometry following propidium iodide staining and analysed for cell cycle phase and induction of cell death. Spiruchostatin A (figure 5-2) was found to cause a very slight (but statistically non-significant) increase in G0/G1 cell fraction and corresponding decrease in S phase fraction at a dose of 10nM, however at higher doses of 100 and 1000nM a marked (and statistically significant) G2M arrest became apparent. This mirrors the dose specific effects described for SAHA where G1 arrest has been shown at lower doses (and shorter treatment durations) and G2M arrest predominating at higher dose (and longer exposure).<sup>136,147,148</sup>

With regards to induction of cell death, as assessed by the pre-G0 cell fraction, a modest effect was seen at 10nM but at doses of 100nM and above this becomes more pronounced compared to DMSO vehicle exposed cells (figure 5-3).

In conclusion therefore, in the dose range in which histone acetylation is seen, Spiruchostatin A exerts cell cycle arrest which predominates in G2M phase and induces cell death in breast cancer cells.

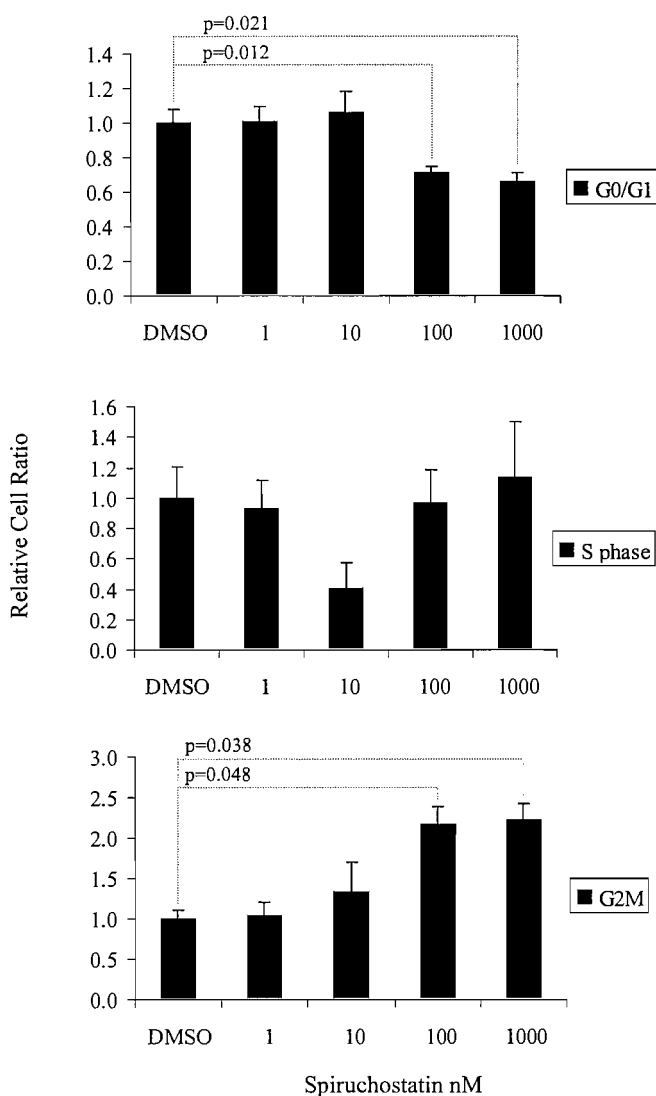


**Figure 5-2 Cell cycle effects of Spiruchostatin A relative to dose in MCF7 breast carcinoma cells**

MCF7 cell mono-layers were exposed to medium containing the indicated concentrations of Spiruchostatin A or DMSO vehicle for 72 hours and stained with propidium iodide for cell cycle analysis by flow cytometry. Mean values +/- sd of three determinations (and representative of two separate experiments) are shown and represent the proportion of cells in the indicated cell cycle phases, of gated cells remaining in cell cycle, relative to DMSO treated cells which are normalised to one. Results reaching statistical significance ( $p < 0.05$ ) compared to DMSO treated samples are indicated.

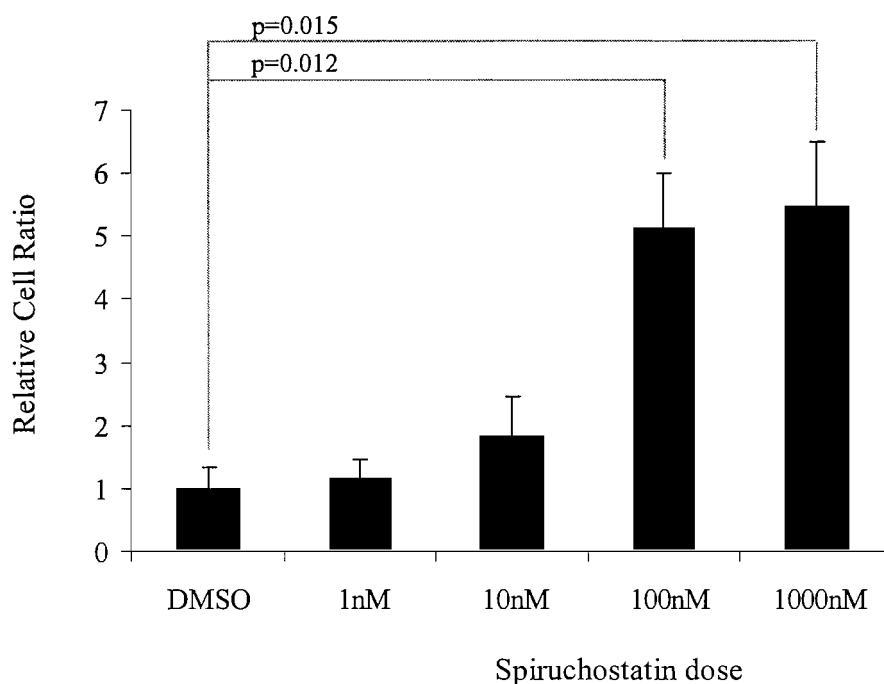


**Figure 5-3 Induction of cell death by Spiruchostatin A with respect to dose in breast cancer cells**

MCF7 cell mono-layers were exposed to medium containing the indicated concentration of Spiruchostatin A or DMSO vehicle and harvested at 72 hours for staining with propidium iodide and analysis by flow cytometry. Cell death was determined as the number of cells in the hypo-diploid pre-G<sub>0</sub> region relative to the total number of gated cells. Mean values +/- sd of three determinations (and representative of two separate experiments) are shown expressed relative to samples treated with DMSO vehicle which have been normalised to one. Results reaching statistical significance ( $p < 0.05$ ) compared to DMSO treated controls are indicated.

#### **5.4 Spiruchostatin A Induces Differentiation in Breast Cancer Cells**

In addition to the ability to induce cell cycle arrest and cell death, HDAC inhibitors are also recognized to induce differentiation of malignant cells in-vitro and this is likely to be relevant to their therapeutic efficacy in vivo.<sup>131,136</sup> It was therefore important to determine if Spiruchostatin A was able to produce a differentiating effect in addition to its cell cycle and cell death effects. To assess this for breast cancer cells, MCF7 cells were grown on microscope cover slips and treated with increasing doses of Spiruchostatin A for 24 hours. Samples were then stained with Nile Red to assess for lipid droplet accumulation as a useful marker for induction of differentiation in breast cancer cell lines.<sup>180</sup> Results are shown in figure 5-4. A clear increase in the mean number of cytoplasmic lipid droplets seen per cell of around six fold is demonstrated. Therefore Spiruchostatin A is able to induce differentiation in breast cancer cells in addition to its other effects and in a manner similar to that described for SAHA.<sup>136</sup>

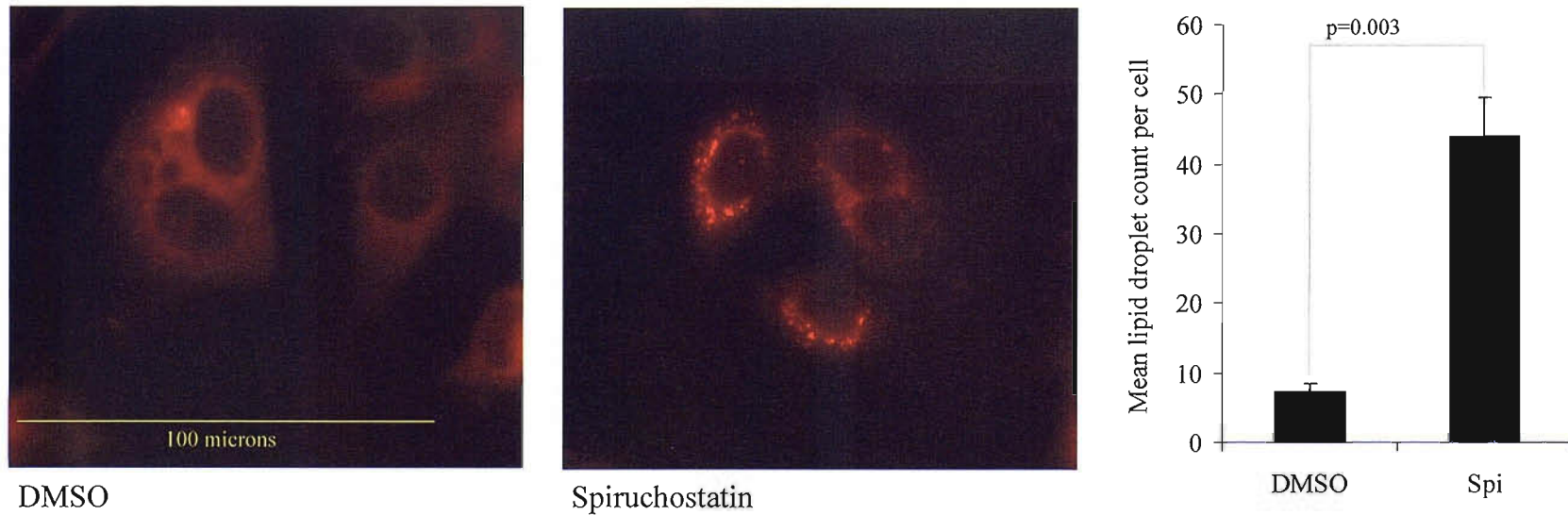


**Figure 5-4 Spiruchostatin A induced differentiation in MCF7 breast carcinoma cells**

MCF7 cell mono-layers plated on microscope cover slips were exposed to medium supplemented with 10nM Spiruchostatin A for 24 hours or DMSO vehicle. Samples were then fixed and stained with Nile Red and imaged by fluorescent microscopy. Representative cell sample images from multiple experiments are shown at 40x magnification. Results of mean lipid droplet count per cell are shown graphically and indicate mean lipid droplet counts per cell +/- SEM from two separate counts of five cells each representative of multiple experiments.



## **5.5 Spiruchostatin A Has Greater Potency In Malignant Compared To Normal Cells In-Vitro**

HDAC inhibitors have been shown to have greater potency for inhibiting cell proliferation for malignant rather than normal cells in-vitro and this is mirrored by the comparative tolerability of these compounds compared to conventional cytotoxics seen during in-vivo administration.<sup>147</sup> This may be an important feature for this class of compounds in terms of their potential use as anti-cancer agents, as histone and non-histone protein acetylation is a ubiquitous phenomenon seen in all cell types. The ability to optimise such a therapeutic window clinically may allow for improvement in efficacy/toxicity ratios.

Initial experiments to assess comparative effects of Spiruchostatin A between normal and malignant cells addressed the effect on cell proliferation. Assays were performed in parallel on MCF7 breast carcinoma cells and normal human dermal fibroblasts. Cells were exposed to drug in serial dilutions for 6 days and cell proliferation was determined using the CyQuant assay system which utilises a DNA binding fluorescent dye as a surrogate marker for cell number. Results are shown in figure 5-5. Non linear regression analysis of the data in this experiment shows that Spiruchostatin A has a higher IC<sub>50</sub> value in normal human dermal fibroblasts of 23.9nM (95% CI 18.81 to 30.41) compared to 5.80nM (95% CI 5.04 to 6.66) for MCF7 cells.

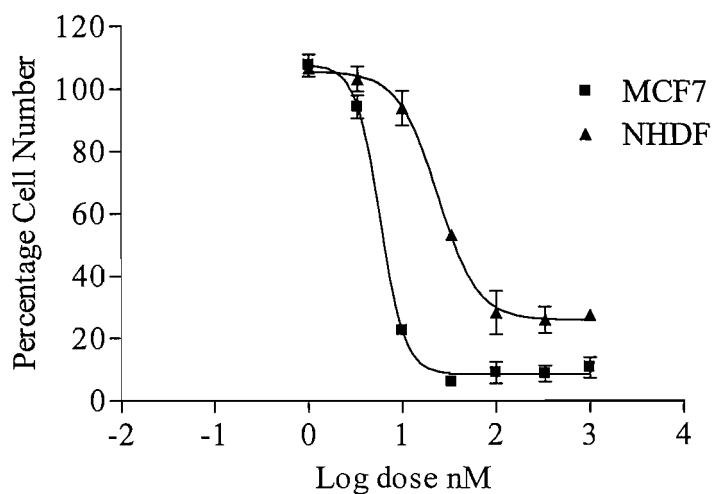


**Figure 5-5 Cell proliferation following Spiruchostatin A exposure for MCF7 versus normal human dermal fibroblasts**

MCF7 and normal human dermal fibroblast (NHDF) cell mono-layers were exposed to medium supplemented with Spiruchostatin A at serial dilutions as indicated for 6 days. Samples were then analysed for cell number using the CyQuant fluorescent assay system. Results show mean values +/- SEM for duplicate samples expressed as percentages relative to untreated cells together with non-linear regression curves. Samples exposed to cell culture medium supplemented with DMSO vehicle alone showed no significant deviation in cell proliferation from untreated cells (data not shown).  $IC_{50}$  values are presented in the text. Overall results are representative of multiple experiments.

## **5.6 Spiruchostatin A Exhibits Differences In Induction Of Cell Cycle Arrest And Cell Death Between Malignant And Normal Cells**

To determine whether differences in potency for inhibition of cell proliferation, between MCF7 breast carcinoma cells and normal human dermal fibroblasts, translated into biological differences in cell behaviour in response to these drugs, experiments were performed to assess protein acetylation, cell cycle progression and apoptosis. Firstly in dose response experiments for Spiruchostatin A, Western blot analysis at 24 hours showed that normal human dermal fibroblasts underwent histone acetylation at specific lysine residues. The pattern of acetylation appears to be broadly the same as for MCF7 cells in terms of dose response and the fact that all histone lysine residues assessed seem responsive to increased acetylation after Spiruchostatin A (figure 5-6). Therefore differences in biological effect and inhibition of cell proliferation, seen between malignant and normal cells are not likely to be due to differences in the way that Spiruchostatin A and perhaps other HDAC inhibitors interact with HDAC enzymes per se in these differing cells.

Secondly, parallel experiments to assess the effect on cell cycle progression (figure 5-7) and cell death (figure 5-8) were performed in these two cell lines in dose response assessments for Spiruchostatin A exposure at 72 hours. Results indicate that the G2M arrest and a corresponding decrease in G0/G1 fraction seen in MCF7 cells, is not found in the non-malignant fibroblasts. Instead the fibroblasts undergo cell cycle arrest during S phase from doses of 10nM upwards. Induction of cell death (pre-G0 fraction) is more pronounced in MCF7 cells than fibroblasts with approximately double the number of cells progressing to cell death as a ratio to DMSO treated cells at Spiruchostatin A doses of 100nM and above. Fibroblasts however, can clearly be made to undergo cell death but have a comparative rather than an absolute resistance. This mirrors the IC<sub>50</sub> results for cell proliferation discussed elsewhere.

Therefore, results comparing Spiruchostatin A effects in malignant versus normal cells indicate that normal cells are resistant to G2M cell cycle arrest effects seen in malignant cells but instead arrest in S phase. With respect to induction of cell death and cell proliferation, there seems instead to be a relative sparing of effects rather than an absolute resistance at lower doses for normal versus malignant cells.

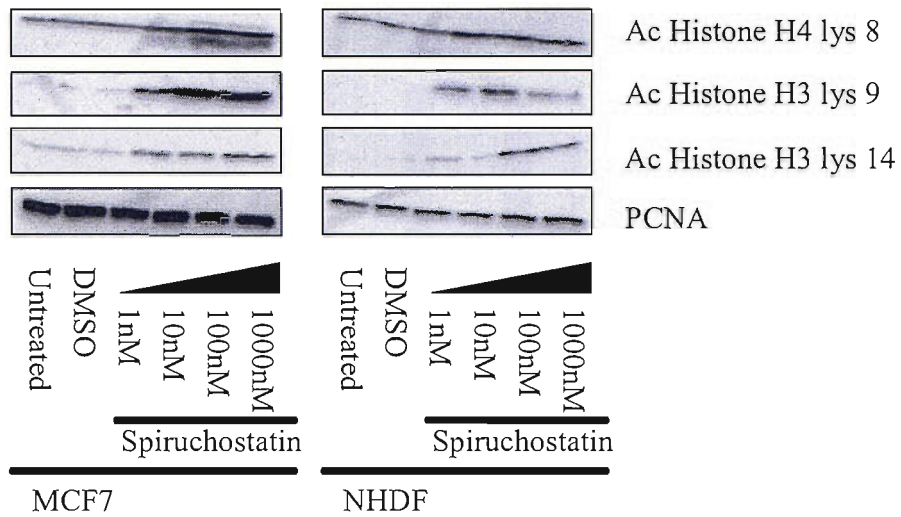


**Figure 5-6 Comparison of histone acetylation status following Spiruchostatin A exposure in MCF7 breast carcinoma cells and normal human dermal fibroblasts**

Cell mono-layers were exposed to medium supplemented with Spiruchostatin A at the indicated concentrations or DMSO vehicle for 24 hours. Samples were then harvested for analysis by Western blot using the indicated antibodies. PCNA is shown as a control for sample loading. The data for MCF7 cells is that presented in figure 5-1 shown here for comparison.

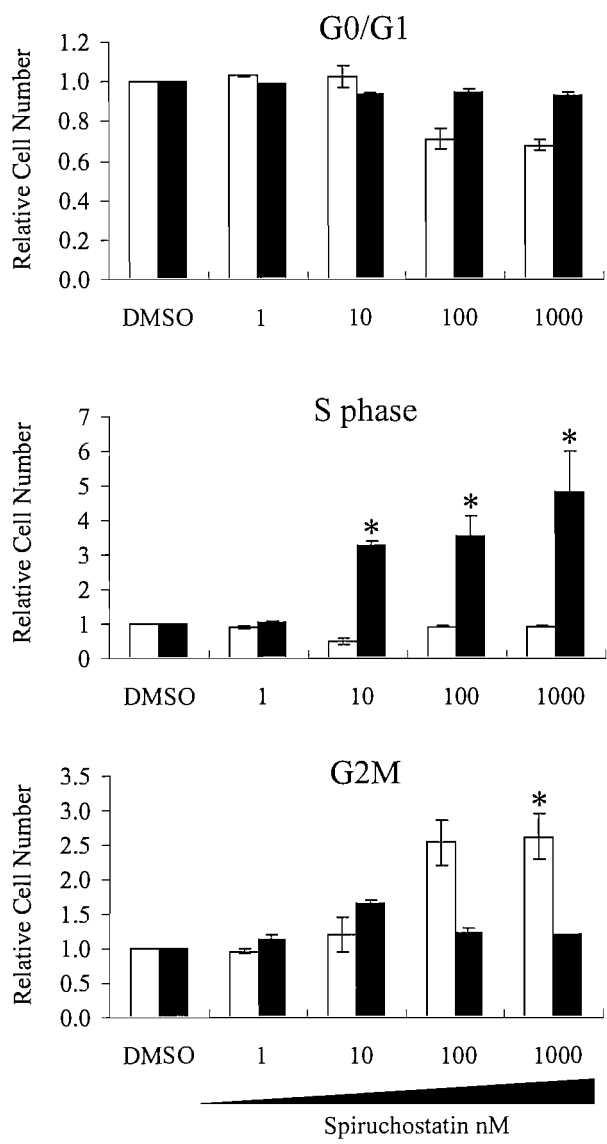


**Figure 5-7 Cell cycle progression following Spiruchostatin A exposure in MCF7 breast carcinoma cells and normal human dermal fibroblasts**

MCF7 (white bars) and NHDF (black bars) mono-layers were exposed to medium supplemented with indicated concentrations of Spiruchostatin A or DMSO vehicle and stained at 72 hours with propidium iodide for cell cycle phase analysis by flow cytometry. Results are mean values +/- SEM for two separate experiments, of the proportion of cells in the indicated cell cycle phase, of total gated cells in cell cycle, relative to DMSO treated samples which are normalised to one. Results reaching statistical significance ( $p < 0.05$ ) relative to DMSO treated samples are indicated.

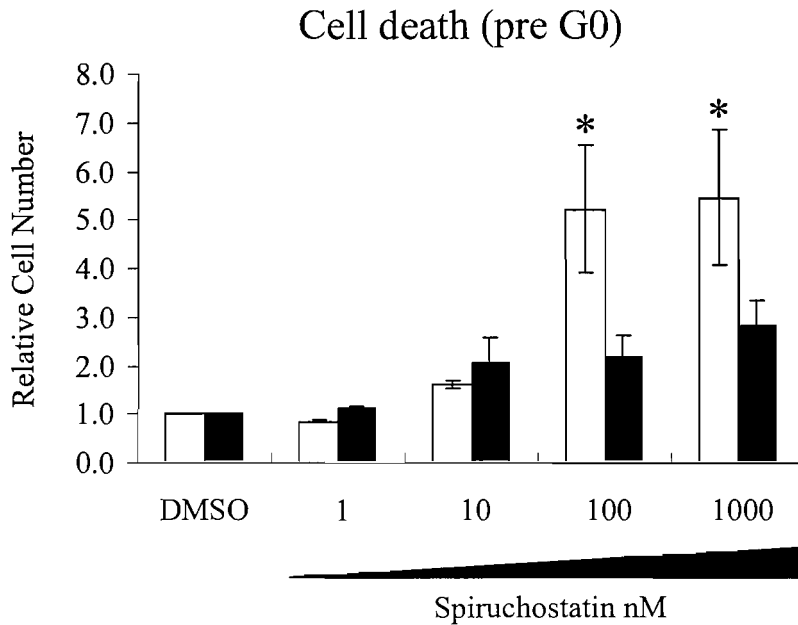


**Figure 5-8 Induction of cell death following Spiruchostatin A exposure in MCF7 breast carcinoma cells and normal human dermal fibroblasts**

MCF7 (white bars) and NHDF (black bars) mono-layers were exposed to medium supplemented with the indicated concentrations of Spiruchostatin A or DMSO vehicle and harvested at 72 hours. Samples were stained with propidium iodide and analysed for cell cycle phase by FACS. Results depict mean values +/- SEM for two separate experiments showing the proportion of dead cells (pre-G0 fraction), as a proportion of total gated cells, and are shown relative to DMSO treated samples which are normalised to one. Results reaching statistical significance ( $p < 0.05$ ) relative to DMSO treated samples are indicated.

## **5.7 Spiruchostatin A Causes Detachment of Adherent Cell Mono-Layers and Inhibits Differentiation Markers Prior To Inducing Cell Death**

The results presented so far show that Spiruchostatin A is a potent HDAC inhibitor which is able to inhibit cell proliferation, and induce cell cycle arrest, differentiation and cell death. One feature of Spiruchostatin A treatment noted in cell mono-layers of all cell types tested to date has been detachment in response to Spiruchostatin A exposure but with viability largely maintained. This effect was both time and dose dependant. Having made these observations, a hypothesis was suggested that Spiruchostatin A had altered the adhesion phenotype and caused cells to enter a pathway which might lead to apoptosis, but equally might be recoverable by removal of HDAC inhibition.

To investigate this hypothesis further, experiments to assess histone acetylation by western blot, cell cycle arrest/cell death by flow cytometry and differentiation by Nile Red staining were performed in parallel samples following Spiruchostatin A exposure. Floating and adherent cell fractions were harvested and processed separately to assess each of these biological outcomes. Exposure to 35nM Spiruchostatin A for 48 hours resulted in approximately 50% of the plated cells becoming detached and floating, with the remaining cells still adherent and morphologically normal. Shorter durations of exposure up to 24 hours resulted in very few floating cells. Exposure to DMSO vehicle alone did not induce significant numbers of cells to detach out to at least 6 days of exposure. Results are shown in figure 5-9. Histone acetylation and a decrease in  $\beta$ -catenin expression are seen in both adherent and floating cell populations to the same degree compared to DMSO treated controls. Likewise G2M arrest is seen for both floating and adherent cells, and it is clear that in the floating cell fraction, cells remain in cycle following this degree of exposure to Spiruchostatin A. Cell death as determined by the pre-G0 cell component by flow cytometry is seen in both cell fractions compared to DMSO treated cells, but the proportion of dead cells is approximately double in the floating

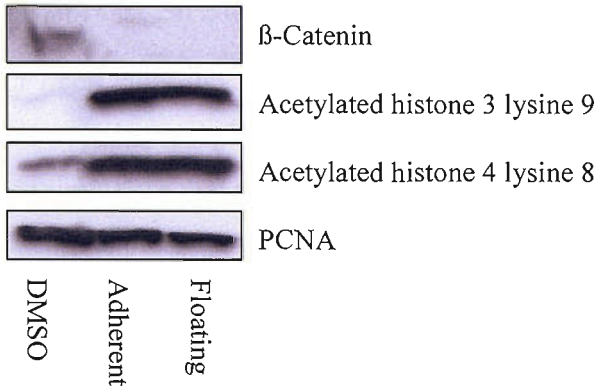


cells compared to the adherent ones. In the samples used to assess differentiation by Nile Red staining, there was a clear difference in that adherent cells showed increased staining of lipid droplets following Spiruchostatin A treatment whereas floating cells did not.

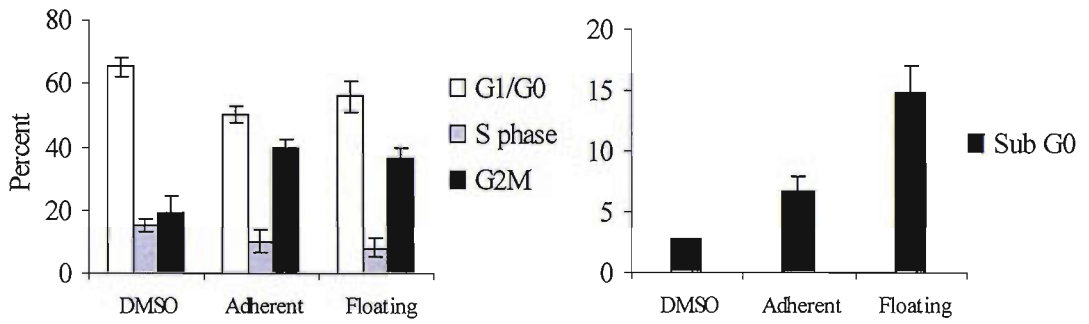
The fact that at least a proportion of cells remained in cell cycle, and had not undergone cell death, raised the question of whether they could be 'rescued' from Spiruchostatin A exposure. This was tested by taking cells from the floating cell fraction, following Spiruchostatin A treatment, and re-suspending in un-supplemented cell culture medium after washing five times. This process failed to rescue these cells, which progressed to cell death over 24 to 48 hours and did not re-adhere.

In conclusion the irreversible detachment of a proportion of adherent cultured breast cancer cells in response to Spiruchostatin A exposure is accompanied by a loss of the differentiated phenotype seen typically in the remaining adherent cell fraction followed by cell death. This is not however mirrored by alterations in the proportion of cells undergoing cell cycle arrest or in histone acetylation status or of  $\beta$ -catenin expression.

A



B



C

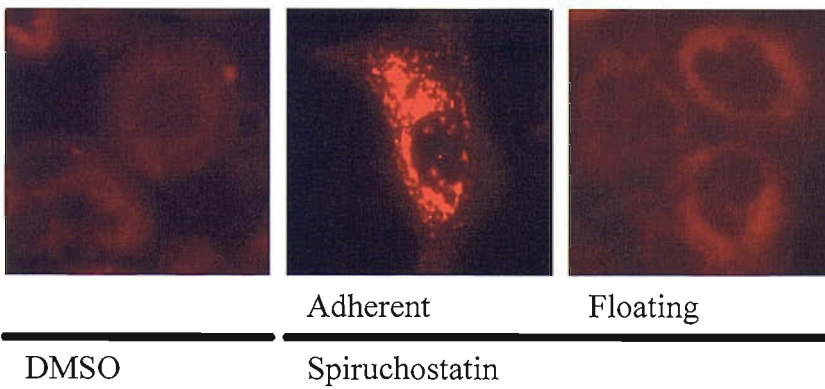


**Figure 5-9 Effects of Spiruchostatin A in floating and adherent cell fractions in MCF7 breast carcinoma cells**

MCF7 cell mono-layers exposed to 35nM Spiruchostatin A or DMSO vehicle for 48 hours were harvested separately as floating and adherent cell fractions which were approximately equal in number. A: Western blot analysis of histone acetylation and  $\beta$ -catenin expression using the indicated antibodies. PCNA is shown as a control for sample loading. Images are representative of two separate experiments. B: Flow cytometry analysis with propidium iodide staining showing percentages of cells in the indicated cell cycle divisions of total cells in cycle and percentage of total gated cells undergoing cell death (pre-G0 fraction), expressed as means +/- SEM for two separate experiments. C: Fluorescent microscopy images to show cytoplasmic Nile Red stained lipid droplets. Representative images derived from two separate experiments are shown.

## 5.8 Discussion

Work presented here has shown that Spiruchostatin A induces histone acetylation in breast cancer cells with nanomolar potency. All specific histone lysine residues assessed to date have undergone acetylation in response to Spiruchostatin A. This was predicted by its close structural similarity to FK228, one of the furthest developed examples of HDAC inhibitors in early phase clinical trials for cancer. Spiruchostatin A, although a natural compound, is amenable to chemical synthesis as previously described following collaborative work within the author's laboratory.<sup>141</sup> This raises the potential for structural analogues to be developed to allow for investigation and optimisation of functional activity of these compounds. Spiruchostatin A analogue analysis may represent a particularly useful tool to dissect HDAC inhibitor function with respect to the HDAC enzyme selectivity which FK-228 and Spiruchostatin A exhibit, which is explored further in the following chapter. Having confirmed that Spiruchostatin A induces histone acetylation, it was important to characterise the downstream biological effects, and this work has been presented in this chapter. Breast cancer cells were utilised as a model for this work as there is initial evidence for the efficacy of these drugs in this disease. In addition there is some preliminary data to suggest the potential of HDAC inhibitors to produce synergistic interactions with some cytotoxic chemotherapeutics used in breast cancer, as well as with breast cancer targeted therapy in the form of the monoclonal antibody trastuzumab.<sup>134,162</sup>

In addition to histone acetylation, Spiruchostatin A was found to also alter protein expression of known HDAC inhibitor targets relevant to breast cancer pathogenesis and progression including the EGFR and HER2 neu receptors. HER2 represents a key receptor for initiation of downstream signalling whose expression is amplified in a subset of poor prognosis breast carcinomas. It is a conventional therapeutic target for the monoclonal antibody trastuzumab in both the metastatic and adjuvant settings

and so HDAC inhibitor modulation of this and other signalling mechanisms are of interest.

In the case of  $\beta$ -catenin, modulation of protein expression has been shown which may be relevant to adhesion and breast cancer cell proliferation characteristics. At the time that these experiments were performed, reduced  $\beta$ -catenin expression in response to HDAC inhibition had not previously been documented.  $\beta$ -catenin acts as a key central axis of the developmental signalling pathway for the secreted extracellular glycoprotein Wnt, via the Frizzled family of cell surface receptors. Wnt signalling leading to  $\beta$ -catenin accumulation, via prevention of proteasomal degradation, and its nuclear relocalisation leads to expression of genes which include c-myc, cyclin D1 and metalloproteinase 7. Mutations of  $\beta$ -catenin and abnormalities in its turnover are implicated in a range of malignancies. Subsequently two papers have appeared that have confirmed reduced  $\beta$ -catenin expression in response to HDAC inhibition in U937 human leukaemic cells and the mouse uterus.<sup>182,183</sup> Therefore the Wnt/ $\beta$ -catenin signalling pathway would seem to represent a novel target for HDAC inhibitor effect that had not previously been identified.

Having determined that Spiruchostatin A induces histone acetylation, work was performed to address its biological effects. A predominant G2M cell cycle arrest was demonstrated in addition to the induction of cell death. The cell death is presumed to be apoptotic although this was not directly tested. It would be important to confirm this, for example with annexin V staining. Certainly induction of apoptosis would be consistent with published data considering other HDAC inhibitors, however another mode of induction of cell death shown to occur with HDAC inhibition is autophagy.<sup>153</sup> This mode of cell death is less well understood and its analysis is hampered by difficulties regarding its quantification. Further assessment of this mechanism would be interesting as it is a mode of tumour cell killing which is not targeted by most other forms of anti-cancer therapy. In addition to cell cycle and cell death effects, Spiruchostatin A produced rapid differentiation of breast cancer cells as assessed by the induction of intra-cytoplasmic lipid droplet accumulation. Finally

the assessment of the ability of Spiruchostatin A to modify breast cancer cell proliferation confirmed that it produces a clear dose response curve in MCF7 breast cancer cells with a low nanomolar  $IC_{50}$  value. Thus Spiruchostatin A induces the expected downstream biological effects of HDAC inhibition in breast cancer cells; namely cell cycle arrest, cell death, induction of differentiation and inhibition of proliferation. This raises the potential for investigation into therapeutic intervention for breast cancer with this and other HDAC inhibitors, and as a new tool for the investigation of the effects of transcriptional regulation via modification of histone acetylation in breast cancer cells.

Following from the initial characterisation of biological activity induced by Spiruchostatin A, the contrasting effects that it exerts between breast cancer and normal cells were addressed. Firstly it was demonstrated that Spiruchostatin A has a lower potency in normal human dermal fibroblasts compared to MCF7 cells in proliferation experiments. This is consistent with similar findings for SAHA which has been shown to have greater potency in malignant versus normal cells.<sup>147</sup> It remained unclear from this published work however what the reasons for these differences might be. Initial testing of the underlying causes for these differences in potency focussed on the histone acetylation characteristics induced by Spiruchostatin A between these two cell lines, however no difference was found. In contrast the fibroblast cell line was found to enter S phase arrest rather than the characteristic G2M arrest seen in breast cancer cells. In the same experiment, induction of cell death was more marked in the breast cancer cells compared to that seen in fibroblasts. This suggests that variation in cell cycle check point controls between the malignant and normal cells result in variation in response to HDAC inhibition in terms of cell cycle progression. The implication is that the aberrant signalling and cell proliferation mechanisms within the malignant cell, leading to abnormal phenotype, are more susceptible to modulation by the relatively specific translational modification resulting from HDAC inhibition. It is possible that while normal cells show S phase arrest from which recovery is possible, malignant cells are subject to different checkpoints, with different consequences. Gene expression

analysis by micro array would provide a starting point to investigate further the differences that lead to this differential response to Spiruchostatin A between malignant and normal cells. It should be possible to assess the expression of genes which contribute as controlling factors at cell cycle check points. In addition these differences in cell cycle arrest characteristics might be relevant for devising strategies to use HDAC inhibitors as part of combination therapy. If malignant cells are sensitive to modification of differing cell cycle checkpoints, this might be relevant to their combination and sequencing with cell cycle specific cytotoxic agents. There is some question as to the relevance of NHDFs as a non malignant cell line for extrapolation to normal tissue toxicology. They were chosen because they provide a useful model for comparison to the adherent breast cancer cell lines used in this work, with broadly similar proliferation characteristics. It will be important to move on to comparison of non-malignant breast cell lines. In addition it would be of interest to compare normal and malignant cells from other cell systems, such as lymphocytes, which might allow for confirmation as to whether the differences seen here are global differences or tissue specific.

Finally in this section, work has been presented to investigate the effect of Spiruchostatin A in inducing detachment of adherent cells in conjunction with their progression through other biological processes including cell cycle arrest and cell death. From these experiments it appears that the detached cell fraction seen after treatment with Spiruchostatin A is destined for cell death, despite remaining in cell cycle in the same proportions as adherent cells which can be rescued. Adherent cells show evidence of differentiation in response to Spiruchostatin A that was not seen in floating cells. Proportions of both fractions of cells undergo apoptosis, although more so in the floating fraction. These differences are not explained by histone acetylation differences and all cells ultimately undergo apoptosis either with increased time or dose exposure. Therefore it is proposed that cells treated in these samples are at varying points along a continuum of biological effect, which passes through cellular differentiation, cell cycle arrest and ultimately to apoptosis that at

some stage becomes an irreversible outcome. The extent of this progression within a cell sample is both time and dose dependant.

In conclusion, Spiruchostatin A is an HDAC inhibitor and produces characteristic effects of HDAC inhibition including cell cycle arrest, differentiation, cell death and inhibition of cell proliferation. It might therefore have value in breast cancer and other malignancies. It is highly potent in the low nanomolar range for median effects in each of these biological outcomes. Important differences in its effects in breast cancer cells compared to normal cells have been shown which suggests this is a class effect for HDAC inhibitors generally in conjunction with published data for SAHA. This may explain some of the therapeutic benefit which appears to be achievable with these compounds.



## 6 Comparison Between Bicyclic Tetrapeptide and Hydroxamate HDAC Inhibitors

### 6.1 Introduction

In-vitro and early phase clinical trial development of HDAC inhibitors has indicated encouraging efficacy against a range of malignancies. However toxicity has been seen with each of these compounds predominantly with nausea, fatigue, myelosuppression and cardiac effects. It may be that the efficacy and toxicity of these compounds could be improved by considering their structure specific characteristics. The bicyclic tetrapeptide FK228 is one of the furthest developed in terms of clinical trials. It has been shown to exhibit relative class I HDAC selectivity. Using an in-vitro assay for HDAC activity, FK228 has been shown to have a predominant effect on HDAC1 and 2 (class I enzymes) and comparatively little on HDAC4 and 6 (class II enzymes). TSA by comparison showed a broad inhibitory activity across all these enzymes.<sup>133</sup> However, at present it remains unclear whether FK228 class selectivity might translate a specific biological effect, and if so whether this might produce useful differences in therapeutic profile. The close structural similarity between this compound and Spiruchostatin A suggests that if bicyclic compounds, as a structural class, exhibit HDAC class selectivity, then the ability to modify Spiruchostatin A to produce synthetic structural analogues might allow for exploitation of these characteristics. Theoretically it might be possible to select for benefits in therapeutic efficacy and/or against drug induced toxicity. It is not clear whether, and to what degree, the class I selective action shown for FK228 might apply to structural variants such as Spiruchostatin A or its synthetic derivatives. It may also be possible to use analogues of Spiruchostatin A as chemical tools to dissect class I versus class II HDAC effects and expand our understanding of their function. Thus the use of Spiruchostatin A, in addition to FK228 which had previously been the sole example

of a cyclic tetrapeptide natural product HDAC inhibitor, provides a unique opportunity to dissect potential differences in HDAC inhibitor classes.

The class I HDAC selectivity of FK228 has previously been confirmed.<sup>133</sup> The prediction that Spiruchostatin A would also exhibit Class I selectivity was assessed in collaboration between the author's laboratory and that of Dr Minoru Yoshida, Department of Biotechnology, University of Tokyo, Japan, whose group had performed the original confirmation of HDAC selectivity for FK228. By in-vitro enzyme assays performed by Dr Yoshida's group, Spiruchostatin A was found to exhibit an approximately 600 fold lower potency for inhibition of HDAC6 (class II) than HDAC1 (class I). In the same experiments, TSA has found to have broadly equivalent potency for these two enzymes. (Unpublished data, Table 6-1) Spiruchostatin A therefore provides a unique opportunity in combination with FK228 to examine HDAC class selective effects of bicyclic inhibitors, compared to pan-HDAC inhibitor compounds.

With these considerations in mind, experiments were performed to compare the ability of two hydroxamates (TSA and SAHA) and two bicyclic tetrapeptides (FK228 and Spiruchostatin A) to affect cancer cell proliferation and gene expression. Subsequent work addressed downstream biological effects of these compounds in the form of cell cycle progression and induction of cell death. Tubulin acetylation activity is a downstream effect of HDAC6 indicative of class II HDAC inhibition and Spiruchostatin A was tested for activity in this system in order to determine how selective its effect may be. Finally the role of histone acetylation pharmacodynamic differences was considered as a marker of biological effect, as this has been used as a surrogate marker for drug efficacy both in-vitro and in the setting of early phase clinical trials.

<b>Compound</b>	<b>HDAC1 IC<sub>50</sub> (nmol)</b>	<b>HDAC6 IC<sub>50</sub> (nmol)</b>
Trichostatin A	15	61
Spiruchostatin A (with DTT)	0.6	360

**Table 6-1 Inhibition values of Spiruchostatin A and TSA against HDAC1 and HDAC6**

In-vitro IC<sub>50</sub> values for TSA and Spiruchostatin A (Data courtesy of Dr Minoru Yoshida). Description of the methodological processes have previously been described (for FK-228 and TSA) by Dr Yoshida's group.<sup>133</sup>

## 6.2 Comparison Of The Effects Of Bicyclic Tetrapeptides And Hydroxamates On Cell Proliferation, Gene Expression And Cell Cycle Progression

To assess the relative abilities of bicyclic tetrapeptide and hydroxamate HDAC inhibitors to modify breast cancer cell proliferation, experiments were performed to determine dose response relationships for Spiruchostatin A, FK228, TSA and SAHA. These were performed using the CyQuant cell proliferation assay system. As can be seen in figure 6-1 each of these compounds produces a sigmoidal dose response curve against a log x axis of increasing dose. Each has an  $IC_{50}$  within the nanomolar range and the values calculated were highly consistent between experiments. The relative potency for each drug was found to be  $FK228 > Spiruchostatin\ A > TSA > SAHA$  in all experiments performed and indeed this relationship is held up in experiments looking at specific drug effects such as histone acetylation and cell cycle arrest elsewhere in this section. Previous data presented in section 5 has suggested differences for inhibition of cell proliferation between normal human dermal fibroblasts and MCF7 breast cancer cells. This was investigated for each of these compounds and the resulting cell proliferation curves are shown in figure 6-2. From these curves it is apparent that both the bicyclic tetrapeptide and hydroxamate HDAC inhibitors exhibit similar differences in potency between these two cell types. Figure 6-3 shows the relative  $IC_{50}$  values for each drug as mean values for all experiments performed.

Next experiments were performed to assess the gene expression patterns of all four of these drugs. Unpublished work within the author's laboratory using micro array analysis of a 20K human gene array has indicated that a small proportion of genes have their gene expression altered in response to TSA treatment in MCF7 cells, and that as many genes are down as up regulated. This is consistent with results published by other groups.<sup>135,149</sup> A selection of seven of these genes (FOXC2, SIRT4, RGL, ICB1, MDR1, CTGF and RAB33A) and in addition the cell cycle regulator p21<sup>(WAF1/Cip1)</sup> were investigated further to determine whether the bicyclic

tetrapeptides also altered gene expression at the transcriptional level in a similar pattern in MCF7 breast cancer cells, using quantitative RT-PCR. The genes assessed are relevant to a diverse range of cellular processes including transcriptional regulation (FOXC2), differentiation and cell proliferation (ICB-1), cell cycle progression (p21<sup>(WAF1/Cip1)</sup>), multi drug resistance (MDR1), intracellular vesicle transport (RAB33A), cell adhesion (CTGF), protein acetylation (SIRT4) and cell signalling (RGL1). Cells were exposed to each drug for 16 hours at equipotent concentrations (based on using multiples of IC<sub>50</sub> estimations from the cell proliferation studies shown in this section). In this experiment each drug was used at a concentration approximately five times its IC<sub>50</sub> value. In addition each gene was assessed after exposure to an epimer of Spiruchostatin A which has been shown during work performed in the author's laboratory to be inactive in terms of induction of histone acetylation.<sup>141</sup> mRNA expression of these genes was then determined by quantitative RT-PCR. Each of the genes assessed in this manner had shown increased expression in response to HDAC inhibition in the micro array analysis. As shown in figure 6-4 each gene shows increased transcriptional expression compared to samples exposed to DMSO vehicle. In each case also the epimer of Spiruchostatin A was found to be inactive. For the selected genes assessed here, expression patterns in terms of which genes are altered by hydroxamates and bicyclic compounds were found to be the same albeit at different levels.

In addition to the genes indicated to have altered transcriptional expression following TSA exposure, experiments were conducted to assess the expression patterns of HDAC enzymes themselves in response to HDAC inhibitor exposure. As shown in figure 6-4, HDAC 5 exhibited increased expression levels in response to HDAC inhibition either with hydroxamate or bicyclic compounds. In the case of each of the other class I or II HDAC enzymes, expression was not altered by HDAC inhibitor exposure (data not shown). Thus in breast cancer cells, inhibition of HDAC activity, either as a global class I and II HDAC effect, or as a selective class I effect (in the case of FK228 and Spiruchostatin A), results in increased activity of at least one HDAC enzyme. The mechanism and reason for this are uncertain but may

represent a feedback loop in response to the global switch to a protein acetylated state.

Following on from these experiments to assess cell proliferation and gene expression characteristics in response to HDAC inhibition, investigation was performed to assess the effects of these inhibitor classes on cell cycle progression and induction of cell death. MCF7 cells were exposed to Spiruchostatin A, TSA or SAHA, again to equipotent doses based on the cell proliferation assays previously described and assessed by flow cytometry following propidium iodide staining over a time course to 72 hours. As shown in figure 6-5 each drug induces G2M arrest with a corresponding decrease in the proportion of cells in G0/G1 or S phases. These effects were minor at 24 hours but became progressively more pronounced with 48 and 72 hours exposure. At these equipotent doses for cell proliferation, the extent of G2M arrest seen is equivalent for each drug. Furthermore the induction of cell death by HDAC inhibition in this experiment as assessed by the proportion of cells in the pre-G0 fraction of cells shows again that cell death is induced by equivalent amounts by each drug.

In conclusion, comparison of the class I HDAC selective inhibitors Spiruchostatin A and FK228 to the pan class I/II inhibitors TSA and SAHA has shown that equivalent effects are seen with respect to malignant versus normal cell proliferation, cell cycle progression, cell death and a selection of transcriptional gene expression targets at equipotent doses.

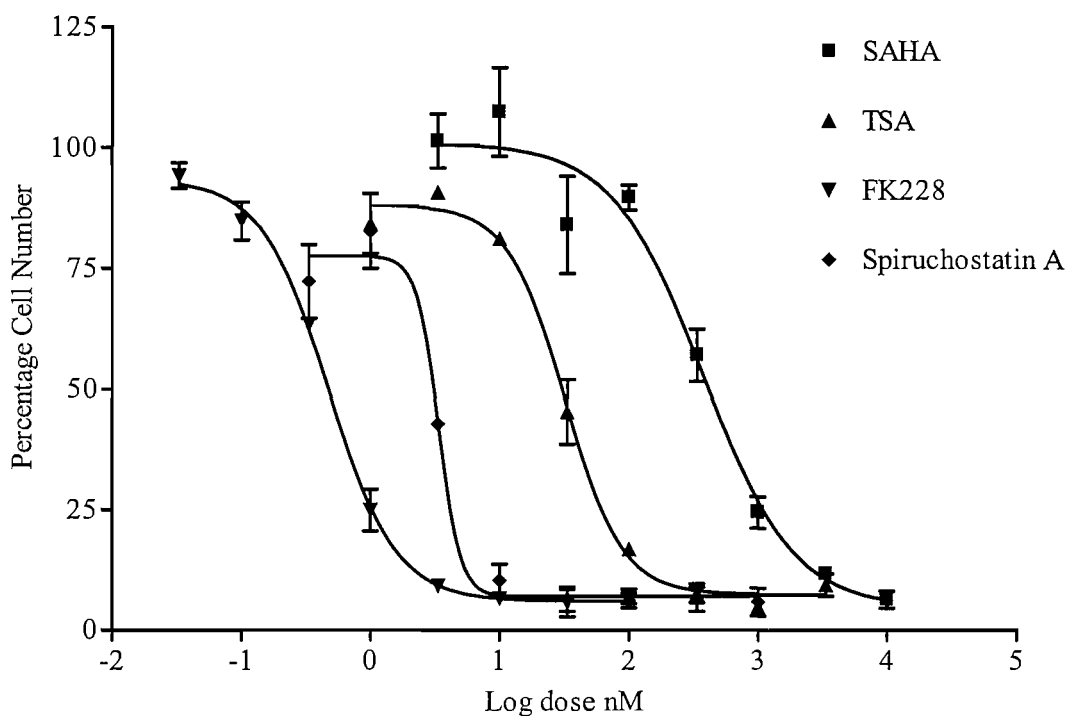


**Figure 6-1 Cell proliferation curves for Spiruchostatin A, FK228, TSA and SAHA in MCF7 breast cancer cells**

MCF7 cell mono-layers were exposed to medium containing the indicated serial dilutions of HDAC inhibitors for 6 days. Cell number was then determined using the CyQuant fluorescent assay system. Results show mean values  $\pm$  SEM for duplicate samples expressed as percentages relative to untreated cells together with non-linear regression curves. Samples exposed to cell culture medium supplemented with DMSO vehicle alone showed no significant deviation in cell proliferation from untreated cells (data not shown). Overall results are representative of multiple experiments.

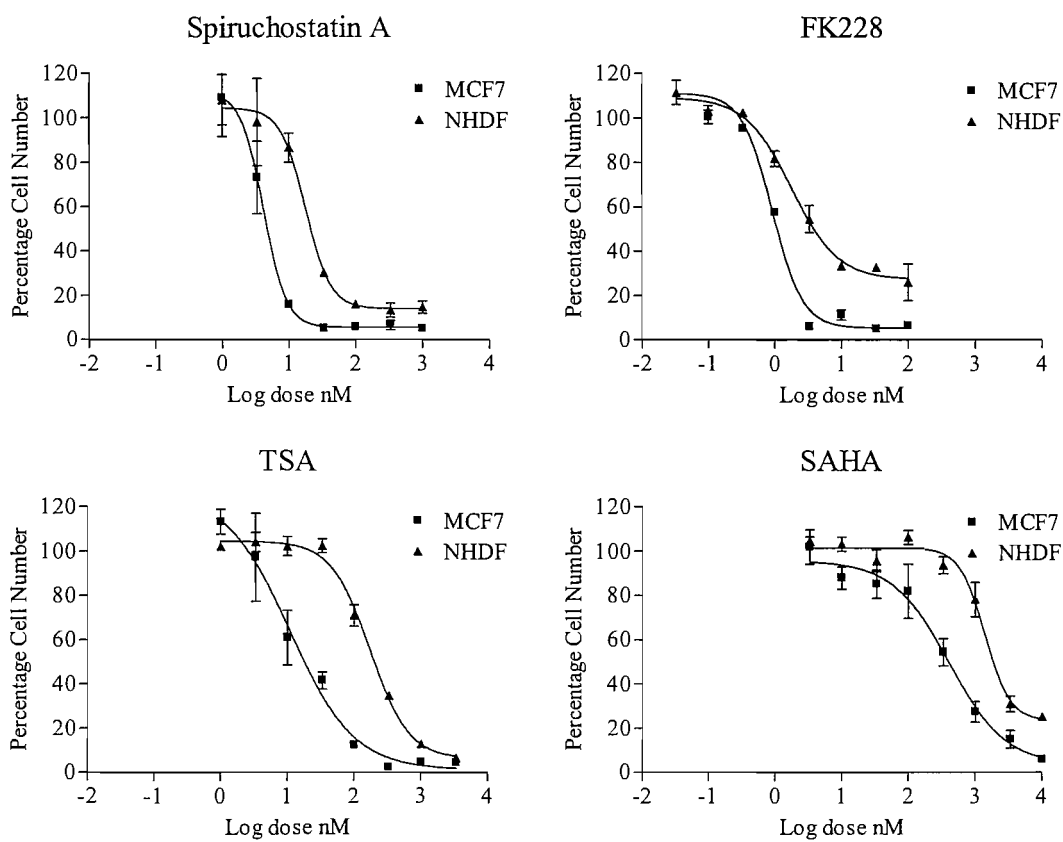
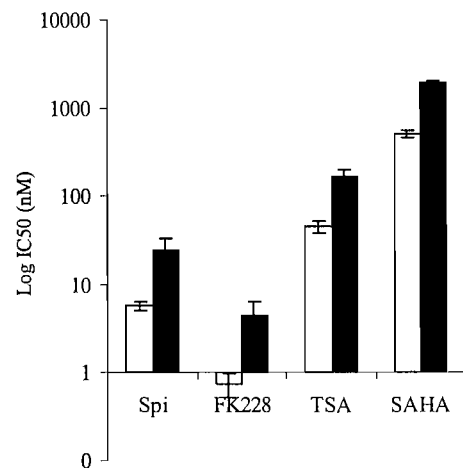


**Figure 6-2 Cell proliferation following bicyclic tetrapeptide or hydroxamate HDAC inhibitor exposure, in MCF7 breast carcinoma cells versus normal human dermal fibroblasts**

MCF7 and normal human dermal fibroblast (NHDF) cell mono-layers were exposed to medium supplemented with Spiruchostatin A, FK228, TSA or SAHA at serial dilutions as indicated for 6 days. Plates were then analysed for cell number using the CyQuant fluorescent assay system. Results for individual data points show mean values +/- SEM for duplicate samples, expressed as percentages relative to untreated cells. Samples exposed to cell culture medium supplemented with DMSO vehicle alone showed no significant deviation in cell proliferation from untreated cells (data not shown). Overall results are representative of multiple experiments.





Drug	IC <sub>50</sub> nM ± SEM		p
	MCF7	NHDF	
Spiruchostatin	5.7 ± 0.7	25 ± 7.7	0.0035
FK228	0.75 ± 0.2	4.5 ± 1.9	0.08
TSA	44 ± 6.7	165 ± 35	0.0011
SAHA	510 ± 42	2000 ± 50	0.0001

**Figure 6-3 Mean IC<sub>50</sub> values for Spiruchostatin A, FK228, TSA and SAHA in MCF7 breast carcinoma cells and normal human dermal fibroblasts**

MCF7 (open bars) and normal human dermal fibroblast (NHDF, closed bars) cell mono-layers were exposed to medium containing serial dilutions of Spiruchostatin A, FK228, TSA or SAHA and analysed after 6 days for cell number using the CyQuant fluorescent assay system. Results show mean values +/- SEM for multiple separate experiments. Each IC<sub>50</sub> determination was from a minimum of three separate experiments for each drug in each cell line with IC<sub>50</sub> values determined from dose response curves obtained with duplicate determinations of each dose level. Statistical significance of differences between mean values for MCF7 and NHDF cell lines for each drug is indicated as a p value calculated by unpaired t test.

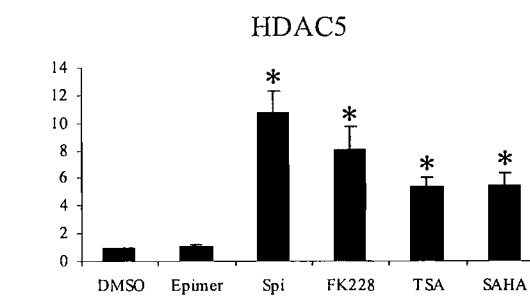
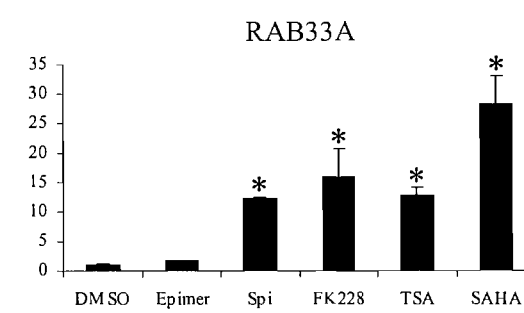
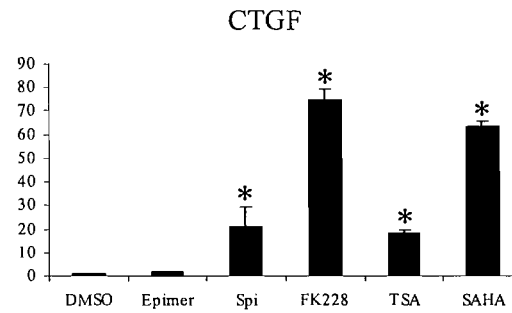
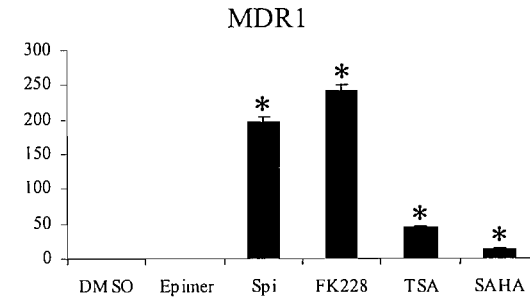
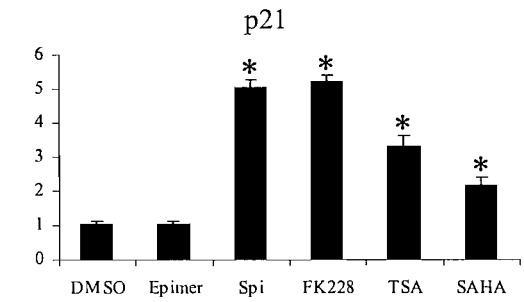
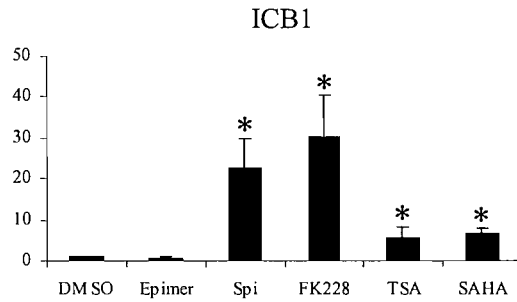
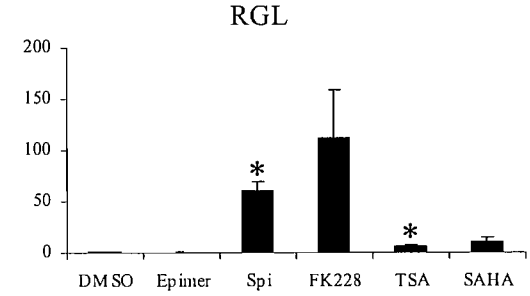
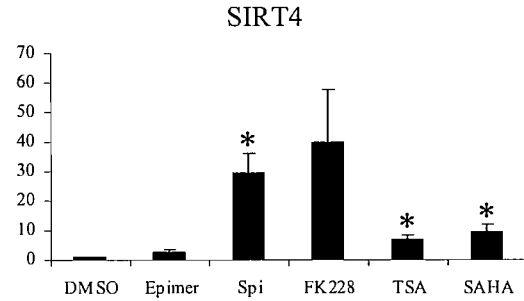
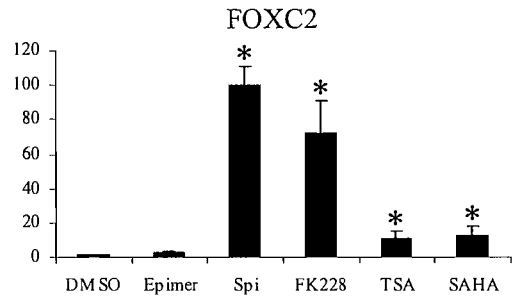


**Figure 6-4 Gene expression analysis following exposure to Spiruchostatin A, its structural epimer or FK228, TSA or SAHA**

MCF7 cell monolayers were exposed for 16 hours to DMSO vehicle or an epimer of Spiruchostatin A or equipotent doses of the indicated HDAC inhibitors (30nM Spiruchostatin A, 3.75nM FK228, 200nM TSA, 2.5 $\mu$ M SAHA). Following reverse transcription, samples were analysed for gene expression by quantitative PCR for the indicated genes. Results indicate mean expression +/- sd, corrected for GAPDH expression, of triplicate samples and are representative of two separate experiments. Results reaching criteria for statistical significance in comparison to DMSO exposed samples are indicated ( $p < 0.05$ ).

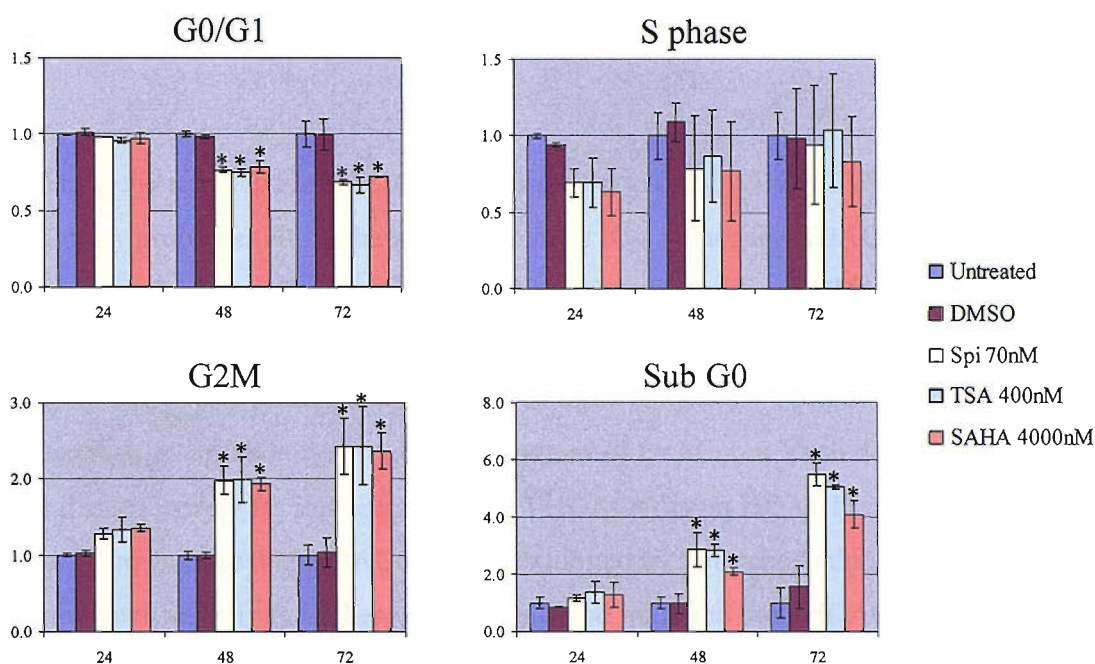


**Figure 6-5 Cell cycle progression and apoptosis in MCF7 breast carcinoma cells following HDAC inhibition with Spiruchostatin A, TSA or SAHA**

MCF7 cell mono-layers were exposed to culture medium supplemented with HDAC inhibitors at the indicated doses (~10 times the respective  $IC_{50}$  values) and harvested at the times shown. Samples were stained with propidium iodide and analysed by flow cytometry. Results show ratios for cells in the indicated cell cycle phases, as a proportion of cells in cycle or of the dead cell sub-G0 cell fraction as proportion of total cells, relative to DMSO treated cells which are normalised to one. Results are mean values +/- SEM for two separate experiments. Results reaching statistical significance ( $p < 0.05$ ) compared to untreated samples for each time point are indicated.

### 6.3 Spiruchostatin A Exhibits Class I HDAC Selective Effects

The bicyclic tetrapeptide FK228 has been shown to exhibit HDAC Class I selective inhibitory properties. It has been found to have IC<sub>50</sub> values for HDAC1 and HDAC2 (both Class I enzymes) more than 10 fold less than that seen for HDAC4 and 300 to 400 fold less than that for HDAC6 (both class II enzymes). TSA in this study was roughly equipotent for inhibition of each of these enzymes.<sup>133</sup> Unpublished work undertaken in collaboration with the laboratory of Dr Minoru Yoshida confirmed that this selectivity for inhibition of class I HDACs (using HDAC1) compared to class II enzymes (using HDAC6) is also exhibited by Spiruchostatin A. TSA did not exhibit such selectivity in these experiments and inhibited both HDAC classes with roughly equal potency (table 6-1). It was important therefore to assess this selectivity at the level of a biological effect. The class II enzyme HDAC6 is known to exhibit tubulin acetylation activity and this was used to compare selectivity for HDAC class inhibition compared to a key downstream effect of p21<sup>(WAF1/Cip1)</sup> expression as an example of class I HDAC inhibition. MCF7 breast cancer cells were exposed to multiples of the respective IC<sub>50</sub> values of Spiruchostatin A, FK228, TSA and SAHA for 24 hours and analysed by Western blot for histone acetylation, p21<sup>(WAF1/Cip1)</sup> expression and tubulin acetylation. As seen in figure 6-6, each drug induces acetylation of histone H4 at lysine 8 and induction of p21<sup>(WAF1/Cip1)</sup> expression to broadly similar degrees for equipotent doses. By comparison however, tubulin acetylation is clearly induced by the hydroxamate HDAC inhibitors in doses of double the respective IC<sub>50</sub> values and above but this is not seen with the bicyclic tetrapeptides. (The lack of tubulin acetylation seen in the Spiruchostatin A and FK-228 samples was controlled for in these results by subsequent determination of PCNA and tubulin expression levels and parallel results shown here for the hydroxamates which were confirmed in the same blot.) Tubulin expression levels remain constant in this experiment. Therefore the HDAC class I selectivity seen for FK228 and Spiruchostatin A at the level of in-vitro enzyme inhibition is shown here to translate to downstream biological effect in breast cancer cells.

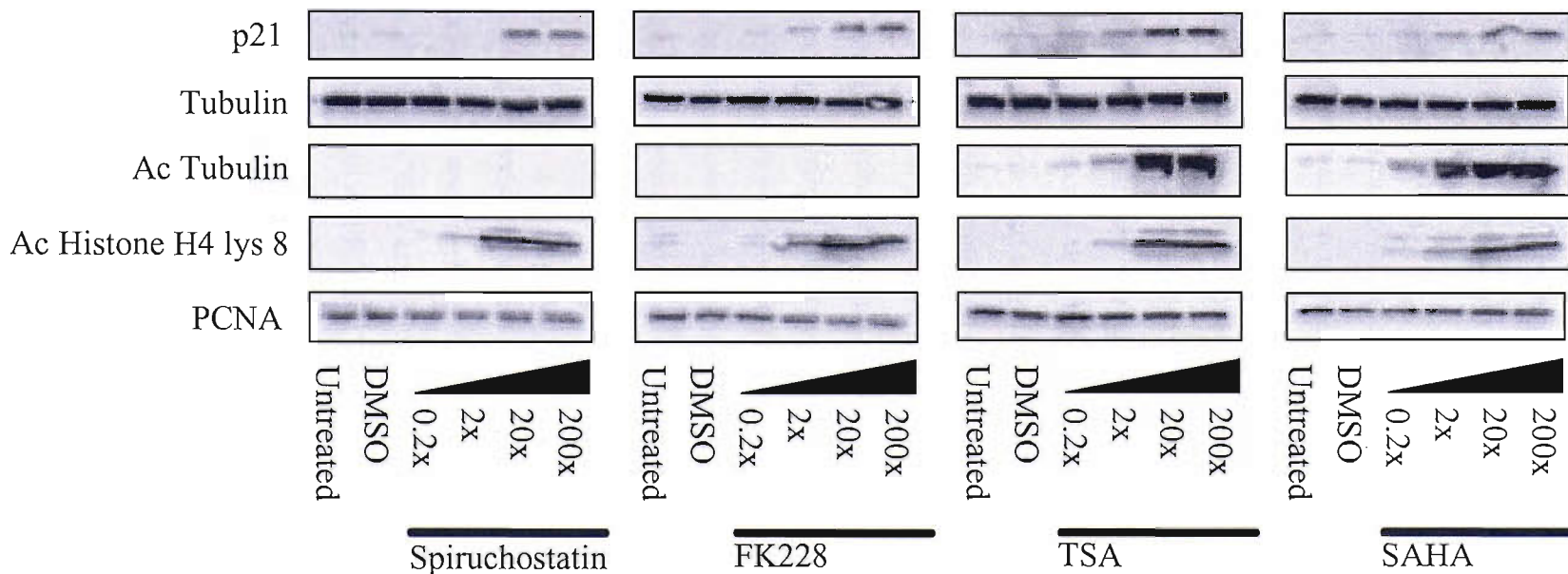


**Figure 6-6 Histone and tubulin acetylation and p21<sup>(WAF1/Cip1)</sup> expression characteristics for bicyclic tetrapeptides compared to hydroxamates in MCF7 breast carcinoma cells**

MCF7 cells were exposed to cell culture medium supplemented with the indicated HDAC inhibitors at multiples of their respective IC<sub>50</sub> values for 24 hours. Samples were then harvested and processed for Western blot analysis of protein expression and acetylation status using the indicated antibodies. PCNA is shown as a control for sample loading and the results shown are representative of two such experiments.

#### **6.4 Bicyclic and Hydroxamate HDAC Inhibitors Exhibit Differences In Histone Acetylation Pharmacodynamics**

Having determined that each of the hydroxamate and bicyclic HDAC inhibitors assessed was able to induce inhibition of cell proliferation, similar gene expression changes, G2M cell cycle arrest and induction of cell death, experiments were then performed to assess the pharmacodynamics characteristics of histone acetylation. This was done following exposure to modest and equipotent doses of Spiruchostatin A and TSA. Samples were assessed for acetylation status at specific lysine residues of core histones by Western blot analysis over a time course of continuous exposure from 15 minutes out to 72 hours. As shown in figure 6-7, differences exist between the pharmacodynamics of histone acetylation (in this case of lysine 9 on histone H3 and lysine 8 of histone H4) in response to exposure to either Spiruchostatin A or TSA. The hydroxamate induces histone acetylation from as early as 15 minutes of exposure, whereas Spiruchostatin A induced acetylation occurs later at around four to eight hours of exposure. However in the case of TSA there is clear waning of acetylation from 24 hours of exposure onwards. By comparison, Spiruchostatin A produces a prolonged effect lasting to at least 72 hours. This pattern of acetylation was seen to be the same for all core histone lysine acetylation sites assessed.

To further assess the nature of these differences in acetylation pharmacodynamics, experiments were performed to address the effect of drug washout on histone acetylation. Cells were exposed to a time course of HDAC inhibitor exposure using Spiruchostatin A, FK228, TSA and SAHA. At various time points, samples were then either harvested in a simple time course determination of histone acetylation out to 24 hours or were washed repeatedly and maintained in fresh cell culture medium to 24 hours and harvested at this point. As shown in figure 6-8, despite seeing early histone acetylation again occurring with the hydroxamate compounds, there was in addition an equally rapid loss of acetylation following drug washout. By comparison the bicyclic tetrapeptides Spiruchostatin A and FK228 were seen to exhibit a

prolonged change in histone acetylation status despite removal of drug lasting out to between eight and twenty four hours. These results therefore indicate differences between the histone acetylation pharmacodynamics produced by hydroxamates and bicyclic tetrapeptides. These effects appear to be determined by the structural class to which the respective inhibitors belong.



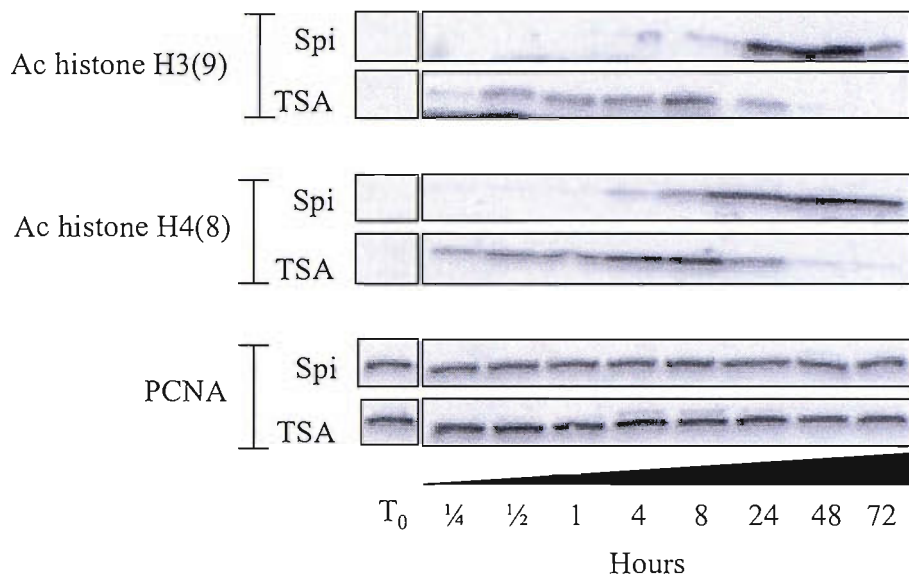


**Figure 6-7 Histone acetylation with respect to time for Spiruchostatin A and TSA treatment in MCF7 breast cancer cells**

MCF7 cell mono-layers were exposed to culture medium supplemented with 15nM Spiruchostatin A (Spi) or 80nM TSA (i.e. approximately double the respective IC<sub>50</sub> values) and harvested at the indicated time points for Western blot analysis using the indicated antibodies. PCNA is shown as a control for sample loading. Results are representative of multiple experiments.

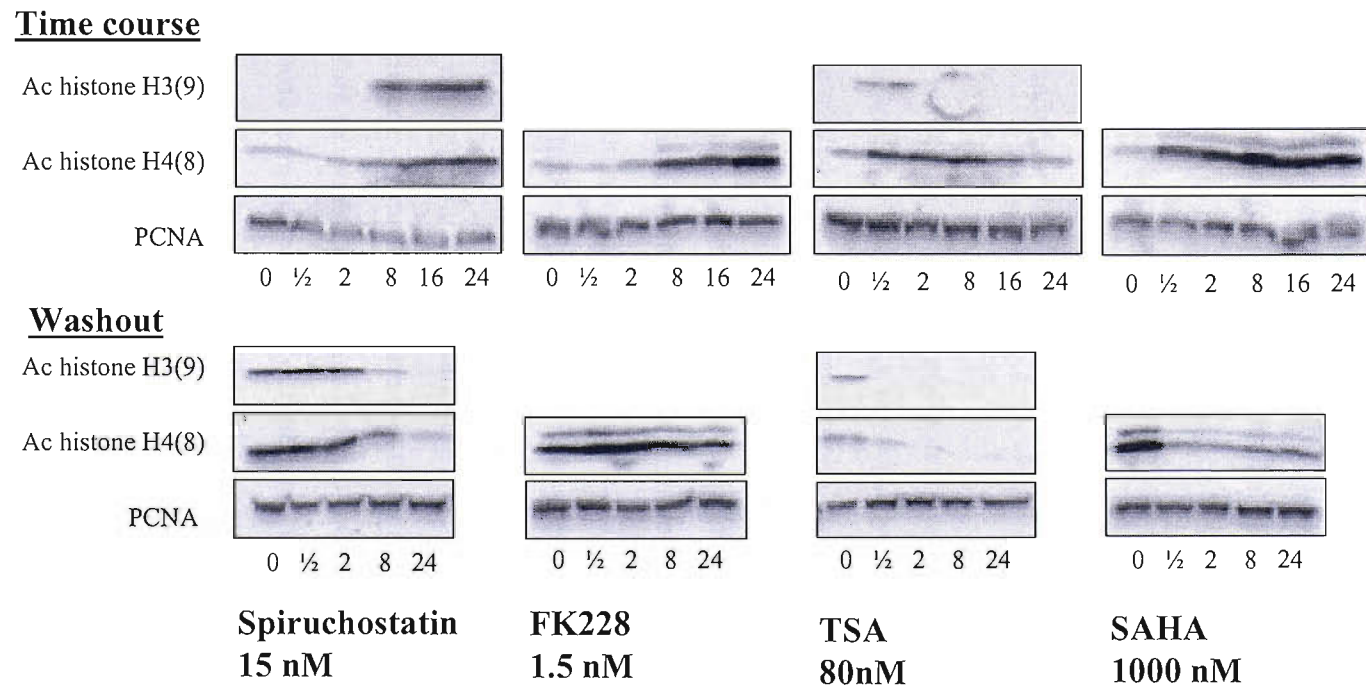


**Figure 6-8 Histone acetylation following exposure to, and washout of, Spiruchostatin A, FK228, TSA or SAHA in MCF7 breast cancer cells**

MCF7 cells were exposed to culture medium supplemented with the indicated HDAC inhibitors and analysed for histone acetylation by Western blot using the indicated antibodies. In the top panel samples were harvested at the indicated time points. In the bottom panel, at the indicated time points, samples were washed five times and maintained to 24 hours in fresh non-supplemented medium and then harvested. PCNA is shown as a control for sample loading. Results are representative of multiple experiments.

## **6.5 The Effect of Histone Acetylation Pharmacodynamics on Cell Cycle Progression**

Having determined that there are clear differences between the histone acetylation pharmacodynamics induced between the bicyclic tetrapeptides and hydroxamates, it was important to determine what effect this might have on the biological effects of these drugs. Experiments were performed, to assess the outcome from pulsed exposure of these two structural HDAC inhibitor groups on cell cycle progression characteristics.

MCF7 cells were exposed to equipotent doses based on proliferation assays of Spiruchostatin A, FK228, TSA or SAHA by comparison to untreated and DMSO vehicle treated cells. Cells were exposed to these drugs for either 2, 16 or 72 hours with samples treated for the earlier two time points being washed repeatedly to remove all trace of drug. These washed samples were then maintained in fresh un-supplemented cell culture medium. Samples were then harvested at 72 hours, stained with propidium iodide and assessed for cell cycle progression characteristics by flow cytometry. In parallel to this, samples were also produced which were analysed for histone acetylation status by Western blot at each time point and following each pulse exposure duration to characterise the histone acetylation patterns through this experiment. As shown in figure 6-9, the characteristic G2M arrest induced by exposure to each of these drugs is again seen after 72 hours continuous exposure. For those samples treated by pulsed exposure to these drugs there is no evidence that two hours exposure either to the hydroxamates or bicyclic tetrapeptides induces an effect on cell cycle progression after 72 hours. By comparison, the samples exposed to a pulse of either class of inhibitor for 16 hours are shown to exhibit G2M arrest after 72 hours. The degree of effect is comparable to the samples exposed continuously for the full 72 hour period.

Figure 6-10 indicates the histone acetylation characteristics of parallel samples produced in this experiment. Consistent with data already presented it can readily be seen that the hydroxamates have produced a rapid induction of histone acetylation which is reversed on drug washout by 16 hours of incubation. Continued exposure to sixteen hours maintains strong histone acetylation at 16 hours, but following washout the effect has disappeared by 72 hours. Continuous exposure to 72 hours shows that hydroxamate induced histone acetylation disappears despite the drug remaining present. By comparison, the bicyclic tetrapeptides have produced a delayed histone acetylation which becomes strong by 16 hours and persists out to 72 hours with continuous exposure and also to a modest degree at 72 hours with 16 hours of pulsed exposure.

In conclusion therefore, the immediate acetylation induced by pulsed exposure to the hydroxamate HDAC inhibitors for two hours is not sufficient to induce the downstream biological effect of cell cycle arrest. Thus early histone acetylation through hydroxamates is not sufficient to determine this particular downstream biological effect. By comparison, 16 hours of pulsed drug exposure to either class of inhibitor is able to induce characteristic G2M cell cycle arrest at 72 hours.

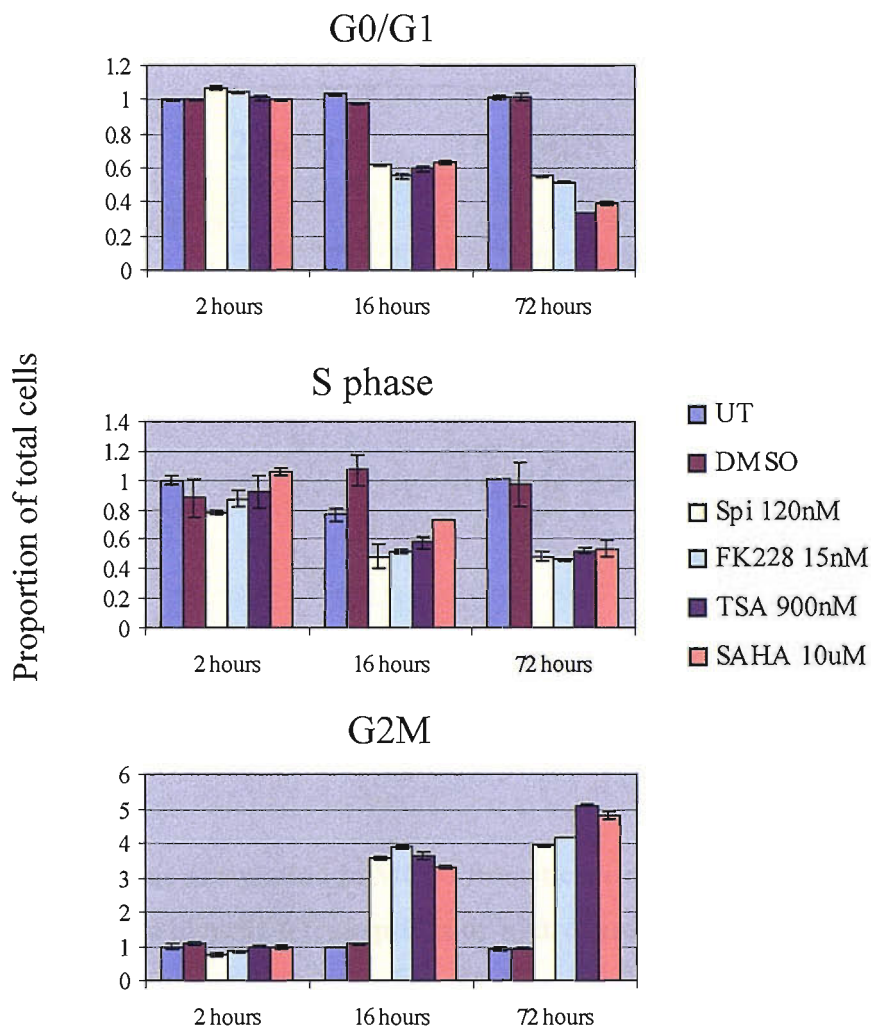


**Figure 6-9 Cell cycle progression in MCF7 breast carcinoma cells following pulsed exposure to Spiruchostatin A, FK228, TSA or SAHA**

MCF7 cell mono-layers were left untreated or exposed to culture medium supplemented with DMSO vehicle or HDAC inhibitors at the indicated doses. At the time points shown, samples were washed five times and maintained to 72 hours in fresh unsupplemented cell culture medium. All samples were then harvested at 72 hours and stained with propidium iodide for analysis by flow cytometry. Results show proportions of cells in the indicated cell cycle phases, as a percentage of cells in cycle. Results are mean values +/- SEM for duplicate samples and are representative of three separate experiments. (Samples in the experiment shown were produced in parallel to those in figure 6-10)

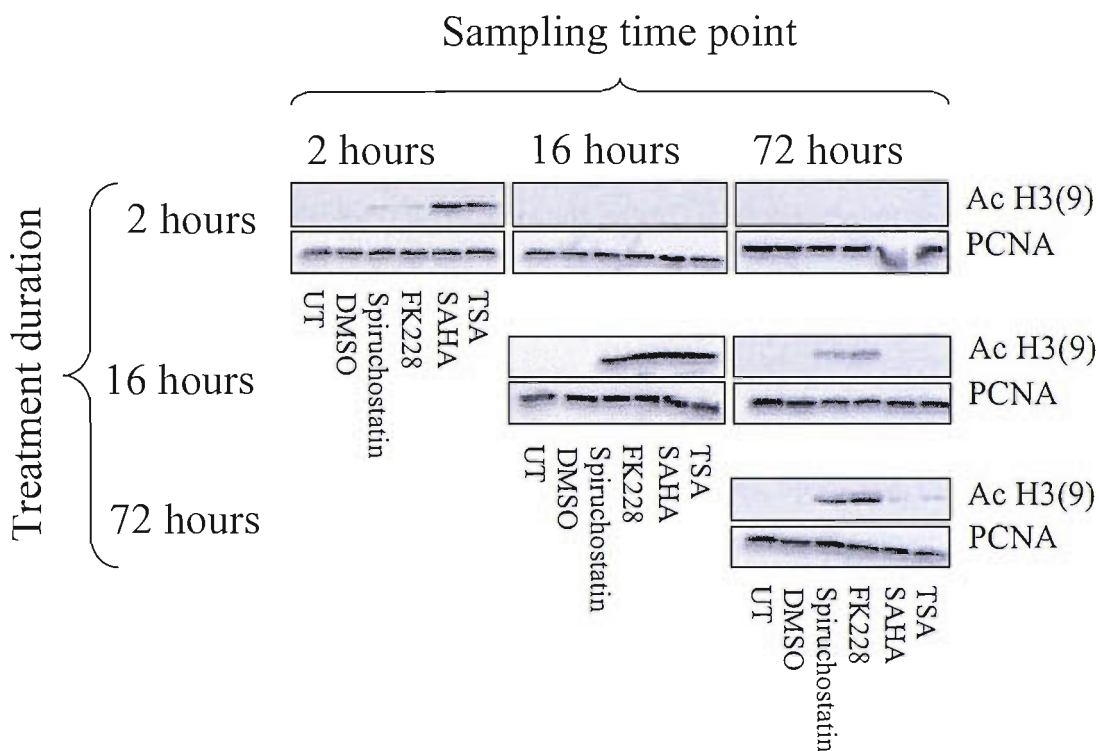


**Figure 6-10 Histone acetylation in MCF7 breast carcinoma cells following pulsed exposure to bicyclic tetrapeptides or hydroxamates**

MCF7 cell mono-layers were left untreated or exposed to culture medium supplemented with DMSO vehicle or 120nM Spiruchostatin A, 15nM FK228, 900nM TSA or 10 $\mu$ M SAHA as indicated. At the treatment duration time points indicated, samples were washed five times in fresh unsupplemented cell culture medium. Samples were then maintained to the sampling time points indicated in unsupplemented cell culture medium and harvested for analysis by Western blot, for acetylated histone three (lysine nine) and PCNA as a loading control. Results are representative of multiple experiments. (Samples in the experiment shown were produced in parallel to those in figure 6-9)

## 6.6 Investigation of Bicyclic Tetrapeptide Cellular Entry and Internal Reduction Mechanisms

Having established that the bicyclic tetrapeptide HDAC inhibitors Spiruchostatin A and FK228 exhibit delayed and prolonged histone acetylation pharmacodynamics by comparison to the hydroxamates, initial investigation was performed to assess potential reasons for these differences. FK228 undergoes a reduction of its internal disulfide bond on cellular entry.<sup>133</sup> This allows for the active site of the molecule to access and interact with the active site of the HDAC enzymes. Spiruchostatin A would be presumed to function in the same manner based on its close structural similarity. Work within the author's laboratory has confirmed that that reduction of Spiruchostatin A does activate its in-vitro activity (Dr Packham, personal communication). Having hypothesised that this internal reduction was likely to occur immediately on cellular entry, investigation was performed to test this by assessing histone acetylation following exposure to Spiruchostatin A that had been pre-exposed to a high molar concentration of the reducing agent DTT. Samples were assessed by Western blot analysis as a time course out to 24 hours. As can be seen in figure 6-11A) pre-exposure of Spiruchostatin A with a reducing agent to render it in its active state does not alter its pharmacodynamics in terms of histone acetylation time course. This suggests that the requirement for Spiruchostatin A to undergo internal reduction is not the determining factor in the observed delay in producing histone acetylation as an effect.

One common determining factor in drug pharmacodynamics is the interaction between drug and serum proteins such as albumin. Drug binding to serum proteins can exert a reservoir effect and limit drug activity in either an absolute manner or by altering time course features. Thus if cellular uptake of the drug can be presumed to be equilibrium/concentration driven, then serum protein binding will modify this process by reducing the effective concentration of drug available for cellular entry. To look at whether this was a contributing factor for the observed histone acetylation

pharmacodynamics seen with the bicyclic HDAC inhibitors, the experiment shown in figure 6-11A also included samples for which Spiruchostatin A was supplemented into serum free cell culture medium after extensive washing out of serum from these samples. This again produced no alteration in the time course of histone acetylation seen following drug exposure. This provides preliminary evidence that serum proteins do not interact with Spiruchostatin A to modify its pharmacodynamics effects.

A further mechanism by which bicyclic compounds might have their pharmacodynamics influenced is through drug entry into and exit from the cell, and also by the dynamics of their interactions with the HDAC active sites. Investigation to begin to elucidate the potential role of both of these factors was performed by co-administration of Spiruchostatin A and its functionally inactive epimer. In figure 6-11B, MCF7 cells were exposed to two different concentrations of Spiruchostatin A either with or without an excess concentration of the epimer. This did not alter the histone acetylation status induced by Spiruchostatin A. Thus Spiruchostatin A induced histone acetylation is not blocked, at least at this time point by competitive interaction with its structural epimer.



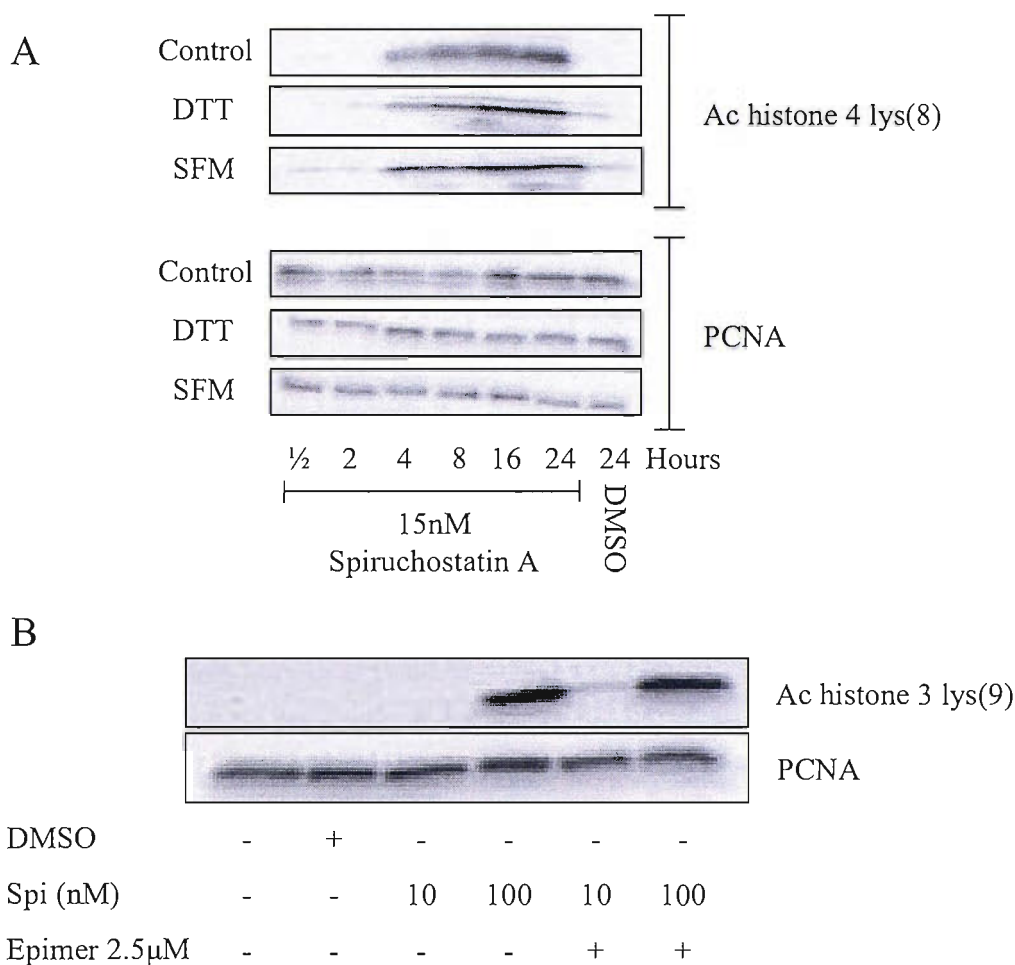


**Figure 6-11 Effects of internal reduction, the presence of serum proteins and co-treatment with an inactive epimer on Spiruchostatin A induced histone acetylation**

MCF7 cell monolayers were exposed to Spiruchostatin A as shown. Samples were then harvested for western blot analysis using antibodies to the indicated acetylated histone lysine residues and PCNA as a loading control. (A) Cells were exposed to 15nM Spiruchostatin A or DMSO vehicle for the indicated durations either in normal cell culture medium (control), or using Spiruchostatin A pre-exposed to a 10mM concentration of the reducing agent dithiothreitol (DTT) or in serum free cell culture medium (SFM) after washing five times. (B) Exposure for 16 hours to Spiruchostatin A with or without its structural epimer at 2.5μM.

## 6.7 Discussion

Work presented in this chapter has considered comparative differences between the HDAC class I selective bicyclic tetrapeptides and the pan class I and II inhibitory hydroxamates in breast cancer cells. The fact that the bicyclic tetrapeptides exhibit a consistently greater potency against breast cancer cells is encouraging for their potential clinical use. However SAHA, the least potent HDAC inhibitor investigated here, is in fact (alongside FK228) one of the most developed compounds to date in the clinical setting and cannot be said to have a worse activity profile in terms of either efficacy or toxicity. Therefore the relevance of yet more potent compounds is perhaps not the most important point to consider in future development. Rather the key may be to consider the potential differences in biological effect between these structural classes to attempt to exploit efficacy/toxicity benefits.

As predicted based on its structure, Spiruchostatin A is a class I selective HDAC inhibitor. This has been confirmed both in collaborative work at the level of in-vitro HDAC inhibition, and in work presented here regarding the downstream effect of tubulin acetylation. Until now, a detailed comparison of the more class I-selective depsipeptide HDAC inhibitor exemplified by FK228 and the simpler class I/II-selective hydroxamates has not been possible, because FK228 was the only example of a natural bicyclic HDAC inhibitor, and this compound has been in limited supply to the academic research community. Characterisation of Spiruchostatin A therefore provided an ideal opportunity to compare directly the activity of multiple members of these different classes. At equipotent doses, both bicyclic tetrapeptides and hydroxamates induce the same degree of histone acetylation and protein expression using p21<sup>(WAF1/Cip1)</sup> as an example. It remains unclear what significance class I HDAC selectivity might have in terms of differences in biological outcome. Early phase I and II clinical trial data has yet to demonstrate clear differences between say the class I HDAC selective inhibitor FK228 and non class selective inhibitors such

as SAHA. Nevertheless there remains the prospect that structural analogue development of class I selective molecules such as Spiruchostatin A might allow for intelligent design of molecules with more favourable efficacy/toxicity profiles. One initial aim that would help in pursuing this line of investigation, would be to have examples of gene expression targets for class I selective inhibitors versus non-selective inhibitors as a starting point for determining differences in biological effect. At the moment we are limited to the ability to assess tubulin acetylation as a class II (HDAC6) effect as shown in this work. A comparative array experiment for Spiruchostatin A and FK228 versus TSA and SAHA would be an obvious initial means to pursue this. By comparison, one example of class II HDAC enzyme downstream biological effect that has been characterised is of HDAC5 and 9 activity providing protection against cardiac hypertrophy in response to specific stress pathways based on work in knockout mice.<sup>150</sup> It remains unclear if this would provide an example for response differences between HDAC class selective and non-selective inhibitors in the form of a murine model. Although class I HDAC selectivity has been demonstrated in this work to be a class effect for bicyclic inhibitors, it remains unclear if FK228 and Spiruchostatin A exhibit the exact same patterns of selectivity or if future development of Spiruchostatin A analogues might lead to yet further subclass selectivity and specificity of HDAC inhibition. This is hampered by the difficulties of in-vitro testing of such selectivity beyond what has been achieved for FK228 and Spiruchostatin A. The ability to create a more complete in-vitro HDAC selectivity profile for these and other inhibitors would be of great value.

In looking at downstream biological effects of the bicyclic versus the hydroxamate inhibitors, it is clear from work presented in this chapter, that much of the fundamental biological endpoint of drug treatment with these compounds, in terms of G2M cell cycle arrest and induction of cell death, is equivalent at equipotent treatment doses. Thus each of these drugs induces cell death and cell cycle arrest and the work presented here does not indicate structure specific differences in these outcomes. The fact that all four drugs are able to show differences in potency for

inhibition of cell proliferation between malignant and normal cells, implies that this is a generalised feature of HDAC inhibition. Thus the proliferation differences in normal cells appear to be a result of a class effect for HDAC inhibitors which does not seem to be altered by HDAC class I selectivity of the bicyclic compounds. Work presented in the previous chapter has shown that S phase arrest is seen with normal cells (fibroblasts) compared to G2M arrest in breast cancer cells in response to Spiruchostatin A. It would seem reasonable to predict that the same differences would be seen with the other HDAC inhibitors but this should be confirmed. Again array data might be a useful first approach to elucidate differences in gene expression in the non malignant cells compared to breast cancer cells. The work discussed in the introduction regarding differences in the effects on TRAIL and Fas death receptor pathways in acute myeloid leukaemia cells compared to normal haematopoietic progenitors and separately of protective induction of thioredoxin levels in normal cells and subsequent death relating to reactive oxygen species for malignant cells may also provide starting points to explain differential effects in other cell systems.<sup>158-160</sup>

With regard to gene expression changes induced by bicyclic tetrapeptides and hydroxamates, the data presented here is consistent with the array data (which used TSA) from which the genes assessed were picked. Both the bicyclic tetrapeptides and the hydroxamates induced increased expression of each of the genes assessed. Thus differences in structural class of these inhibitors, and of the HDAC class selectivity that they exhibit, did not alter downstream gene expression effects at least at these doses and time points and for these particular genes. However further assessment of gene expression at the mRNA level would be of interest to try to identify gene expression changes that differentiate between bicyclic tetrapeptides and hydroxamates. This might be best achieved by initially repeating gene array experiments following exposure to these differing structural classes of inhibitor. In terms of the specific genes assessed, the fact that Spiruchostatin A induces MDR1 expression is important. This finding is consistent with published effects on MDR1 expression of other HDAC inhibitors which are confirmed here. Thus HDAC

inhibition induces its own potential mechanism of drug resistance which has implications for therapeutic use in p-glycoprotein expressing tumours and for combination therapy with other therapeutic modalities. The fact that the epimer of Spiruchostatin A failed to induce MDR1 expression is of interest because it implies that the increase in MDR1 gene expression is a specific effect of HDAC inhibition rather than the effect of a simple xenobiotic sensing mechanism to a foreign drug like molecule. Moreover, the general failure of the Spiruchostatin A epimer to modulate the other genes shown to have their expression altered by Spiruchostatin A, and the other HDAC inhibitors used, helps to confirm that Spiruchostatin A is indeed functioning through the mechanism of protein acetylation by HDAC inhibition.

Although overall effects of different classes of HDAC inhibitor were similar when tested at equipotent concentrations, some striking differences were seen. In work to compare histone acetylation pharmacodynamics, data have been presented to show differences at the level of histone acetylation in cell culture with the bicyclic tetrapeptides producing a delayed but prolonged acetylation response compared to the hydroxamates. The mechanisms for these effects are not clear, but many rate-limiting steps in the action of depsipeptides can be envisioned and may contribute to the slow onset of action and protracted effects. For example, these larger compounds might be expected to accumulate within and exit cells more slowly than lower molecular weight hydroxamates. It is also possible that efficient uptake of the compounds may require active transporters, and these may be saturable or take time to be induced. Alternately, reduction of the compounds may be a rate limiting step.

This raises questions regarding the effect of inhibition of the HDAC enzymes, the measurable immediate outcome of this in the form of histone acetylation and subsequent downstream biological effects leading to tumour cell kill. Better understanding of these interactions may have importance in the design of drug delivery protocols in the clinical setting, which has so far been largely empirical to optimise efficacy/toxicity ratios. For the cyclic tetrapeptides questions arise

regarding the way in which the effect of drug, in producing histone acetylation, relates to drug/cell interactions. Data presented here suggest that we may need other surrogate markers for drug efficacy in early phase clinical trials and basic research because they imply that histone acetylation at a given time point and subsequent biological effect are not necessarily related. Therefore, as a pharmacodynamic endpoint, the duration, rather than magnitude of in vivo HDAC inhibition may better predict clinical response in trials.

Certainly in the data presented to assess cell cycle arrest in breast cancer cells it has been demonstrated that the effects of either class of inhibitor and outcome in terms of G2M arrest are not linked to histone acetylation at an early time point of 2 hours exposure. One aspect of these time course events not assessed in these experiments is whether the 2 hour pulsed exposure induction of early acetylation seen with the hydroxamates is able to affect cell cycle arrest if samples were harvested at an earlier time point, say within the first 24 hours of the experiment. However the results presented already in section 6.2 (figure 6-5) suggest that at 24 hours of continuous exposure, for both structural class of inhibitor, only minimal evidence of cell cycle arrest has begun to occur. Thus it appears that there is a minimal duration of exposure, somewhere between 2 and 16 hours, that is a requirement to induce cell cycle arrest that is durable at least out to 72 hours. It is not the case however that continuous drug exposure beyond a set time point (16 hours in the experiment presented) is required in order to produce a maximal degree of cell cycle arrest. Furthermore, it can be argued that the key marker for assessment of particular biological effect in this experiment was maximal histone acetylation status at 16 hours. The acetylation status at 2 hours of exposure, or at the nominal endpoint of this experiment at 72 hours, was essentially misleading as surrogate markers for this biological effect. This raises questions regarding the use of histone acetylation as a surrogate marker for biological outcome of in-vitro, in-vivo and clinical investigations of HDAC inhibitors which has been widespread in the literature. It may be the case that histone acetylation status needs to be considered as separate to

the underlying transcriptional regulation that underpins the drive to a biological effect such as cell cycle arrest.

## 7 Future Work

Data presented here have provided novel insights into the mechanisms of PPAR $\gamma$  ligands and HDAC inhibitors as potential therapeutic interventions to induce cell cycle arrest, cell death and differentiation in breast cancer cells. A number of avenues for ongoing investigation exist.

With respect to NHR interactions with BAG-1 in breast cancer, it remains of importance to understand how PPAR $\gamma$  agonists, as a potential therapeutic modality, might interact with the known interaction between BAG-1 and the ER. As BAG-1 is known to potentiate the ER, but has been shown here to fail to modulate PPAR $\gamma$ , it would be useful to assess effectiveness of co-administration of PPAR $\gamma$  agonists, with and without conventional ER directed hormonal therapy, in breast cancer cells with respect to BAG-1 expression status. One could envisage modelling these approaches in systems such as the BAG-1 over expressing MCF-7 clones used in this work, to assess the relevance of BAG-1 on the combined effect of ER directed interventions, with selective oestrogen receptor modulators such as tamoxifen or with aromatase inhibitors, and in conjunction with PPAR $\gamma$  agonists. The inability of BAG-1 to modulate PPAR $\gamma$  action might provide a mechanism to perturb the BAG-1 activation of the ER in BAG-1 over expressing cells. This could subsequently be modelled at the level of tumour xenografts, again using clones to determine BAG-1 expression levels. An alternative approach would be to try to affect BAG-1 activity directly by the use of small molecule inhibition. This approach has been explored within the author's laboratory (Sharp A, Crabb S et al, manuscript submitted). The identification of such 'BAG-1 inhibitors' warrants investigation into the ability to modify hormonal intervention strategies in breast cancer, either through conventional modulation of the ER, or potentially via PPAR $\gamma$  agonists.

Turning to HDAC inhibition, it is of importance to further characterise the differences between non-selective inhibitors and the HDAC class I selective



compounds FK-228 and Spiruchostatin A. An initial aim will be to identify differences in protein expression profiles for the selective compounds as a tool to determine how they might distinguish themselves from non-selective inhibitors. A comparative array experiment would be a starting point to achieve this at the mRNA level with subsequent confirmation at the levels of gene assays for mRNA expression and protein expression. It might be expected that the selective class I inhibitors would induce a more narrow range of protein expression changes but this remains to be confirmed. In addition it will be important to determine if any expression changes are seen with these but not the non-selective compounds. Following on from this, other Spiruchostatin A analogues are being produced by the Southampton collaboration that has developed the parent compound. These compounds will equally need to be validated for their activity in breast cancer models as has been described here, as well as other cancer experimental systems. This gives the potential to select for desirable characteristics. Initial definition of gene expression signatures afforded by differing structures is a first step in this process.

The description of differences in cell cycle progression between malignant and normal cells following HDAC inhibition, and the demonstration that this appears to be a class effect for HDAC inhibitors, builds on previous work using SAHA.<sup>147</sup> This will need to be confirmed in other cell systems because it implies that malignant cells have perturbed cell cycle checkpoint mechanisms that predispose them to HDAC inhibitor therapy. Analysis and identification of the key cell cycle modulators that underpin these observations to elucidate the mechanism for this is required. The microarray experiment using TSA performed in the author's laboratory detected, amongst the overall change in mRNA expression following HDAC inhibition, a number of cell cycle regulatory proteins that underwent altered expression in response to treatment (Howell M, Crabb S et al, manuscript in preparation). The next step to determining how normal cells differ in response to HDAC inhibition would be to repeat this as a comparative experiment in malignant and normal cells and to confirm it with other HDAC inhibitors.

The time course characteristics for hydroxamates versus the bicyclic HDAC inhibitors are intriguing because they require us to reconsider the relevance of histone acetylation as a marker of efficacy with respect to subsequent biological outcome and tumour cell kill. It has been argued here that duration rather than magnitude of histone acetylation is perhaps more relevant as a surrogate marker for efficacy, based on the finding of delayed but prolonged acetylation with Spiruchostatin A and FK-228. This needs to be formally tested however, first through modelling in cell culture systems. In addition time course experiments using gene expression assays at the mRNA level are of interest to model changes in genes whose expression is altered by HDAC inhibition with respect to exposure duration. This will provide comparison to the time course histone acetylation changes described here.

Clearly the development of Spiruchostatin A to date raises the question of its in-vivo activity and a number of animal experiments suggest themselves at this stage. Firstly the fundamental need for the molecule to be active and avoid metabolic degradation needs to be confirmed. The close similarity to FK-288 is encouraging in this regard as this compound has been shown to be stable and active in development up to the level of phase II clinical trials. The efficacy and toxicity of the compound then need to be assessed in murine xenograft models. The questions of histone acetylation and its use as a subsequent marker of efficacy (and toxicity) should be examined at this level both in malignant and normal tissues as extensions of the work presented here in cell lines. The aim would be to model histone acetylation over time in either tumour tissue, or a surrogate such as peripheral blood lymphocytes, to tumour response and determine the relevance of acetylation duration. The subsequent in-vivo assessment of Spiruchostatin A analogues will allow for assessment of the potential to design for optimisation of therapeutic outcome. It is perhaps more likely that benefit will lie more in improvement in toxicity patterns than efficacy for the analogues of Spiruchostatin A. One major aim must be to attempt to produce

compounds without the potential for cardiac toxicity which have been a concern with FK-228.

Finally the likelihood for the development of many therapeutics strategies aimed at malignant cells is that combination treatment will be an appropriate manner in which to utilise them. Initial work with other targeted therapeutic interventions such as trastuzumab and with conventional cytotoxics have suggested synergistic activity and this warrants further exploration.<sup>162</sup> Little is understood about the nature of such synergism and gene expression profiling would be a starting point to indicate where the pathways relevant to interaction lie. The combination of a broad transcriptional modifier in the form of an HDAC inhibitor and more targeted intervention of known key mediators for cell proliferation, such as HER2 or the ER, is an attractive area for development.

## References

1. CancerStats Monograph 2004. Cancer Research UK; 2004.
2. Schwartz GK, Shah MA. Targeting the cell cycle: a new approach to cancer therapy. *J Clin Oncol* 2005; 23:9408-9421.
3. Leszczyniecka M, Roberts T, Dent P, Grant S, Fisher PB. Differentiation therapy of human cancer: basic science and clinical applications. *Pharmacol Ther* 2001; 90:105-156.
4. Cutress RI, Townsend PA, Sharp A, Maison A, Wood L, Lee R, Brimmell M, Mullee MA, Johnson PW, Royle GT, Bateman AC, Packham G. The nuclear BAG-1 isoform, BAG-1L, enhances oestrogen-dependent transcription. *Oncogene* 2003; 22:4973-4982.
5. Cato AC, Mink S. BAG-1 family of cochaperones in the modulation of nuclear receptor action. *J Steroid Biochem Mol Biol* 2001; 78:379-388.
6. Rumi MA, Ishihara S, Kazumori H, Kadowaki Y, Kinoshita Y. Can PPAR gamma ligands be used in cancer therapy? *Curr Med Chem Anti -Canc Agents* 2004; 4:465-477.
7. Cutress RI, Townsend PA, Brimmell M, Bateman AC, Hague A, Packham G. BAG-1 expression and function in human cancer. *Br J Cancer* 2002; 87:834-839.
8. Tang SC. BAG-1, an anti-apoptotic tumour marker. *IUBMB Life* 2002; 53:99-105.
9. Townsend PA, Cutress RI, Sharp A, Brimmell M, Packham G. BAG-1: a multifunctional regulator of cell growth and survival. *Biochim Biophys Acta* 2003; 1603:83-98.

10. Sharp A, Crabb SJ, Cutress RI, Brimmell M, Wang XH, Packham G, Townsend PA. BAG-1 in carcinogenesis. *Expert Rev Mol Med* 2004; 2004:1-15.
11. Townsend PA, Stephanou A, Packham G, Latchman DS. BAG-1: a multi-functional pro-survival molecule. *Int J Biochem Cell Biol* 2005; 37:251-259.
12. Di Gennaro E, Bruzzese F, Caraglia M, Abruzzese A, Budillon A. Acetylation of proteins as novel target for antitumor therapy: review article. *Amino Acids* 2004; 26:435-441.
13. McLaughlin F, La Thangue NB. Histone deacetylase inhibitors open new doors in cancer therapy. *Biochem Pharmacol* 2004; 68:1139-1144.
14. Zhu WG, Otterson GA. The interaction of histone deacetylase inhibitors and DNA methyltransferase inhibitors in the treatment of human cancer cells. *Curr Med Chem Anti -Canc Agents* 2003; 3:187-199.
15. Takayama S, Sato T, Krajewski S, Kochel K, Irie S, Millan JA, Reed JC. Cloning and functional analysis of BAG-1: a novel Bcl-2-binding protein with anti-cell death activity. *Cell* 1995; 80:279-284.
16. Zeiner M, Gehring U. A protein that interacts with members of the nuclear hormone receptor family: identification and cDNA cloning. *Proc Natl Acad Sci U S A* 1995; 92:11465-11469.
17. Takayama S, Kochel K, Irie S, Inazawa J, Abe T, Sato T, Druck T, Huebner K, Reed JC. Cloning of cDNAs encoding the human BAG1 protein and localization of the human BAG1 gene to chromosome 9p12. *Genomics* 1996; 35:494-498.
18. Packham G, Brimmell M, Cleveland JL. Mammalian cells express two differently localized Bag-1 isoforms generated by alternative translation initiation. *Biochem J* 1997; 328 ( Pt 3):807-813.

19. Takayama S, Krajewski S, Krajewska M, Kitada S, Zapata JM, Kochel K, Knee D, Scudiero D, Tudor G, Miller GJ, Miyashita T, Yamada M, Reed JC. Expression and location of Hsp70/Hsc-binding anti-apoptotic protein BAG-1 and its variants in normal tissues and tumor cell lines. *Cancer Res* 1998; 58:3116-3131.
20. Yang X, Chernenko G, Hao Y, Ding Z, Pater MM, Pater A, Tang SC. Human BAG-1/RAP46 protein is generated as four isoforms by alternative translation initiation and overexpressed in cancer cells. *Oncogene* 1998; 17:981-989.
21. Coldwell MJ, deSchoolmeester ML, Fraser GA, Pickering BM, Packham G, Willis AE. The p36 isoform of BAG-1 is translated by internal ribosome entry following heat shock. *Oncogene* 2001; 20:4095-4100.
22. Merrick WC. Cap-dependent and cap-independent translation in eukaryotic systems. *Gene* 2004; 332:1-11.
23. Pickering BM, Mitchell SA, Spriggs KA, Stoneley M, Willis AE. Bag-1 internal ribosome entry segment activity is promoted by structural changes mediated by poly(rC) binding protein 1 and recruitment of polypyrimidine tract binding protein 1. *Mol Cell Biol* 2004; 24:5595-5605.
24. Sourisseau T, Desbois C, Debure L, Bowtell DD, Cato AC, Schneikert J, Moyse E, Michel D. Alteration of the stability of Bag-1 protein in the control of olfactory neuronal apoptosis. *J Cell Sci* 2001; 114:1409-1416.
25. Takayama S, Reed JC. Molecular chaperone targeting and regulation by BAG family proteins. *Nat Cell Biol* 2001; 3:E237-E241.
26. Briknarova K, Takayama S, Brive L, Havert ML, Knee DA, Velasco J, Homma S, Cabezas E, Stuart J, Hoyt DW, Satterthwait AC, Llinas M, Reed JC, Ely KR. Structural analysis of BAG1 cochaperone and its interactions with Hsc70 heat shock protein. *Nat Struct Biol* 2001; 8:349-352.

27. Sondermann H, Scheufler C, Schneider C, Hohfeld J, Hartl FU, Moarefi I. Structure of a Bag/Hsc70 complex: convergent functional evolution of Hsp70 nucleotide exchange factors. *Science* 2001; 291:1553-1557.
28. Takayama S, Xie Z, Reed JC. An evolutionarily conserved family of Hsp70/Hsc70 molecular chaperone regulators. *J Biol Chem* 1999; 274:781-786.
29. Song J, Takeda M, Morimoto RI. Bag1-Hsp70 mediates a physiological stress signalling pathway that regulates Raf-1/ERK and cell growth. *Nat Cell Biol* 2001; 3:276-282.
30. Wang HG, Takayama S, Rapp UR, Reed JC. Bcl-2 interacting protein, BAG-1, binds to and activates the kinase Raf-1. *Proc Natl Acad Sci U S A* 1996; 93:7063-7068.
31. Luders J, Demand J, Hohfeld J. The ubiquitin-related BAG-1 provides a link between the molecular chaperones Hsc70/Hsp70 and the proteasome. *J Biol Chem* 2000; 275:4613-4617.
32. Alberti S, Demand J, Esser C, Emmerich N, Schild H, Hohfeld J. Ubiquitylation of BAG-1 suggests a novel regulatory mechanism during the sorting of chaperone substrates to the proteasome. *J Biol Chem* 2002; 277:45920-45927.
33. Schneikert J, Hubner S, Martin E, Cato AC. A nuclear action of the eukaryotic cochaperone RAP46 in downregulation of glucocorticoid receptor activity. *J Cell Biol* 1999; 146:929-940.
34. Bardelli A, Longati P, Albero D, Goruppi S, Schneider C, Ponzetto C, Comoglio PM. HGF receptor associates with the anti-apoptotic protein BAG-1 and prevents cell death. *EMBO J* 1996; 15:6205-6212.

35. Clevenger CV, Thickman K, Ngo W, Chang WP, Takayama S, Reed JC. Role of Bag-1 in the survival and proliferation of the cytokine-dependent lymphocyte lines, Ba/F3 and Nb2. *Mol Endocrinol* 1997; 11:608-618.
36. Kullmann M, Schneikert J, Moll J, Heck S, Zeiner M, Gehring U, Cato AC. RAP46 is a negative regulator of glucocorticoid receptor action and hormone-induced apoptosis. *J Biol Chem* 1998; 273:14620-14625.
37. Lin J, Hutchinson L, Gaston SM, Raab G, Freeman MR. BAG-1 is a novel cytoplasmic binding partner of the membrane form of heparin-binding EGF-like growth factor: a unique role for proHB-EGF in cell survival regulation. *J Biol Chem* 2001; 276:30127-30132.
38. Townsend PA, Cutress RI, Sharp A, Brimmell M, Packham G. BAG-1 prevents stress-induced long-term growth inhibition in breast cancer cells via a chaperone-dependent pathway. *Cancer Res* 2003; 63:4150-4157.
39. Yang X, Hao Y, Ferenczy A, Tang SC, Pater A. Overexpression of anti-apoptotic gene BAG-1 in human cervical cancer. *Exp Cell Res* 1999; 247:200-207.
40. Yawata A, Adachi M, Okuda H, Naishiro Y, Takamura T, Hareyama M, Takayama S, Reed JC, Imai K. Prolonged cell survival enhances peritoneal dissemination of gastric cancer cells. *Oncogene* 1998; 16:2681-2686.
41. Arhel NJ, Packham G, Townsend PA, Collard TJ, Zadeh AM, Sharp A, Cutress RI, Malik K, Hague A, Paraskeva C, Williams AC. The retinoblastoma protein interacts with Bag-1 in human colonic adenoma and carcinoma derived cell lines. *Int J Cancer* 2003; 106:364-371.
42. King FW, Wawrzynow A, Hohfeld J, Zylicz M. Co-chaperones Bag-1, Hop and Hsp40 regulate Hsc70 and Hsp90 interactions with wild-type or mutant p53. *EMBO J* 2001; 20:6297-6305.



43. Hung WJ, Roberson RS, Taft J, Wu DY. Human BAG-1 proteins bind to the cellular stress response protein GADD34 and interfere with GADD34 functions. *Mol Cell Biol* 2003; 23:3477-3486.
44. Niyaz Y, Frenz I, Petersen G, Gehring U. Transcriptional stimulation by the DNA binding protein Hap46/BAG-1M involves hsp70/hsc70 molecular chaperones. *Nucleic Acids Res* 2003; 31:2209-2216.
45. Sondermann H, Ho AK, Listenberger LL, Siegers K, Moarefi I, Wente SR, Hartl FU, Young JC. Prediction of novel Bag-1 homologs based on structure/function analysis identifies Snl1p as an Hsp70 co-chaperone in *Saccharomyces cerevisiae*. *J Biol Chem* 2002; 277:33220-33227.
46. Takayama S, Bimston DN, Matsuzawa S, Freeman BC, Aime-Sempe C, Xie Z, Morimoto RI, Reed JC. BAG-1 modulates the chaperone activity of Hsp70/Hsc70. *EMBO J* 1997; 16:4887-4896.
47. Zeiner M, Gebauer M, Gehring U. Mammalian protein RAP46: an interaction partner and modulator of 70 kDa heat shock proteins. *EMBO J* 1997; 16:5483-5490.
48. Luders J, Demand J, Papp O, Hohfeld J. Distinct isoforms of the cofactor BAG-1 differentially affect Hsc70 chaperone function. *J Biol Chem* 2000; 275:14817-14823.
49. Nollen EA, Kabakov AE, Brunsting JF, Kanon B, Hohfeld J, Kampinga HH. Modulation of in vivo HSP70 chaperone activity by Hip and Bag-1. *J Biol Chem* 2001; 276:4677-4682.
50. Nollen EA, Brunsting JF, Song J, Kampinga HH, Morimoto RI. Bag1 functions in vivo as a negative regulator of Hsp70 chaperone activity. *Mol Cell Biol* 2000; 20:1083-1088.
51. Brimmell M, Burns JS, Munson P, McDonald L, O'Hare MJ, Lakhani SR, Packham G. High level expression of differentially localized BAG-1

- isoforms in some oestrogen receptor-positive human breast cancers. *Br J Cancer* 1999; 81:1042-1051.
52. Knee DA, Froesch BA, Nuber U, Takayama S, Reed JC. Structure-function analysis of Bag1 proteins. Effects on androgen receptor transcriptional activity. *J Biol Chem* 2001; 276:12718-12724.
  53. Turner BC, Krajewski S, Krajewska M, Takayama S, Gumbs AA, Carter D, Rebeck TR, Haffty BG, Reed JC. BAG-1: a novel biomarker predicting long-term survival in early-stage breast cancer. *J Clin Oncol* 2001; 19:992-1000.
  54. Sjostrom J, Blomqvist C, von Boguslawski K, Bengtsson NO, Mjaaland I, Malmstrom P, Ostenstadt B, Wist E, Valvere V, Takayama S, Reed JC, Saksela E. The predictive value of bcl-2, bax, bcl-xL, bag-1, fas, and fasL for chemotherapy response in advanced breast cancer. *Clin Cancer Res* 2002; 8:811-816.
  55. Tang SC, Shehata N, Chernenko G, Khalifa M, Wang X, Shaheta N. Expression of BAG-1 in invasive breast carcinomas. *J Clin Oncol* 1999; 17:1710-1719.
  56. Townsend PA, Dublin E, Hart IR, Kao RH, Hanby AM, Cutress RI, Poulson R, Ryder K, Barnes DM, Packham G. BAG-1 expression in human breast cancer: interrelationship between BAG-1 RNA, protein, HSC70 expression and clinico-pathological data. *J Pathol* 2002; 197:51-59.
  57. Cutress RI, Townsend PA, Bateman AC, Johnson PW, Ryder K, Barnes DM, Packham G. BAG-1 immunostaining and survival in early breast cancer. *J Clin Oncol* 2001; 19:3706-3707.
  58. Pusztai L, Krishnamurti S, Perez CJ, Sneige N, Esteva FJ, Volchenok M, Breitenfelder P, Kau SW, Takayama S, Krajewski S, Reed JC, Bast RC, Jr., Hortobagyi GN. Expression of BAG-1 and Bcl-2 proteins before and after

- neoadjuvant chemotherapy of locally advanced breast cancer. *Cancer Invest* 2004; 22:248-256.
59. Noguchi T, Takeno S, Shibata T, Fumoto S, Uchida Y, Yokoyama S, Gabbert HE, Muller W. Nuclear BAG-1 expression is a biomarker of poor prognosis in esophageal squamous cell carcinoma. *Dis Esophagus* 2003; 16:107-111.
  60. Kikuchi R, Noguchi T, Takeno S, Funada Y, Moriyama H, Uchida Y. Nuclear BAG-1 expression reflects malignant potential in colorectal carcinomas. *Br J Cancer* 2002; 87:1136-1139.
  61. Xie X, Clausen OP, Boysen M. Bag-1 expression as a prognostic factor in tongue squamous cell carcinomas. *Laryngoscope* 2004; 114:1785-1790.
  62. Rorke S, Murphy S, Khalifa M, Chernenko G, Tang SC. Prognostic significance of BAG-1 expression in nonsmall cell lung cancer. *Int J Cancer* 2001; 95:317-322.
  63. Kitada S, Andersen J, Akar S, Zapata JM, Takayama S, Krajewski S, Wang HG, Zhang X, Bullrich F, Croce CM, Rai K, Hines J, Reed JC. Expression of apoptosis-regulating proteins in chronic lymphocytic leukemia: correlations with In vitro and In vivo chemoresponses. *Blood* 1998; 91:3379-3389.
  64. Yamauchi H, Adachi M, Sakata K, Hareyama M, Satoh M, Himi T, Takayama S, Reed JC, Imai K. Nuclear BAG-1 localization and the risk of recurrence after radiation therapy in laryngeal carcinomas. *Cancer Lett* 2001; 165:103-110.
  65. Roth W, Grimm C, Rieger L, Strik H, Takayama S, Krajewski S, Meyermann R, Dichgans J, Reed JC, Weller M. Bag-1 and Bcl-2 gene transfer in malignant glioma: modulation of cell cycle regulation and apoptosis. *Brain Pathol* 2000; 10:223-234.

66. Moriyama T, Littell RD, Debernardo R, Oliva E, Lynch MP, Rueda BR, Duska LR. BAG-1 expression in normal and neoplastic endometrium. *Gynecol Oncol* 2004; 94:289-295.
67. Hague A, Packham G, Huntley S, Shefford K, Eveson JW. Deregulated Bag-1 protein expression in human oral squamous cell carcinomas and lymph node metastases. *J Pathol* 2002; 197:60-71.
68. Shindoh M, Adachi M, Higashino F, Yasuda M, Hida K, Nishioka T, Ono M, Takayama S, Reed JC, Imai K, Totsuka Y, Kohgo T. BAG-1 expression correlates highly with the malignant potential in early lesions (T1 and T2) of oral squamous cell carcinoma. *Oral Oncol* 2000; 36:444-449.
69. Rau KM, Kang HY, Cha TL, Miller SA, Hung MC. The mechanisms and managements of hormone-therapy resistance in breast and prostate cancers. *Endocr Relat Cancer* 2005; 12:511-532.
70. Olefsky JM. Nuclear receptor minireview series. *J Biol Chem* 2001; 276:36863-36864.
71. Rosenfeld MG, Glass CK. Coregulator codes of transcriptional regulation by nuclear receptors. *J Biol Chem* 2001; 276:36865-36868.
72. Cheung J, Smith DF. Molecular chaperone interactions with steroid receptors: an update. *Mol Endocrinol* 2000; 14:939-946.
73. Nollen EA, Morimoto RI. Chaperoning signaling pathways: molecular chaperones as stress-sensing 'heat shock' proteins. *J Cell Sci* 2002; 115:2809-2816.
74. Kanelakis KC, Morishima Y, Dittmar KD, Galigniana MD, Takayama S, Reed JC, Pratt WB. Differential effects of the hsp70-binding protein BAG-1 on glucocorticoid receptor folding by the hsp90-based chaperone machinery. *J Biol Chem* 1999; 274:34134-34140.

75. Schneikert J, Hubner S, Langer G, Petri T, Jaattela M, Reed J, Cato AC. Hsp70-RAP46 interaction in downregulation of DNA binding by glucocorticoid receptor. *EMBO J* 2000; 19:6508-6516.
76. Froesch BA, Takayama S, Reed JC. BAG-1L protein enhances androgen receptor function. *J Biol Chem* 1998; 273:11660-11666.
77. Shatkina L, Mink S, Rogatsch H, Klocker H, Langer G, Nestl A, Cato AC. The cochaperone Bag-1L enhances androgen receptor action via interaction with the NH2-terminal region of the receptor. *Mol Cell Biol* 2003; 23:7189-7197.
78. Schmidt U, Wochnik GM, Rosenhagen MC, Young JC, Hartl FU, Holsboer F, Rein T. Essential role of the unusual DNA-binding motif of BAG-1 for inhibition of the glucocorticoid receptor. *J Biol Chem* 2003; 278:4926-4931.
79. Liu R, Takayama S, Zheng Y, Froesch B, Chen GQ, Zhang X, Reed JC, Zhang XK. Interaction of BAG-1 with retinoic acid receptor and its inhibition of retinoic acid-induced apoptosis in cancer cells. *J Biol Chem* 1998; 273:16985-16992.
80. Guzey M, Takayama S, Reed JC. BAG1L enhances trans-activation function of the vitamin D receptor. *J Biol Chem* 2000; 275:40749-40756.
81. Witcher M, Yang X, Pater A, Tang SC. BAG-1 p50 isoform interacts with the vitamin D receptor and its cellular overexpression inhibits the vitamin D pathway. *Exp Cell Res* 2001; 265:167-173.
82. Berger J, Moller DE. The mechanisms of action of PPARs. *Annu Rev Med* 2002; 53:409-435.
83. Debril MB, Renaud JP, Fajas L, Auwerx J. The pleiotropic functions of peroxisome proliferator-activated receptor gamma. *J Mol Med* 2001; 79:30-47.

84. Kersten S, Desvergne B, Wahli W. Roles of PPARs in health and disease. *Nature* 2000; 405:421-424.
85. Sporn MB, Suh N, Mangelsdorf DJ. Prospects for prevention and treatment of cancer with selective PPARgamma modulators (SPARMs). *Trends Mol Med* 2001; 7:395-400.
86. Rosen ED, Sarraf P, Troy AE, Bradwin G, Moore K, Milstone DS, Spiegelman BM, Mortensen RM. PPAR gamma is required for the differentiation of adipose tissue in vivo and in vitro. *Mol Cell* 1999; 4:611-617.
87. Barak Y, Nelson MC, Ong ES, Jones YZ, Ruiz-Lozano P, Chien KR, Koder A, Evans RM. PPAR gamma is required for placental, cardiac, and adipose tissue development. *Mol Cell* 1999; 4:585-595.
88. Clay CE, Namen AM, Atsumi G, Willingham MC, High KP, Kute TE, Trimboli AJ, Fonteh AN, Dawson PA, Chilton FH. Influence of J series prostaglandins on apoptosis and tumorigenesis of breast cancer cells. *Carcinogenesis* 1999; 20:1905-1911.
89. Elstner E, Muller C, Koshizuka K, Williamson EA, Park D, Asou H, Shintaku P, Said JW, Heber D, Koeffler HP. Ligands for peroxisome proliferator-activated receptor gamma and retinoic acid receptor inhibit growth and induce apoptosis of human breast cancer cells in vitro and in BNX mice. *Proc Natl Acad Sci U S A* 1998; 95:8806-8811.
90. Keller H, Givel F, Perroud M, Wahli W. Signaling cross-talk between peroxisome proliferator-activated receptor/retinoid X receptor and estrogen receptor through estrogen response elements. *Mol Endocrinol* 1995; 9:794-804.
91. Wang X, Kilgore MW. Signal cross-talk between estrogen receptor alpha and beta and the peroxisome proliferator-activated receptor gamma1 in MDA-

- MB-231 and MCF-7 breast cancer cells. *Mol Cell Endocrinol* 2002; 194:123-133.
92. Rubin GL, Zhao Y, Kalus AM, Simpson ER. Peroxisome proliferator-activated receptor gamma ligands inhibit estrogen biosynthesis in human breast adipose tissue: possible implications for breast cancer therapy. *Cancer Res* 2000; 60:1604-1608.
  93. Pignatelli M, Cortes-Canteli M, Lai C, Santos A, Perez-Castillo A. The peroxisome proliferator-activated receptor gamma is an inhibitor of ErbBs activity in human breast cancer cells. *J Cell Sci* 2001; 114:4117-4126.
  94. Suh N, Wang Y, Williams CR, Risingsong R, Gilmer T, Willson TM, Sporn MB. A new ligand for the peroxisome proliferator-activated receptor-gamma (PPAR-gamma), GW7845, inhibits rat mammary carcinogenesis. *Cancer Res* 1999; 59:5671-5673.
  95. Kroll TG, Sarraf P, Pecciarini L, Chen CJ, Mueller E, Spiegelman BM, Fletcher JA. PAX8-PPARgamma1 fusion oncogene in human thyroid carcinoma [corrected]. *Science* 2000; 289:1357-1360.
  96. McIver B, Grebe SK, Eberhardt NL. The PAX8/PPAR gamma fusion oncogene as a potential therapeutic target in follicular thyroid carcinoma. *Curr Drug Targets Immune Endocr Metabol Disord* 2004; 4:221-234.
  97. Badawi AF, Badr MZ. Expression of cyclooxygenase-2 and peroxisome proliferator-activated receptor-gamma and levels of prostaglandin E2 and 15-deoxy-delta12,14-prostaglandin J2 in human breast cancer and metastasis. *Int J Cancer* 2003; 103:84-90.
  98. Jiang WG, Douglas-Jones A, Mansel RE. Expression of peroxisome-proliferator activated receptor-gamma (PPARgamma) and the PPARgamma co-activator, PGC-1, in human breast cancer correlates with clinical outcomes. *Int J Cancer* 2003; 106:752-757.

99. Govindarajan R, Ratnasinghe L, Midathada M, Kim P, Darbe M, Barnhart S, Siegel E, Simmons D, Kim L, Lang N. Association between the use of thiazolidinediones and the risk of cancer in diabetic patients. 2005. Proc ASCO.
100. Burstein HJ, Demetri GD, Mueller E, Sarraf P, Spiegelman BM, Winer EP. Use of the peroxisome proliferator-activated receptor (PPAR) gamma ligand troglitazone as treatment for refractory breast cancer: a phase II study. *Breast Cancer Res Treat* 2003; 79:391-397.
101. Hisatake JI, Ikezoe T, Carey M, Holden S, Tomoyasu S, Koeffler HP. Down-Regulation of prostate-specific antigen expression by ligands for peroxisome proliferator-activated receptor gamma in human prostate cancer. *Cancer Res* 2000; 60:5494-5498.
102. Mueller E, Smith M, Sarraf P, Kroll T, Aiyer A, Kaufman DS, Oh W, Demetri G, Figg WD, Zhou XP, Eng C, Spiegelman BM, Kantoff PW. Effects of ligand activation of peroxisome proliferator-activated receptor gamma in human prostate cancer. *Proc Natl Acad Sci U S A* 2000; 97:10990-10995.
103. Tontonoz P, Singer S, Forman BM, Sarraf P, Fletcher JA, Fletcher CD, Brun RP, Mueller E, Altiock S, Oppenheim H, Evans RM, Spiegelman BM. Terminal differentiation of human liposarcoma cells induced by ligands for peroxisome proliferator-activated receptor gamma and the retinoid X receptor. *Proc Natl Acad Sci U S A* 1997; 94:237-241.
104. Demetri GD, Fletcher CD, Mueller E, Sarraf P, Naujoks R, Campbell N, Spiegelman BM, Singer S. Induction of solid tumor differentiation by the peroxisome proliferator-activated receptor-gamma ligand troglitazone in patients with liposarcoma. *Proc Natl Acad Sci U S A* 1999; 96:3951-3956.



105. Debrock G, Vanhentenrijk V, Sciot R, Debiec-Rychter M, Oyen R, Van Oosterom A. A phase II trial with rosiglitazone in liposarcoma patients. *Br J Cancer* 2003; 89:1409-1412.
106. Kulke MH, Demetri GD, Sharpless NE, Ryan DP, Shivdasani R, Clark JS, Spiegelman BM, Kim H, Mayer RJ, Fuchs CS. A phase II study of troglitazone, an activator of the PPARgamma receptor, in patients with chemotherapy-resistant metastatic colorectal cancer. *Cancer J* 2002; 8:395-399.
107. Clay CE, Atsumi GI, High KP, Chilton FH. Early de novo gene expression is required for 15-deoxy-Delta 12,14-prostaglandin J2-induced apoptosis in breast cancer cells. *J Biol Chem* 2001; 276:47131-47135.
108. Biel M, Wascholowski V, Giannis A. Epigenetics--an epicenter of gene regulation: histones and histone-modifying enzymes. *Angew Chem Int Ed Engl* 2005; 44:3186-3216.
109. Strahl BD, Allis CD. The language of covalent histone modifications. *Nature* 2000; 403:41-45.
110. Marmorstein R, Roth SY. Histone acetyltransferases: function, structure, and catalysis. *Curr Opin Genet Dev* 2001; 11:155-161.
111. Allfrey VG, FAULKNER R, MIRSKY AE. Acetylation and methylation of histones and their possible role in the regulation of RNA synthesis. *Proc Natl Acad Sci U S A* 1964; 51:786-794.
112. Marks PA, Miller T, Richon VM. Histone deacetylases. *Curr Opin Pharmacol* 2003; 3:344-351.
113. Gregory PD, Wagner K, Horz W. Histone acetylation and chromatin remodeling. *Exp Cell Res* 2001; 265:195-202.

114. Cress WD, Seto E. Histone deacetylases, transcriptional control, and cancer. *J Cell Physiol* 2000; 184:1-16.
115. Marks P, Rifkind RA, Richon VM, Breslow R, Miller T, Kelly WK. Histone deacetylases and cancer: causes and therapies. *Nat Rev Cancer* 2001; 1:194-202.
116. Hubbert C, Guardiola A, Shao R, Kawaguchi Y, Ito A, Nixon A, Yoshida M, Wang XF, Yao TP. HDAC6 is a microtubule-associated deacetylase. *Nature* 2002; 417:455-458.
117. Youn HD, Grozinger CM, Liu JO. Calcium regulates transcriptional repression of myocyte enhancer factor 2 by histone deacetylase 4. *J Biol Chem* 2000; 275:22563-22567.
118. Grant PA, Berger SL. Histone acetyltransferase complexes. *Semin Cell Dev Biol* 1999; 10:169-177.
119. Kouzarides T. Acetylation: a regulatory modification to rival phosphorylation? *EMBO J* 2000; 19:1176-1179.
120. He LZ, Tolentino T, Grayson P, Zhong S, Warrell RP, Jr., Rifkind RA, Marks PA, Richon VM, Pandolfi PP. Histone deacetylase inhibitors induce remission in transgenic models of therapy-resistant acute promyelocytic leukemia. *J Clin Invest* 2001; 108:1321-1330.
121. Lin RJ, Nagy L, Inoue S, Shao W, Miller WH, Jr., Evans RM. Role of the histone deacetylase complex in acute promyelocytic leukaemia. *Nature* 1998; 391:811-814.
122. Dhordain P, Lin RJ, Quief S, Lantoine D, Kerckaert JP, Evans RM, Albagli O. The LAZ3(BCL-6) oncoprotein recruits a SMRT/mSIN3A/histone deacetylase containing complex to mediate transcriptional repression. *Nucleic Acids Res* 1998; 26:4645-4651.

123. Gayther SA, Batley SJ, Linger L, Bannister A, Thorpe K, Chin SF, Daigo Y, Russell P, Wilson A, Sowter HM, Delhanty JD, Ponder BA, Kouzarides T, Caldas C. Mutations truncating the EP300 acetylase in human cancers. *Nat Genet* 2000; 24:300-303.
124. Yang XJ. Lysine acetylation and the bromodomain: a new partnership for signaling. *Bioessays* 2004; 26:1076-1087.
125. Martinez-Balbas MA, Bauer UM, Nielsen SJ, Brehm A, Kouzarides T. Regulation of E2F1 activity by acetylation. *EMBO J* 2000; 19:662-671.
126. Chan HM, Krstic-Demonacos M, Smith L, Demonacos C, La Thangue NB. Acetylation control of the retinoblastoma tumour-suppressor protein. *Nat Cell Biol* 2001; 3:667-674.
127. Gu W, Roeder RG. Activation of p53 sequence-specific DNA binding by acetylation of the p53 C-terminal domain. *Cell* 1997; 90:595-606.
128. Imai T, Adachi S, Nishijo K, Ohgushi M, Okada M, Yasumi T, Watanabe K, Nishikomori R, Nakayama T, Yonehara S, Toguchida J, Nakahata T. FR901228 induces tumor regression associated with induction of Fas ligand and activation of Fas signaling in human osteosarcoma cells. *Oncogene* 2003; 22:9231-9242.
129. Keen JC, Yan L, Mack KM, Pettit C, Smith D, Sharma D, Davidson NE. A novel histone deacetylase inhibitor, scriptaid, enhances expression of functional estrogen receptor alpha (ER) in ER negative human breast cancer cells in combination with 5-aza 2'-deoxycytidine. *Breast Cancer Res Treat* 2003; 81:177-186.
130. Plumb JA, Finn PW, Williams RJ, Bandara MJ, Romero MR, Watkins CJ, La Thangue NB, Brown R. Pharmacodynamic response and inhibition of growth of human tumor xenografts by the novel histone deacetylase inhibitor PXD101. *Mol Cancer Ther* 2003; 2:721-728.

131. Vigushin DM, Ali S, Pace PE, Mirsaidi N, Ito K, Adcock I, Coombes RC. Trichostatin A is a histone deacetylase inhibitor with potent antitumor activity against breast cancer in vivo. *Clin Cancer Res* 2001; 7:971-976.
132. Finnin MS, Donigian JR, Cohen A, Richon VM, Rifkind RA, Marks PA, Breslow R, Pavletich NP. Structures of a histone deacetylase homologue bound to the TSA and SAHA inhibitors. *Nature* 1999; 401:188-193.
133. Furumai R, Matsuyama A, Kobashi N, Lee KH, Nishiyama M, Nakajima H, Tanaka A, Komatsu Y, Nishino N, Yoshida M, Horinouchi S. FK228 (depsipeptide) as a natural prodrug that inhibits class I histone deacetylases. *Cancer Res* 2002; 62:4916-4921.
134. Fuino L, Bali P, Wittmann S, Donapaty S, Guo F, Yamaguchi H, Wang HG, Atadja P, Bhalla K. Histone deacetylase inhibitor LAQ824 down-regulates Her-2 and sensitizes human breast cancer cells to trastuzumab, taxotere, gemcitabine, and epothilone B. *Mol Cancer Ther* 2003; 2:971-984.
135. Glaser KB, Staver MJ, Waring JF, Stender J, Ulrich RG, Davidsen SK. Gene expression profiling of multiple histone deacetylase (HDAC) inhibitors: defining a common gene set produced by HDAC inhibition in T24 and MDA carcinoma cell lines. *Mol Cancer Ther* 2003; 2:151-163.
136. Munster PN, Troso-Sandoval T, Rosen N, Rifkind R, Marks PA, Richon VM. The histone deacetylase inhibitor suberoylanilide hydroxamic acid induces differentiation of human breast cancer cells. *Cancer Res* 2001; 61:8492-8497.
137. Blaheta RA, Cinatl J, Jr. Anti-tumor mechanisms of valproate: a novel role for an old drug. *Med Res Rev* 2002; 22:492-511.
138. Sasakawa Y, Naoe Y, Inoue T, Sasakawa T, Matsuo M, Manda T, Mutoh S. Effects of FK228, a novel histone deacetylase inhibitor, on tumor growth and expression of p21 and c-myc genes in vivo. *Cancer Lett* 2003; 195:161-168.

139. Ueda H, Nakajima H, Hori Y, Fujita T, Nishimura M, Goto T, Okuhara M. FR901228, a novel antitumor bicyclic depsipeptide produced by *Chromobacterium violaceum* No. 968. I. Taxonomy, fermentation, isolation, physico-chemical and biological properties, and antitumor activity. *J Antibiot (Tokyo)* 1994; 47:301-310.
140. Ueda H, Manda T, Matsumoto S, Mukumoto S, Nishigaki F, Kawamura I, Shimomura K. FR901228, a novel antitumor bicyclic depsipeptide produced by *Chromobacterium violaceum* No. 968. III. Antitumor activities on experimental tumors in mice. *J Antibiot (Tokyo)* 1994; 47:315-323.
141. Yurek-George A, Habens F, Brimmell M, Packham G, Ganesan A. Total synthesis of spiruchostatin A, a potent histone deacetylase inhibitor. *J Am Chem Soc* 2004; 126:1030-1031.
142. Furumai R, Komatsu Y, Nishino N, Khochbin S, Yoshida M, Horinouchi S. Potent histone deacetylase inhibitors built from trichostatin A and cyclic tetrapeptide antibiotics including trapoxin. *Proc Natl Acad Sci U S A* 2001; 98:87-92.
143. Prakash S, Foster BJ, Meyer M, Wozniak A, Heilbrun LK, Flaherty L, Zalupski M, Radulovic L, Valdivieso M, LoRusso PM. Chronic oral administration of CI-994: a phase 1 study. *Invest New Drugs* 2001; 19:1-11.
144. Balasubramanyam K, Swaminathan V, Ranganathan A, Kundu TK. Small molecule modulators of histone acetyltransferase p300. *J Biol Chem* 2003; 278:19134-19140.
145. Howitz KT, Bitterman KJ, Cohen HY, Lamming DW, Lavu S, Wood JG, Zipkin RE, Chung P, Kisielewski A, Zhang LL, Scherer B, Sinclair DA. Small molecule activators of sirtuins extend *Saccharomyces cerevisiae* lifespan. *Nature* 2003; 425:191-196.

146. Posakony J, Hirao M, Stevens S, Simon JA, Bedalov A. Inhibitors of Sir2: evaluation of splitomicin analogues. *J Med Chem* 2004; 47:2635-2644.
147. Huang L, Pardee AB. Suberoylanilide hydroxamic acid as a potential therapeutic agent for human breast cancer treatment. *Mol Med* 2000; 6:849-866.
148. Marchion DC, Bicaku E, Daud AI, Richon V, Sullivan DM, Munster PN. Sequence-specific potentiation of topoisomerase II inhibitors by the histone deacetylase inhibitor suberoylanilide hydroxamic acid. *J Cell Biochem* 2004; 92:223-237.
149. Mitsiades CS, Mitsiades NS, McMullan CJ, Poulaki V, Shringarpure R, Hideshima T, Akiyama M, Chauhan D, Munshi N, Gu X, Bailey C, Joseph M, Libermann TA, Richon VM, Marks PA, Anderson KC. Transcriptional signature of histone deacetylase inhibition in multiple myeloma: biological and clinical implications. *Proc Natl Acad Sci U S A* 2004; 101:540-545.
150. Chang S, McKinsey TA, Zhang CL, Richardson JA, Hill JA, Olson EN. Histone deacetylases 5 and 9 govern responsiveness of the heart to a subset of stress signals and play redundant roles in heart development. *Mol Cell Biol* 2004; 24:8467-8476.
151. Roychowdhury S, Baiocchi RA, Vourganti S, Bhatt D, Blaser BW, Freud AG, Chou J, Chen CS, Xiao JJ, Parthun M, Chan KK, Eisenbeis CF, Ferketich AK, Grever MR, Chen CS, Caligiuri MA. Selective efficacy of depsipeptide in a xenograft model of Epstein-Barr virus-positive lymphoproliferative disorder. *J Natl Cancer Inst* 2004; 96:1447-1457.
152. Henderson C, Mizzau M, Paroni G, Maestro R, Schneider C, Brancolini C. Role of caspases, Bid, and p53 in the apoptotic response triggered by histone deacetylase inhibitors trichostatin-A (TSA) and suberoylanilide hydroxamic acid (SAHA). *J Biol Chem* 2003; 278:12579-12589.

153. Shao Y, Gao Z, Marks PA, Jiang X. Apoptotic and autophagic cell death induced by histone deacetylase inhibitors. *Proc Natl Acad Sci U S A* 2004; 101:18030-18035.
154. Chen JS, Faller DV. Histone deacetylase inhibition-mediated post-translational elevation of p27KIP1 protein levels is required for G1 arrest in fibroblasts. *J Cell Physiol* 2005; 202:87-99.
155. Peart MJ, Tainton KM, Ruefli AA, Dear AE, Sedelies KA, O'Reilly LA, Waterhouse NJ, Trapani JA, Johnstone RW. Novel mechanisms of apoptosis induced by histone deacetylase inhibitors. *Cancer Res* 2003; 63:4460-4471.
156. Sutheesophon K, Nishimura N, Kobayashi Y, Furukawa Y, Kawano M, Itoh K, Kano Y, Ishii H, Furukawa Y. Involvement of the tumor necrosis factor (TNF)/TNF receptor system in leukemic cell apoptosis induced by histone deacetylase inhibitor depsipeptide (FK228). *J Cell Physiol* 2005; 203:387-397.
157. Kosugi H, Ito M, Yamamoto Y, Towatari M, Ito M, Ueda R, Saito H, Naoe T. In vivo effects of a histone deacetylase inhibitor, FK228, on human acute promyelocytic leukemia in NOD / Shi-scid/scid mice. *Jpn J Cancer Res* 2001; 92:529-536.
158. Insinga A, Monestiroli S, Ronzoni S, Gelmetti V, Marchesi F, Viale A, Altucci L, Nervi C, Minucci S, Pelicci PG. Inhibitors of histone deacetylases induce tumor-selective apoptosis through activation of the death receptor pathway. *Nat Med* 2005; 11:71-76.
159. Nebbioso A, Clarke N, Voltz E, Germain E, Ambrosino C, Bontempo P, Alvarez R, Schiavone EM, Ferrara F, Bresciani F, Weisz A, de Lera AR, Gronemeyer H, Altucci L. Tumor-selective action of HDAC inhibitors involves TRAIL induction in acute myeloid leukemia cells. *Nat Med* 2005; 11:77-84.

160. Ungerstedt JS, Sowa Y, Xu WS, Shao Y, Dokmanovic M, Perez G, Ngo L, Holmgren A, Jiang X, Marks PA. Role of thioredoxin in the response of normal and transformed cells to histone deacetylase inhibitors. *Proc Natl Acad Sci U S A* 2005; 102:673-678.
161. Piekarz RL, Robey R, Sandor V, Bakke S, Wilson WH, Dahmouh L, Kingma DM, Turner ML, Altemus R, Bates SE. Inhibitor of histone deacetylation, depsipeptide (FR901228), in the treatment of peripheral and cutaneous T-cell lymphoma: a case report. *Blood* 2001; 98:2865-2868.
162. Bali P, Pranpat M, Swaby R, Fiskus W, Yamaguchi H, Balasis M, Rocha K, Wang HG, Richon V, Bhalla K. Activity of suberoylanilide hydroxamic Acid against human breast cancer cells with amplification of her-2. *Clin Cancer Res* 2005; 11:6382-6389.
163. Marshall JL, Rizvi N, Kauh J, Dahut W, Figuera M, Kang MH, Figg WD, Wainer I, Chaissang C, Li MZ, Hawkins MJ. A phase I trial of depsipeptide (FR901228) in patients with advanced cancer. *J Exp Ther Oncol* 2002; 2:325-332.
164. Sandor V, Bakke S, Robey RW, Kang MH, Blagosklonny MV, Bender J, Brooks R, Piekarz RL, Tucker E, Figg WD, Chan KK, Goldspiel B, Fojo AT, Balcerzak SP, Bates SE. Phase I trial of the histone deacetylase inhibitor, depsipeptide (FR901228, NSC 630176), in patients with refractory neoplasms. *Clin Cancer Res* 2002; 8:718-728.
165. Byrd JC, Marcucci G, Parthun MR, Xiao JJ, Klisovic RB, Moran M, Lin TS, Liu S, Sklenar AR, Davis ME, Lucas DM, Fischer B, Shank R, Tejaswi SL, Binkley P, Wright J, Chan KK, Grever MR. A phase 1 and pharmacodynamic study of depsipeptide (FK228) in chronic lymphocytic leukemia and acute myeloid leukemia. *Blood* 2005; 105:959-967.
166. Kelly WK, Richon VM, O'Connor O, Curley T, MacGregor-Curtelli B, Tong W, Klang M, Schwartz L, Richardson S, Rosa E, Drobnjak M, Cordon-



- Cordo C, Chiao JH, Rifkind R, Marks PA, Scher H. Phase I clinical trial of histone deacetylase inhibitor: suberoylanilide hydroxamic acid administered intravenously. *Clin Cancer Res* 2003; 9:3578-3588.
167. Gore SD, Weng LJ, Figg WD, Zhai S, Donehower RC, Dover G, Grever MR, Griffin C, Grochow LB, Hawkins A, Burks K, Zabelena Y, Miller CB. Impact of prolonged infusions of the putative differentiating agent sodium phenylbutyrate on myelodysplastic syndromes and acute myeloid leukemia. *Clin Cancer Res* 2002; 8:963-970.
168. Gilbert J, Baker SD, Bowling MK, Grochow L, Figg WD, Zabelina Y, Donehower RC, Carducci MA. A phase I dose escalation and bioavailability study of oral sodium phenylbutyrate in patients with refractory solid tumor malignancies. *Clin Cancer Res* 2001; 7:2292-2300.
169. Ryan QC, Headlee D, Acharya M, Sparreboom A, Trepel JB, Ye J, Figg WD, Hwang K, Chung EJ, Murgo A, Melillo G, Elsayed Y, Monga M, Kalnitskiy M, Zwiebel J, Sausville EA. Phase I and pharmacokinetic study of MS-275, a histone deacetylase inhibitor, in patients with advanced and refractory solid tumors or lymphoma. *J Clin Oncol* 2005; 23:3912-3922.
170. Undevia SD, Kindler HL, Janisch L, Olson SC, Schilsky RL, Vogelzang NJ, Kimmel KA, Macek TA, Ratain MJ. A phase I study of the oral combination of CI-994, a putative histone deacetylase inhibitor, and capecitabine. *Ann Oncol* 2004; 15:1705-1711.
171. Bug G, Ritter M, Wassmann B, Schoch C, Heinzl T, Schwarz K, Romanski A, Kramer OH, Kampfmann M, Hoelzer D, Neubauer A, Ruthardt M, Ottmann OG. Clinical trial of valproic acid and all-trans retinoic acid in patients with poor-risk acute myeloid leukemia. *Cancer* 2005; 104:2717-2725.
172. Kuendgen A, Schmid M, Schlenk R, Knipp S, Hildebrandt B, Steidl C, Germing U, Haas R, Dohner H, Gattermann N. The histone deacetylase

- (HDAC) inhibitor valproic acid as monotherapy or in combination with all-trans retinoic acid in patients with acute myeloid leukemia. *Cancer* 2006; 106:112-119.
173. Kuendgen A, Strupp C, Aivado M, Bernhardt A, Hildebrandt B, Haas R, Germing U, Gattermann N. Treatment of myelodysplastic syndromes with valproic acid alone or in combination with all-trans retinoic acid. *Blood* 2004; 104:1266-1269.
174. Adachi M, Zhang Y, Zhao X, Minami T, Kawamura R, Hinoda Y, Imai K. Synergistic effect of histone deacetylase inhibitors FK228 and m-carboxycinnamic acid bis-hydroxamide with proteasome inhibitors PSI and PS-341 against gastrointestinal adenocarcinoma cells. *Clin Cancer Res* 2004; 10:3853-3862.
175. Nakajima H, Kim YB, Terano H, Yoshida M, Horinouchi S. FR901228, a potent antitumor antibiotic, is a novel histone deacetylase inhibitor. *Exp Cell Res* 1998; 241:126-133.
176. Piekarz RL, Robey RW, Zhan Z, Kayastha G, Sayah A, Abdeldaim AH, Torrico S, Bates SE. T-cell lymphoma as a model for the use of histone deacetylase inhibitors in cancer therapy: impact of depsipeptide on molecular markers, therapeutic targets, and mechanisms of resistance. *Blood* 2004; 103:4636-4643.
177. Yu X, Guo ZS, Marcu MG, Neckers L, Nguyen DM, Chen GA, Schrupp DS. Modulation of p53, ErbB1, ErbB2, and Raf-1 expression in lung cancer cells by depsipeptide FR901228. *J Natl Cancer Inst* 2002; 94:504-513.
178. Koeller KM, Haggarty SJ, Perkins BD, Leykin I, Wong JC, Kao MC, Schreiber SL. Chemical genetic modifier screens: small molecule trichostatin suppressors as probes of intracellular histone and tubulin acetylation. *Chem Biol* 2003; 10:397-410.

179. Emmans VC, Rodway HA, Hunt AN, Lillycrop KA. Regulation of cellular processes by PPARgamma ligands in neuroblastoma cells is modulated by the level of retinoblastoma protein expression. *Biochem Soc Trans* 2004; 32:840-842.
180. Greenspan P, Mayer EP, Fowler SD. Nile red: a selective fluorescent stain for intracellular lipid droplets. *J Cell Biol* 1985; 100:965-973.
181. Clay CE, Monjazebe A, Thorburn J, Chilton FH, High KP. 15-Deoxy-delta12,14-prostaglandin J2-induced apoptosis does not require PPARgamma in breast cancer cells. *J Lipid Res* 2002; 43:1818-1828.
182. Gunin AG, Kapitova IN, Suslonova NV. Effects of histone deacetylase inhibitors on estradiol-induced proliferation and hyperplasia formation in the mouse uterus. *J Endocrinol* 2005; 185:539-549.
183. Woo HJ, Lee SJ, Choi BT, Park YM, Choi YH. Induction of apoptosis and inhibition of telomerase activity by trichostatin A, a histone deacetylase inhibitor, in human leukemic U937 cells. *Exp Mol Pathol* 2006.